THE STUDY OF BACTERIA THAT METABOLIZE AROMATIC HYDROCARBONS BY STABLE ISOTOPE PROBING, SECONDARY ION MASS SPECTROMETRY, AND IN VITRO EXPERIMENTS WITH *POLAROMONAS NAPHTHALENIVORANS* CJ2

A Dissertation

Presented to the Faculty of the Graduate School

of Cornell University

In Partial Fulfillment of the Requirements for the Degree of

Doctor of Philosophy

by

Graham Michael Pumphrey

August 25 2008

THE STUDY OF BACTERIA THAT METABOLIZE AROMATIC HYDROCARBONS BY STABLE ISOTOPE PROBING, SECONDARY ION MASS SPECTROMETRY, AND IN VITRO EXPERIMENTS WITH *POLAROMONAS NAPHTHALENIVORANS* CJ2

Graham Michael Pumphrey, Ph.D.

Cornell University 2008

Stable isotope probing is a cultivation-independent technique that allows researchers to identify microorganisms that metabolize substrates that are labeled with stable isotopes. However, to understand the genetics and physiology of microbial processes, experiments using pure culture are often necessary. *Polaromonas naphthalenivorans* CJ2 was identified as a key member of the naphthalene-degrading community in coal tar-contaminated sediment, and was successfully isolated in pure culture. Using respirometry, metabolite detection by gas chromatography/mass spectrometry, and cell-free enzyme assays, strain CJ2 was shown to metabolize naphthalene via gentisate. Growth assays revealed that strain CJ2 is inhibited by naphthalene concentrations of 78 μM (10 ppm) and higher. Despite being able to use naphthalene as a carbon and energy source, strain CJ2 must balance naphthalene utilization against two types of toxicity. Naphthalene directly inhibited growth, and the accumulation of putative naphthalene metabolites resulted in the loss of cell viability. Stable isotope probing of benzoic acid metabolizing bacteria in agricultural soil revealed the role of *Burkholderia* species, and cultivation efforts led to isolation of a representative of the benzoic acid-degrading population, *Burkholderia sp*. strain EBA09. Growth of the population represented by EBA09 in the field was demonstrated using MPN-PCR. The potential for dynamic secondary ion mass spectrometry (SIMS) ion microscopy to complement SIP studies by measuring ^{13}C assimilation into individual bacterial cells

grown on ^{13}C-labeled organic compounds was explored. A clear relationship between mass 27 and 26 signals in cells grown in media containing varying proportions of ^{12}C- to ^{13}C-glucose was observed; a standard curve was generated to predict ^{13}C-enrichment in unknown samples. Differences in ^{13}C signals measured by SIMS were shown to be due to ^{13}C assimilation into cell biomass. The application of SIMS ion microscopy to soil samples from a field experiment receiving ^{12}C- or ^{13}C-phenol revealed that ^{13}C-labeled cells were detected in soil that was dosed a single time with ^{13}C-phenol, and in soil that received 12 doses of ^{13}C-phenol, 27% of the cells in the total community were more than 90% ^{13}C-labeled.

BIOGRAPHICAL SKETCH

Graham Pumphrey was born in Lexington, KY, but he grew up and attended public schools in Kansas. In the fall of 1998, he enrolled into Cornell College, a liberal arts college in Mount Vernon, Iowa. As an undergraduate he worked with Dr. Barbara Christie-Pope in the summer of 2000 conducting research on a neurotoxin that causes Parkinson's disease-like symptoms. The following summer he was a Howard Hughes Undergraduate Research Fellow at the University of Iowa, where he conducted research examining zinc in *Saccharomyces cerevisiae* with Dr. Alan Kay. In the spring of 2002, he earned a B.A. in biochemistry. After entering in the Field of Microbiology graduate program at Cornell University in the fall of 2002, he joined Dr. Eugene Madsen's research group in the summer of 2003.

Dedicated to my parents, Roy and Wanda

ACKNOWLEDGMENTS

To begin, I would like thank my advisor, Dr. Eugene Madsen, for his patience and guidance as he helped me develop into a better scientist. I would like to thank Dr. Subhash Chandra for his collaboration and analyses of samples at the Cornell University Secondary Ion Mass Spectromatry Core Facility. I am also thankful to Buck Hanson, Chris DeRito, Jane Yagi, and Dr. Jack Liou for making time spent in the lab more productive and engaging, while making time spent away from the lab more fun. Buck deserves specific thanks for his help with the analysis of SIMS images.

Much of the work within this dissertation was made possible by a National Institute of Environmental Health Science predoctoral Environmental Training Grant.

I would also like to thank my family for their enduring support. I reserve my deepest gratitude for Amy Audetat, who supported me through graduate school with her humor and thoughtfulness.

TABLE OF CONTENTS

Section Page

LIST OF FIGURES

LIST OF TABLES

1. INTRODUCTION AND LITERATURE REVIEW

1.1 Introduction

The fundamental goals of the discipline of environmental microbiology are to elucidate (1) which microorganisms are present in a given environment, (2) what functions those microorganisms are performing, and (3) how microbial communities organize and interact. The observation that the majority of bacteria are not readily cultivated in a laboratory has led to the use of cultivation-independent techniques to ascertain the presence and function of bacteria in the natural environment (Amann et al., 1995). Applications of molecular techniques that target the 16S rRNA gene have greatly improved our understanding of microbial diversity in complex environments (Hugenholtz, 2002). However, while analysis of 16S rRNA sequences can provide insight into phylogenetic relationships and community diversity, it is difficult and dubious to infer function from a 16S rRNA sequence.

Techniques that combine the metabolism of isotopically labeled substrates with the analysis of 16S rRNA genes can provide a link between a microorganism's identity and substrate-specific function (Neufeld et al., 2007c). Fluorescent in situ hybridization combined with microautoradiography (FISH-MAR) (Ouverney and Fuhrman, 1999) and isotope arrays (Adamczyk et al., 2003) are techniques that use radiolabeled substrates in combination with oligonucleotide probes to identify metabolically active microorganisms. However, both of these techniques require prior knowledge of 16S rRNA sequences for oligonucleotide probe design. Stable isotope probing (SIP) is a technique that can directly link the identity and substrate-specific function of a microorganism without the need for prior knowledge of a 16S rRNA gene sequence (Dumont and Murrell, 2005; Madsen, 2006; Radajewski et al., 2000).

Despite advancements in techniques like SIP, and the development of metagenomics (Handelsman, 2004) and metaproteomics (Maron et al., 2007), experiments with pure cultures provide unmatched control of variables and reproducibility. Pure culture studies provide an important complement to cultivation-independent studies, and they are particularly valuable to detailed investigations of genetic regulation and metabolic pathways. A more complete biological picture can be gained if both studies performed with cultivation-independent methods and studies with pure cultures can be directed towards a microbial process.

Stable isotope probing of bacteria that metabolize aromatic hydrocarbons is a theme that connects the chapters within this dissertation. Both cultivation-independent techniques and pure culture in vitro studies are conducted to better understand (1) which microbial communities successfully metabolize aromatic hydrocarbons in the field, (2) how do those microorganisms metabolize aromatic hydrocarbons, and (3) how do those microbial communities change when aromatic hydrocarbons are added to their environment.

Polaromonas naphthalenivorans CJ2 is a cultivated representative of a naphthalene-degrading population from coal tar-contaminated sediment that was shown to be active in situ by SIP (Jeon et al., 2003). The cultivation of strain CJ2 has provided the opportunity to conduct in vitro studies that could help reveal what factors enabled strain CJ2 to successfully occupy a niche as a naphthalene-degrader in the environment. Chapter 2 of this dissertation is a study of the naphthalene catabolic pathway in strain CJ2, and it describes growth inhibition by naphthalene and naphthalene metabolites. Chapter 2 was published in *Microbiology* (Pumphrey and Madsen, 2007).

Chapter 3 of this dissertation describes a study that used SIP and cultivation to identify benzoic acid metabolizing bacteria in agricultural field soil. Changes in

culturable benzoic acid metabolizing bacteria, and 16S rRNA sequence information obtained through SIP are used to demonstrate the growth of a population of *Burkholderia* species in the field. Chapter 3 was published *Applied and Environmental Microbiology* (Pumphrey and Madsen, 2008).

Secondary ion mass spectrometry (SIMS) is a technique that allows analysis of the elemental and isotopic content of samples (Guerquin-Kern et al., 2005), and SIMS ion microscopy can be used to visualize isotope locations in a sample. SIMS ion microscopy has the potential to complement SIP experiments by microscopically confirming the role of microorganisms that are identified through SIP and measuring the amount of isotopic label that individual cells have incorporated the into their biomass. Chapter 4 of this dissertation is a study that demonstrated the use of a Cameca IMS-3f SIMS ion microscope to measure ^{13}C-incorporation by bacteria in pure culture and in soil, and is in review for the journal *Environmental Microbiology*.

1.2 Stable isotope probing

1.2.1 Stable isotope probing overview

Stable isotope probing (SIP) is a cultivation-independent technique that allows researchers to identify microorganisms that metabolize an exogenously added substrate. Due to the low natural abundance of ^{13}C (~1.1% total carbon) and ^{15}N (~0.37% total nitrogen) the biomass of microorganism that metabolize a substrate labeled with a stable isotope becomes enriched relative to the members of the population that are unable to metabolize the labeled substrate. SIP can help researchers identify populations that perform microbial processes in a variety of natural environments, while avoiding biases associated with culture-based techniques. A link between phylogeny and function is established by analyzing biomarkers, such as DNA (Radajewski et al., 2000), RNA (Manefield et al., 2002), or phospholipid fatty

acids (PFLA) (Boschker et al., 1998), from the biomass of populations that become labeled with ^{13}C or ^{15}N following the metabolism of a labeled substrate. In the case of nucleic acids, labeled RNA and DNA can be separated from non-labeled nucleic acids by density gradient ultracentrifugation due to differences in buoyant density, while lipids can be analyzed by gas chromatography-isotope ratio mass spectrometry (GC-IRMS).

The first study in microbial ecology that applied the principles of SIP examined PFLA that were ^{13}C-labeled due to the metabolism of ^{13}C-acetate or ^{13}C-methane (Boschker et al., 1998). ^{13}C-labeled PFLA are detected by GC-IRMS and do not need to be purified from unlabeled PLFA. Furthermore, only partial incorporation of ^{13}C is needed for analysis. This makes PFLA-SIP well-suited for investigating populations with low cell numbers or low growth rates, and studies of methanotrophic populations in particular have relied on the sensitivity of PFLA-SIP (Boschker et al., 1998; Bull et al., 2000; Crossman et al., 2004; Maxfield et al., 2006; Maxfield et al., 2008; Mohanty et al., 2006; Qiu et al., 2008; Shrestha et al., 2008; Singh and Tate 2007; Singh et al., 2007). PFLA-SIP has also been used to identify populations that metabolize aromatic pollutants such as polychlorinated biphenyl (Tillman et al., 2005) or toluene (Hanson et al., 1999; Mauclaire et al., 2003; Pelz et al., 2001), rhizosphere populations (Butler et al., 2003; Lu et al., 2007; Treonis et al., 2004), and acetate metabolizing populations (Boschker et al., 1998; Pombo et al., 2002; Pombo et al., 2005). However, because analysis of 16S small subunit (SSU) rRNA and its corresponding gene provide greater taxonomic resolution than analysis of lipids, DNA- and RNA-SIP studies are more prevalent in the literature.

The first application of DNA-SIP used ^{13}C-methanol to label DNA of methylotrophs in oak forest soil microcosms (Radajewski et al., 2000), and RNA-SIP was first applied to a phenol-degrading community in an industrial bioreactor

following the addition of ^{13}C-phenol (Manefield et al., 2002). DNA replication is necessary for isotopic labeling of DNA. At minimum, two cycles of replication are needed for the DNA to be fully labeled, which could reduce the likelihood of identifying slow growing organisms by DNA-SIP. Growth is not necessary for isotopic labeling of RNA, and because active cells turn over RNA at high rates, it is a more responsive biomarker that can be labeled with incubation times that are shorter than those needed for DNA-SIP.

Both DNA- and RNA-SIP require separation of stable isotope labeled nucleic acids from unlabeled nucleic acids by density gradient ultracentrifugation. DNA is typically separated in cesium chloride (CsCl) gradients, while RNA is separated using cesium trifluoroacetate (CsTFA). CsTFA prevents visualization of nucleic acids with ethidium bromide, and gradients containing RNA must be fractionated. CsCl gradients on the other hand, can be fractionated or ethidium bromide can be included in the gradient, and DNA bands can be visualized and collected by puncturing the side of an ultracentrifuge tube with a needle. Ultracentrifugation does not provide complete separation of labeled and unlabeled nucleic acids, and RNA tends to have higher levels of background than DNA (Lueders et al., 2004a). Thus, the presence of a nucleic acid sequence in the "heavy" part of a gradient does not necessarily indicate a high degree of labeling. SIP studies that use ^{15}N are far less common because the difference in buoyant density due to ^{15}N-incorporation is nearly identical to differences in buoyant density due to G+C content. A technique that included an intercalating agent during density gradient ultracentrifugation to minimize the effect of G+C content (Buckley et al., 2007a) led to the identification of free-living diazotrophs in soil (Buckley et al., 2007b).

Following ultracentrifugation, a variety of molecular techniques can be used to characterize the nucleic acids present in gradient fractions. The active members of a

microbial community that incorporated the stable isotopic label can be differentiated from inactive community members by comparing the nucleic acids present in "heavy" fractions to those in "light" fractions from the same gradient, as well as by comparing "heavy" fractions from samples treated with a ^{13}C-labeled substrate to "heavy" fractions from control samples treated with a ^{12}C-substrate. The most common techniques used to compare gradient fractions are clone libraries (Jeon et al., 2003; Morris et al., 2002; Padmanabhan et al 2003; Radajewski et al., 2000), terminal-restriction fragment length polymorphism (Lu et al., 2005; Lueders et al 2004b; Lueders et al 2004c), and denaturing gradient gel electrophoresis (Kasai et al., 2006; Manefield et al., 2002; Neufeld et al., 2007). Microarrays can provide a high-throughput method to examine the presence of genes in ^{13}C-labeled DNA (Cebron et al., 2007b; Hery et al., 2008; Leigh et al., 2007). SIP can also be combined with techniques that rely on sequences identified by SIP, such as fluorescent in situ hybridization-microautoradiography (Ginige et al., 2004; Ginige et al., 2005) and quantitative-PCR (Singleton et al., 2007). Metagenomic techniques can be used to detect entire operons as opposed to single gene sequences (Dumont et al., 2006). Additionally, microscopic techniques that can detect isotopic enrichment in cells, such as Raman microscopy (Huang et al., 2004; Huang et al., 2007) or secondary ion mass spectrometry (DeRito et al., 2005), can be used to confirm incorporation of the isotopic label into cellular biomass.

SIP is not without limitations. The availability of isotopically labeled substrates can be limited, particularly uniformly labeled compounds, which are preferred. In order to ensure enough biomass is labeled for subsequent analysis, a substrate may be added at concentrations that exceed concentrations found in situ, which could alter populations or select for populations that are not representative at natural substrate concentrations. Long incubation times can lead to carbon cross-

feeding, where organisms not responsible for metabolism of the added substrate become ^{13}C-labeled by consuming ^{13}C-labeled metabolites from primary degraders (DeRito et al., 2005; Hutchens et al., 2004; Lueders et al., 2004c; Morris et al., 2002). As mentioned above, separation of labeled and unlabeled nucleic acids is often incomplete, and if organisms consume both the exogenous labeled substrate and endogenous unlabeled substrates then they may be overlooked. Finally, the molecular tools used to analyze labeled nucleic acids are subject to biases of PCR amplification (von Wintzingerode et al., 1997).

1.2.2 SIP applications

The versatility of SIP is illustrated by the many substrates and environments to which researchers have applied the technique. SIP has been applied extensively to study methanotrophic and methylotrophic populations in soil (Cebron et al., 2007a; Cebron et al., 2007b; Dumont et al 2006; Hery et al., 2008; Maxfield et al., 2008; Morris et al., 2002; Radajewski et al., 2002; Singh and Tate, 2007; Singh et al., 2007), sediment (Lin et al., 2004; Nercessian et al., 2005), groundwater (Hutchens et al., 2004), activated sludge (Osaka et al., 2006; Osaka et al., 2008), marine (Neufeld et al., 2007; Neufeld et al., 2008), and rice field soil and rhizosphere (Lueders et al., 2004b; Mohanty et al., 2006; Murase and Frenzel, 2007; Noll et al., 2008; Qiu et al., 2008; Shrestha et al., 2008) environments.

Researchers have also applied SIP to investigate populations that degrade organic pollutants. Benzene-degrading populations have been identified in groundwater (Kasai et al., 2006), an iron-reducing enrichment culture (Kunapuli et al., 2007) and freshwater sediment (Liou et al., 2008). A population of biphenyl-metabolizing bacteria was identified in a pine root zone contaminated with polychlorinated biphenyls (Leigh et al., 2007). Populations that metabolize

naphthalene have been investigated by SIP in groundwater (Huang et al., 2007), freshwater sediment (Jeon et al., 2003), a bench-scale bioreactor (Singleton et al., 2005), and agricultural soil (Padmanabhan et al., 2003). Phenol-degrading populations have also been analyzed in agricultural soil (DeRito et al., 2005; Padmanabhan et al., 2003) and bioreactors (Manefield et al., 2002; Manefield et al., 2007). PAH-degrading populations have been investigated for their ability to degrade phenanthrene (Singleton et al., 2005; Singleton et al., 2007) or pyrene (Singleton et al., 2006; Singleton et al., 2007). Populations that degrade chlorinated compounds such as pentachlorophenol (Mahmood et al., 2005), perchloroethene (Kittelmann and Friedrich 2008a; Kittelmann and Friedrich 2008b), and polychlorinated biphenyl (Tillman et al., 2005) have been investigated as well. Other substrates that have been used in SIP studies include acetate (Ginige et al., 2004; Ginige et al., 2005; Hori et al., 2007; Lear et al., 2007; Osaka et al., 2006; Schwartz et al., 2007; Webster et al., 2006), benzoate (Gallagher et al., 2005), cellulose (Haicher et al., 2007), fatty acids (Hatamoto et al., 2007), methyl chloride (Borodina et al., 2005), propionate (Lueders et al., 2005c), monosaccharides (Hamberger et al., 2008), and $^{15}N_2$ (Buckley et al., 2007b). Pulse labeling of plants with $^{13}CO_2$ has been used to study populations that metabolize root exudates (Griffiths et al., 2004; Lu et al., 2005; Lu and Conrad 2005; Lu et al., 2006; Lu et al., 2007; Rangel-Castro et al., 2005).

Although SIP studies have primarily targeted 16S rRNA genes, DNA-SIP allows functional genes to be targeted in addition to taxonomic markers. Functional genes from ^{13}C-labeled have been analyzed with primers targeting specific genes, microarrays, and metagenomic methods. Primers have been used to target methane monooxygenase genes (Cebron et al., 2007b; Hery et al., 2008; Hutchens et al., 2004; Lin et al., 2004; Morris et al., 2002; Nercessian et al., 2005), methanol dehydrogenase and methylamine dehydrogenase genes (Neufeld et al., 2007), nitrite reductase genes

(Osaka et al., 2006), formaldehyde-activating enzyme genes (Nercessian et al., 2005), and a methyltransferase gene involved in methyl-chloride metabolism (Borodina et al., 2005). Methane monooxygenases have also been examined with microarrays (Cebron et al., 2007b; Hery et al., 2008), as have aromatic ring hydroxylating dioxygenase subunits (Leigh et al., 2007). Cloning of ^{13}C-labeled DNA into a bacterial artificial chromosome plasmid led to the identification of a complete methane monooxygenase operon (Dumont et al., 2006).

In the majority of SIP studies, the microorganisms that are identified as active in situ have yet to be cultured. However, a few studies have reported successful cultivation of isolates that are representative of populations identified by SIP. *Polaromonas napththalenivorans* CJ2 was isolated from coal-tar contaminated sediment, and was shown to be a member of the active naphthalene-degrading population by DNA-SIP in the field (Jeon et al 2003). RNA-SIP of anaerobic benzene-degraders in groundwater revealed the role of *Azoarcus* species. Two strains, DN11 and AN9, with 100% sequence homology to the ^{13}C-labeled *Azoarcus* 16S rRNA sequence were subsequently isolated and shown to degrade benzene under denitrifying conditions (Kasai et al., 2006). An investigation of anaerobic, long-chain fatty acid degrading bacteria in methanogenic sludge enrichments identified members of the family *Syntrophomonadaceae* by RNA-SIP as dominant palmitate degraders, and a representative of the dominant *Syntrophomonadaceae* population, strain MPA, was successfully isolated and shown to degrade palmitate to methanol and acetate (Hatamoto et al., 2007). Both cultivation and DNA-SIP detected an *Arthrobacter* spp. as a biphenyl degrader in the polychlorinated biphenyl-contaminated root zone of Austrian pine (Leigh et al., 2007). The cultivation of microorganisms that have been identified by SIP can enable genetic and physiological studies that seek to understand

what makes the organisms successful in their respective environments (Jeon et al., 2006).

1.3 Secondary ion mass spectrometry

1.3.1 Secondary ion mass spectrometry overview

Secondary ion mass spectrometry is a technique that allows selective analysis of elements and isotopes on sample surfaces. The technique was developed in the early 1960s by Castaing and Slodzian (1962), and relies on the mass spectrometry of secondary ions desorbed from the sample surface by a primary ion beam. The resulting secondary ions are focused, and their masses are measured with a magnetic sector, quadrupole, or time-of-flight mass analyzer (Pacholski and Winograd, 1999). SIMS can provide spatially resolved information, and by rastering the primary ion over an area of a sample, SIMS microscopy can provide images that reveal the origin of secondary ions from the sample (Guerquin-Kern et al., 2005). SIMS analyses are generally divided into two categories: static or dynamic. For static SIMS measurements, the number of incident, primary ions is an order of magnitude less than the number of sample surface atoms. Static SIMS is generally used to measure abundant elements from the top monolayer of a sample. In contrast, for dynamic SIMS the number of incident ions exceeds the number of surface atoms on a sample. The high number of incident ions increases the depth of desorbed ions, and allows for investigation of bulk composition and detection of trace elements. Reviews by Pacholksi and Winograd (1999), Chandra et al. (2000), and Guerquin-Kern et al. (2005) provide greater technical detail of SIMS techniques.

SIMS technology has tremendous potential to aid investigations of microbial systems, but there are technical considerations that can limit application of SIMS to biological problems. Perhaps the greatest limitation of SIMS is that in vivo studies

cannot be performed, because the sample must be dehydrated, brought to a potential of several kilovolts, and held under a vacuum (Guerquin-Kern et al., 2005). Sample preparation is key to SIMS analysis, and it is important to minimize changes to the sample during fixation. The resolution of ions with nearly identical masses can be problematic as mass interference from isobaric ion species has the potential to influence the signal of an ion species of interest. Sample degradation due to erosion by the primary ion beam can limit exposure time needed to take images, or may limit the number of images that can be taken if long exposure times are necessary. The lateral resolution of images acquired by SIMS ranges from ~50 nm to 15 μm depending on the model of ion microprobe, and it can be difficult or impossible to distinguish small cells (Neufeld et al 2007c).

1.3.2 SIMS applications in microbiology

The application of SIMS techniques to biological investigations was limited to eukaryotic systems (Chandra et al., 2000; Pacholski and Winograd, 1999) until pioneering studies that applied SIMS to microbial systems using SIMS in combination with fluorescent in-situ hybridization (FISH) to show that methane-consuming *Archaea* in anoxic marine sediments were naturally ^{13}C-depleted (Orphan et al., 2001; Orphan et al., 2002). Using the erosive quality of SIMS analysis, researchers were able to obtain $\delta^{13}C$ profiles from the exterior to the interior of cell aggregates composed of sulfur-reducing bacteria and methanotrophic archaea (Orphan et al., 2001). Consumption of CH_4 and CO_2 by methanotrophic microbial mats in the Black Sea was studied using a combination of SIMS, autoradiography, and FISH (Treude et al., 2007). Time of flight SIMS (TOF-SIMS) has been used to the assimilation of inorganic carbon and nitrogen in pure cultures grown with $NaH^{13}CO_3$ and $(^{15}NH_4)_2SO_4$, and nitrogen incorporation was shown in bacterial cells and fungal

hyphae from riparian soil treated with $(^{15}NH_4)_2SO_4$ (Cliff et al., 2002). TOF-SIMS has also been used as a forensics application to distinguish *Bacillus subtilis* spores according to the type of media they were grown in by using 16 elemental signatures (Cliff et al., 2005). Dynamic SIMS was used to complement a field-based SIP study by showing enhanced ^{13}C-signals from bacteria in soil treated with ^{13}C-phenol compared to soils treated with ^{12}C-phenol (DeRito et al., 2005).

Recent advances in technology have led to improvements in lateral resolution (~50 nm) and the ability to measure 5 masses in simultaneously (Guerquin-Kern et al., 2005). This nanometer-scale SIMS technology is referred to as NanoSIMS or multi-ion imaging mass spectrometry (MIMS). Lechene et al. (2006) demonstrated the use of NanoSIMS to show ^{15}N fixation by *Teredinibacter turnerae* in pure culture, and distinguished ^{15}N-labeled *T. teredinibacter* from unlabeled *Enterococcus faecalis*. To show that NanoSIMS could be applied to soil environments, cells of ^{15}N-enriched *Pseudomonas fluorescens* were imaged after being added to a soil matrix (Herrmann et al., 2007). The application of NanoSIMS to microbial systems has not been limited to cellular biomass. The association between extracellular proteins and biogenic zinc sulfide nanoparticles was detected by NanoSIMS in a biofilm dominated by sulfate-reducing bacteria (Moreau et al., 2007). Two studies have combined NanoSIMS with 16S rRNA-targeted oligonucleotide probes that contain halogens. Oligonucleotides that were labeled with iodized cytidine were combined with NanoSIMS to visualize both *Escherichia coli* grown on different amounts of ^{13}C and ^{15}N, and an archaeal population from a municipal solid waste bioreactor growing on ^{13}C-methanol (Li et al., 2008). Behrens et al. (2008) combined NanoSIMS with element labeling-FISH (EL-FISH), a technique that uses catalyzed reporter deposition (CARD)-FISH (Pernthaler et al., 2002) and halogen-containing, fluorescently labeled tyramides to label cells with bromine or fluorine. This allowed both fluorescent and SIMS imaging

of a consortium consisting of filamentous cyanobacteria and an epibiont. After incubation with ^{13}C-bicarbonate and $^{15}N_2$, researchers observed that carbon and nitrogen fixed by the cyanobacterium were assimilated by the epibiont (Behrens et al., 2008). NanoSIMS was also used to characterize cellular development and metabolite exchange in filamentous cyanobacteria (Popa et al., 2007).

1.4 Naphthalene metabolism by *Polaromonas naphthalenivorans* CJ2

1.4.1 Aerobic naphthalene metabolism by bacteria

Naphthalene is composed of two fused aromatic rings and is the simplest member of the class of compounds known as polycyclic aromatic hydrocarbons, or PAHs. The metabolism of naphthalene has been studied extensively since the 1950s, when researchers began isolating microorganisms capable of using naphthalene as a source of energy and carbon. Naphthalene metabolism has primarily been studied in *Pseudomonas* species, but other Gram-negative and Gram-positive bacteria are capable of metabolizing naphthalene as well (Habe and Omori, 2003). The initial step in aerobic naphthalene metabolism requires a multi-component dioxygenase that introduces molecular oxygen into the 1,2-position of the aromatic ring (Parales, 2003). The product of the dioxygenation, *cis*-1,2-dihydroxyl-dihydronaphthalene, is dehydrogenated to form 1,2-dihydroxynaphthalene (Davies and Evans, 1964). Subsequent intermediate metabolic steps lead to the production of salicylaldehyde, which is transformed to salicylate by salicylaldehyde dehydrogenase (Habe and Omori, 2003). A key difference among naphthalene metabolic pathways pertains to the metabolism of salicylate. In well studied *Pseudomonas* species, salicylate is metabolized to catechol (Yen and Gunsalus, 1982). Alternatively, salicylate can be metabolized to gentisate as observed in *Ralstonia* sp. strain U2 (Fuenmayor et al.,

1998; Zhou et al., 2001). Gentisate and catechol are ultimately metabolized to tricarboxylic acid cycle intermediates.

The salicylate and gentisate metabolic pathways are encoded by distinct naphthalene catabolic genes with differing operon structures. In the archetypal naphthalene-degraders that use the catechol pathway, *Pseudomonas putida* G7 and *P. putida* NCIB 9816-4, the *nah* catabolic genes are arranged into two operons, upper and lower (Dennis and Zylstra, 2004; Sota et al., 2006). The upper operon encodes for the metabolism of naphthalene to salicylate, and the lower operon encodes for the metabolism of catechol to TCA cycle intermediates. A single, LysR-type regulatory protein, NahR, regulates both the upper and lower operons. In *Ralstonia* sp. strain U2, the *nag* catabolic genes that metabolize salicylate via gentisate are arranged as a single, linear operon that is regulated by the LysR-type regulatory protein, NagR (Jones et al 2003).

Other naphthalene catabolic genotypes and operon structures have been characterized. The *phn* genes of *Burkholderia* sp. strain RP007 show low homology to other naphthalene catabolic genes, and are arranged into an upper operon that encodes metabolism of naphthalene and phenanthrene (Laurie and Lloyd-Jones, 1999a). Strain RP007 also carries two distinct lower operons that encode the meta-cleavage of catechol (Laurie and Lloyd-Jones, 1999b). There are several strains of Gram-positive *Rhodococcus* species that carry *nar* naphthalene catabolic genes, which show low similarity to *nah*-like genes found in *Pseudomonas* species. The *nar* genes are not organized into a single operon, but are encoded by several transcription units that differ by strain (Kulakov et al., 2005). In addition, some *Rhodococcus* strains metabolize naphthalene via catechol (Kulakova et al., 1996), while another is known to metabolize naphthalene through gentisate (Allen et al., 1997).

1.4.2 Polaromonas naphthalenivorans CJ2

Polaromonas naphthalenivorans CJ2 was isolated from coal-tar contaminated freshwater sediment for the ability to utilize naphthalene vapor as a sole source of carbon and energy (Jeon et al., 2003; Jeon et al., 2004). Field-based stable isotope probing of the naphthalene-metabolizing community within the coal-tar contaminated sediment revealed strain CJ2 was responsible for naphthalene mineralization in the field (Jeon et al., 2003). The cultivation of strain CJ2 provides the relatively rare opportunity to use culture-based techniques to study the genetics and physiology of a bacterium that was shown to metabolize naphthalene in the field by non-culture based techniques.

Genetic analysis of the naphthalene catabolic operon in strain CJ2 revealed sequence similarity to the *nag* operon in the naphthalene-degrader *Ralstonia* sp. strain U2 (Jeon et al., 2006). However, unlike the *nag* genes in strain U2, which are organized in a single operon, the naphthalene catabolic genes in strain CJ2 are organized into a large cluster (*nagRAaGHAbAcAdBFCQEDJI'orf1tnpA*) and a small cluster (*nagR2orf2I'KL*). A LysR-type transcriptional regulator (*nagR*) positively regulates the large naphthalene catabolic gene cluster. The small cluster is negatively regulated by a MarR-type transcriptional regulator (*nagR2*).

The *nag* genes in strain CJ2 are located on the chromosome, and not on a plasmid as in *Ralstonia* sp. strain U2. The association of two putative *Azoarcus*-related transposases with the large cluster suggests that mobile genetic elements may have been involved in creating the novel arrangement of catabolic and regulatory genes in strain CJ2 (Jeon et al., 2006).

2. NAPHTHALENE METABOLISM AND GROWTH INHIBITION BY NAPHTHALENE IN *POLAROMONAS NAPHTHALENIVORANS* STRAIN CJ2

2.1 Abstract

This study was designed to characterize naphthalene metabolism in *Polaromonas naphthalenivorans* CJ2. Comparisons were made with two archetypal naphthalene-degrading bacteria: *Pseudomonas putida* NCIB 9816-4 and *Ralstonia* sp. strain U2, representative of the catechol and gentisate pathways, respectively. Strain CJ2 carries naphthalene catabolic genes that are homologous to those in *Ralstonia* sp. strain U2. Here we show that strain CJ2 metabolizes naphthalene via gentisate using respirometry, metabolite detection by gas chromatography/mass spectrometry, and cell-free enzyme assays. Unlike *P. putida* NCIB 9816-4 or *Ralstonia* sp. strain U2, strain CJ2 did not grow in minimal media saturated with naphthalene. Growth assays revealed that strain CJ2 is inhibited by naphthalene concentrations of 78 μM (10 ppm) and higher, and the inhibition of growth is accompanied by the accumulation of orange-colored, putative naphthalene metabolites in the culture media. Loss of cell viability coincided with the appearance of the colored metabolites, and analysis by HPLC suggested the accumulated metabolites were 1,2-naphthoquinone and its unstable autooxidation products. The naphthoquinone breakdown products accumulated in inhibited, but not uninhibited, cultures of strain CJ2. Furthermore, naphthalene itself was shown to directly inhibit growth of a regulatory mutant of strain CJ2 that is unable to metabolize naphthalene. These results suggest that, despite being able to use naphthalene as a carbon and energy source, strain CJ2 must balance naphthalene utilization against two types of toxicity.

2.2 Introduction

Polycyclic aromatic hydrocarbons (PAHs) are widely distributed in the environment, and the toxic and carcinogenic characteristics of PAHs have motivated efforts to develop bioremediation technologies to eliminate sources of PAH exposure (Samanta et al., 2002; Xue and Warshawsky, 2005). Naphthalene is commonly used as a model for studying PAH metabolism by bacteria because it is the simplest and most soluble PAH, as well as a frequent constituent of PAH contaminated environments (Peters et al., 1999). Studies of naphthalene degradation have shown that there are two primary pathways for the metabolism of naphthalene, which are distinguished by the conversion of salicylate to catechol or gentisate. Metabolism of naphthalene via catechol has been studied extensively in two *Pseudomonas* species that carry the archetypal catabolic plasmids, NAH7 (in *P. putida* G7) and pDTG1 (in *P. putida* NCIB 9816-4) (Dennis and Zylstra, 2004; Yen and Serdar, 1988; Sota et al., 2006). The *nah* dissimilatory genes are organized into two operons: one coding for the enzymes involved in the conversion of naphthalene to salicylate (naphthalene degradation upper pathway) and another coding for the conversion of salicylate to catechol, followed by *ortho*- or *meta*-cleavage to TCA cycle intermediates (naphthalene degradation lower pathway) (Yen and Gunsalus, 1982). In contrast, the *nag* genes found in *Ralstonia* sp. strain U2 are organized in a single operon and encode the alternative gentisate pathway, which converts naphthalene to fumarate and pyruvate via salicylate and gentisate (Fuenmayor et al., 1998; Zhou et al., 2002).

Although the genetics and biochemistry of naphthalene metabolism have been studied in-depth, the inhibition of naphthalene metabolism due to the toxicity of naphthalene and naphthalene metabolites has received less attention (Auger et al., 1995; Murphy and Stone, 1955; Park et al., 2004). Naphthalene was reported to be directly toxic to *P. putida* G7 under oxygen- and nitrogen-limited conditions; although

it is unclear if the toxicity was due to naphthalene or a naphthalene metabolite (Ahn et al., 1998). Naphthalene was also shown to be toxic to non-naphthalene-degraders, as *P. putida* KT2440 showed reduced viability in soil amended with naphthalene (Park et al., 2004), and a bioluminescent strain of *Escherichia coli* showed reduced bioluminescence in the presence of naphthalene (Lee et al., 2003).

Polaromonas naphthalenivorans CJ2 was isolated from coal-tar-contaminated freshwater sediment for its ability to use naphthalene as its sole carbon source, and was shown to be responsible for in situ naphthalene degradation by field-based stable isotope probing (Jeon et al., 2003). The naphthalene catabolic genes in strain CJ2 are homologous to the *nag* operon of *Ralstonia* sp. strain U2, but the genes are arranged in two separate clusters, each with its own regulatory protein (Jeon et al., 2006). In the present investigation, we show that strain CJ2 metabolizes naphthalene via the gentisate pathway using respirometry, GC/MS, and cell-free enzyme assays. In addition, we explore the inhibitory effects of naphthalene and its metabolites on the growth of strain CJ2.

2.3 Materials and Methods

2.3.1 Bacterial Strains

P. naphthalenivorans strain CJ2 was isolated from freshwater sediment from a coal-tar waste contaminated site (Jeon et al., 2003). Naphthalene degraders *P. putida* NCIB 9816-4 (Yen and Serdar, 1988) and *Ralstonia* sp. strain U2 (Zhou et al., 2002) were included in this study for comparison. Strain CJN110 is a mutant of strain CJ2 in which the regulatory gene *nagR* has been disrupted by a suicide vector carrying a kanamycin resistance gene (Jeon et al., 2006).

2.3.2 Growth Assays

All growth assays were conducted with Stanier mineral salts media (MSB; Stanier et al., 1966) amended with pyruvate (18 mM), glucose (6 mM), and/or naphthalene crystals. The aqueous concentration of naphthalene was lowered with Amberlite® XAD7 resin. Naphthalene binds to the XAD7 resin, which acts as a reservoir, and maintains the aqueous concentration of naphthalene below saturation (230 µM or 30 ppm) while supplying enough naphthalene to support growth over the course of the experiment (Morasch et al., 2001). Six to 14 mg of naphthalene were added to 6 ml MSB containing 0.1 g XAD7 before the tubes were sealed with Teflon®-lined stoppers and autoclaved. Viability of test bacteria was measured by enumerating colony forming units (CFUs) from 10 µl drops of serially diluted cultures on R2A agar. Kanamycin was added to media at 40 $\mu g\, ml^{-1}$ when appropriate.

2.3.3 Respirometry

Bacterial cells were grown to late-log phase in MSB with naphthalene (0.5% w/v) and harvested (6000 *g*). Cells were washed twice and resuspended in 50 mM KH_2PO_4 buffer (pH=7.4). Endogenous respiration was measured with an oxygen electrode (Rank Brothers, Cambridge, UK) after adding 2 ml of washed cell suspension to the incubation chamber, and oxygen consumption was recorded following the addition of 20 mM substrate dissolved in *N,N*-dimethylformamide (DMF). Respiration upon addition of DMF only was included as a control treatment.

2.3.4 Enzyme assays

Bacterial cells were grown in 500 ml of MSB with 18 mM pyruvate or 4 mM salicylate to late-log phase, and cells were harvested by centrifugation (6,000 *g*) and washed once with 50 mM KH_2PO_4 buffer (pH=7.4). Cells were resuspended in buffer

to a concentration of 0.1 g ml^{-1} and sonicated three times for 30-seconds with 60 second cooling intervals. Cellular debris was cleared by centrifugation (25,000 *g* for 45 min.), and protein concentrations were determined with the Bio-Rad Bradford assay (Bio-Rad, Hercules, Calif.). Enzyme assays were performed with a minimum of 50 µg protein. The enzyme substrates, gentisate (0.19 µmol) or catechol (0.9 µmol), were added in 1-ml volumes. Gentisate 1,2-dioxygenase activity was measured spectrophotometrically by measuring the increase of absorption at 334 nm, due to the formation of maleylpyruvate, and was calculated with an extinction coefficient of 10,800 M^{-1} cm^{-1} (Crawford et al., 1975). Catechol 1,2-dioxygenase activity was assayed by measuring the increase in absorption at 260 nm, due to the formation of *cis,cis*-muconate, and was calculated with an extinction coefficient of 16,800 M^{-1} cm^{-1} (Dorn and Knackmuss, 1978). Catechol 2,3-dioxygenase activity was measured by monitoring the increase in 2-hydroxy-*cis,cis*-muconate semialdehyde at 375 nm, and was calculated with an extinction coefficient of 33000 M^{-1} cm^{-1} (Cerdan et al., 1994).

2.3.5 GC/MS detection of naphthalene pathway metabolites

500 ml of cells grown on naphthalene or pyruvate were harvested, washed twice, and resuspended in 10 ml of 50 mM KH_2PO_4 buffer. Fifty microliters of 200 mM naphthalene in DMF were added to 5 ml of concentrated cell suspension, and metabolism was allowed to proceed for 5 min. Suspensions were acidified with HCl to pH=1.5 and extracted twice with 7.5 ml of ethyl acetate, which was then dried over anhydrous Na_2SO_4 and concentrated under an atmosphere of N_2 to a volume of 300 µl. Extracts were derivatized with 25 µl of BSTFA [bis(trimethylsilyl)trifluoroacetimide] for 5 min prior to gas chromatography-mass spectrometry (GC/MS) analysis and quantified using external standard calibration curves.

2.3.6 HPLC analysis of naphthalene and inhibitory compounds.

Naphthalene concentrations were determined by high-performance liquid chromatography. Samples (100 µl) were taken from culture tubes and immediately fixed in an equal volume of methanol. Samples were filtered through tightly packed glass wool prior to injection, and naphthalene was separated using a PAH-Hypersil column (150x4.6 mm, Keystone Scientific) and a Waters model 590 HPLC pump with a mobile phase of methanol-water (65:35) at a flow rate of 1 ml min^{-1}. Eluents were monitored by UV-visible light detection (ABI analytical absorbance detector, Spectroflow 757) at a wavelength of 270 nm and quantified using an external standard calibration curve.

Putative naphthalene metabolites were separated with a Hypersil BDS-C18 column (4.6x250 mm, Agilent) at a flow rate of 1 ml/min with a Spectra-Physics model SP8800 ternary HPLC pump. The mobile phase consisted of 20% methanol and 80% 40 mM acetic acid for 10 minutes, followed by a linear increase in methanol to 50% over 10 minutes; after 5 minutes the methanol concentration was linearly increased to 90% over 10 minutes and held for 15 minutes. Eluents were detected at 260 nm using UV-Vis detector (SPD-10A VP, Shimadzu). Aged 1,2 naphthoquinone solution (50µM final concentration) was prepared by diluting a filter-sterilized 10mM methanolic stock, aseptically adding it to sterile MSB, and allowing the solution to shake for 48 hours.

2.4 Results

2.4.1 Respirometry

To better understand the physiology of *Polaromonas naphthalenivorans* CJ2, we compared strain CJ2 with archetypal naphthalene degrading bacteria *Pseudomonas putida* NCIB 9816-4 and *Ralstonia* sp. strain U2. The simultaneous induction of

enzymes involved in naphthalene metabolism was compared in the three strains by measuring oxygen uptake after the introduction of potential naphthalene metabolites to washed cell suspensions (Figure 2.1). The simultaneous adaptation assays were aimed at confirming that strain CJ2 metabolizes naphthalene via gentisate as suggested by the sequence homology of the naphthalene catabolic operons in *Ralstonia* sp. strain U2 and strain CJ2, as well as to reveal potential physiological effects of the naphthalene catabolic gene arrangement in strain CJ2.

Consistent with the established metabolic pathway in *P. putida* NCIB 9816-4, these cells rapidly consumed oxygen after addition of naphthalene, salicylaldehyde, salicylate, and catechol, while oxygen depletion was not rapid after the addition of gentisate (Figure 2.1). *Ralstonia* sp. strain U2 cells consumed oxygen when exposed to naphthalene, salicylaldehyde, and salicylate. *Ralstonia* sp. strain U2 cells, our positive control for the gentisate pathway, did not display enhanced respiration when exposed to gentisate (Figure 2.1). Strain CJ2 consumed oxygen after addition of naphthalene, salicylaldehyde, and salicylate. However, similar to *Ralstonia* sp. strain U2, neither gentisate nor catechol led to the rapid depletion of oxygen. *Ralstonia* sp. strain U2 is known to lack a gentisate transporter (Xu et al,. 2006), and if the same is true for strain CJ2, this accounts for the absence of enhanced oxygen uptake in the presence of gentisate. Regardless, the lack of enhanced oxygen uptake in the presence of catechol by *Ralstonia* sp. strain U2 and strain CJ2 reveals a key distinction between these two strains and *P. putida* NCIB 9816-4.

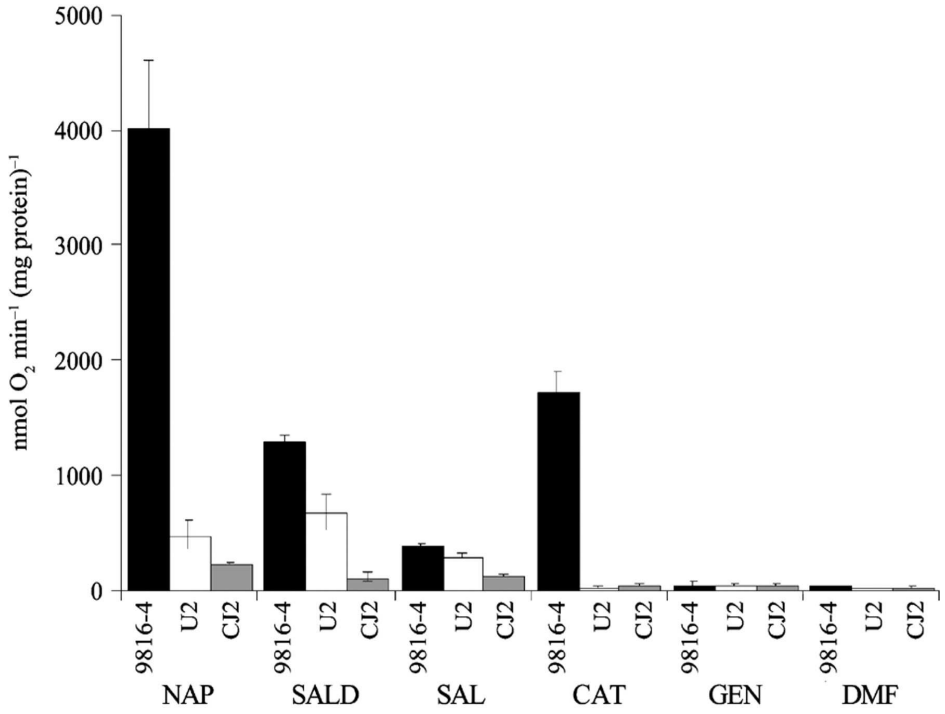

Figure 2.1. Respiration by three strains of bacteria (*P. putida* NCIB 9816-4, *Ralstonia* sp. strain U2, and *P. naphthalenivorans* strain CJ2) grown on naphthalene and exposed to naphthalene and 5 potential metabolites (salicylaldehyde, salicylate, catechol, and gentisate). The oxygen uptake experimental values represent the mean and standard deviation of triplicate experiments. All values are corrected for endogenous respiration of cells. (NAP=naphthalene, SALD=salicylaldehyde, SAL=salicylate, CAT=catechol, GEN=gentisate, and DMF=dimethylformamide)

2.4.2 Metabolite detection

We measured potential naphthalene metabolites with GC/MS to support the respirometry data and to eliminate ambiguity regarding the role of gentisate or catechol in the naphthalene metabolic pathway in strain CJ2. Again, *P. putida* NCIB 9816-4 and *Ralstonia* sp. strain U2 served as controls for the catechol and gentisate pathway, respectively. Table 2.1 shows the detected metabolites from washed cell suspensions that were incubated for 15 minutes after addition of naphthalene in DMF to final concentration of 2 mM.

As expected for the *nah* pathway expressed by *P. putida* NCIB 9816-4 we detected *cis*-1,2-dihydroxydihydronaphthalene, 1,2-dihydroxynaphthalene, salicylaldehyde, salicylate, and catechol. Likewise, as expected for the *nag* pathway expressed by *Ralstonia* sp. strain U2 we detected *cis*-1,2-dihydroxydihydronaphthalene, 1,2-dihydroxynaphthalene, salicylaldehyde, salicylate, and gentisate. As suggested by the respirometry data, the metabolite profile for strain CJ2 is consistent with the genetic similarities between *Ralstonia* sp. strain U2 and strain CJ2. We detected *cis*-1,2-dihydroxydihydronaphthalene, 1,2-dihydroxynaphthalene, salicylaldehyde, salicylate, and gentisate in strain CJ2 cell suspensions. The presence of gentisate and absence of catechol provides clear evidence that strain CJ2 metabolizes naphthalene through the gentisate pathway.

2.4.3 Dioxygenase assays

To provide further evidence for naphthalene metabolism by the gentisate pathway in strain CJ2, dioxygenase assays were conducted with cell-free extract from induced (salicylate grown) and non-induced (pyruvate grown) strain CJ2, *P. putida* NCIB 9816-4, and *Ralstonia* sp. strain U2. Gentisate 1,2-dioxygenase activity was detected in strain *Ralstonia* sp. strain U2 when the cultures were induced by salicylate

Table 2.1.
A survey of metabolites produced by *P. putida* NCIB 9816-4, *Ralstonia* sp. strain U2, and strain CJ2. The experimental values represent the mean and standard deviation of triplicate experiments. 1,2-DHDN=*cis*-1,2-dihydroxydihydronaphthalene, 1,2-DHN=1,2-dihydroxynaphthalene, ND=not detected.

	Naphthalene Metabolites Detected (μg/mg protein)					
Bacteria	1,2-DHDN	1,2-DHN	Salicylaldehyde	Salicylate	Catechol	Gentisate
Pp NCIB 9816-4	2870±1280	1450±600	2.3±2.2	1520±86	3.4±2.7	ND
Ralstonia U2	1260±560	1060±90	4.0±3.3	390±130	ND	2.0±1.3
Strain CJ2	2000±1320	450±300	3.6±1.4	8.7±6.4	ND	2.6±2.2

(0.150 µmol/min/mg protein), but not when grown on pyruvate (0.004 µmol/min/mg protein). Although gentisate dioxygenase activity was not as pronounced in strain CJ2, activity was induced by salicylate (0.032 µmol/min/mg protein) and not by pyruvate (0.003 µmol/min/mg protein). Neither *ortho*- nor *meta*-cleavage of catechol was observed in strain CJ2 or *Ralstonia* sp. strain U2. As expected, *P. putida* NCIB 9816-4, displayed catechol 1,2-dioxygenase activity and no gentisate dioxygenase activity.

2.4.4 Growth inhibition of strain CJ2 by naphthalene

Although strain CJ2 was isolated under naphthalene vapor as a carbon source, a comparison of growth on naphthalene in minimal media (MSB) between strain CJ2, *P. putida* NCIB 9816-4, and *Ralstonia* sp. strain U2 revealed unusual growth characteristics in strain CJ2. Both *P. putida* NCIB 9816-4 and *Ralstonia* sp. strain U2 grew equally well in MSB broth amended with 18 mM pyruvate or saturated with naphthalene crystals (~230 µM). In contrast, strain CJ2 was unable to grow in MSB broth amended with naphthalene crystals (Figure 2.2a), but grew well in MSB broth with 18 mM pyruvate (Figure 2.2b), demonstrating the inhibition of growth is substrate specific. Additionally, the lack of growth in MSB amended with naphthalene was accompanied by the appearance of a light orange color in the medium, indicating the possible accumulation of naphthalene metabolites.

2.4.5 Naphthalene concentration and growth inhibition

To test the effect of naphthalene concentration on growth inhibition, we grew strain CJ2 in MSB broth with 0.1 g XAD7 resin that has been equilibrated with

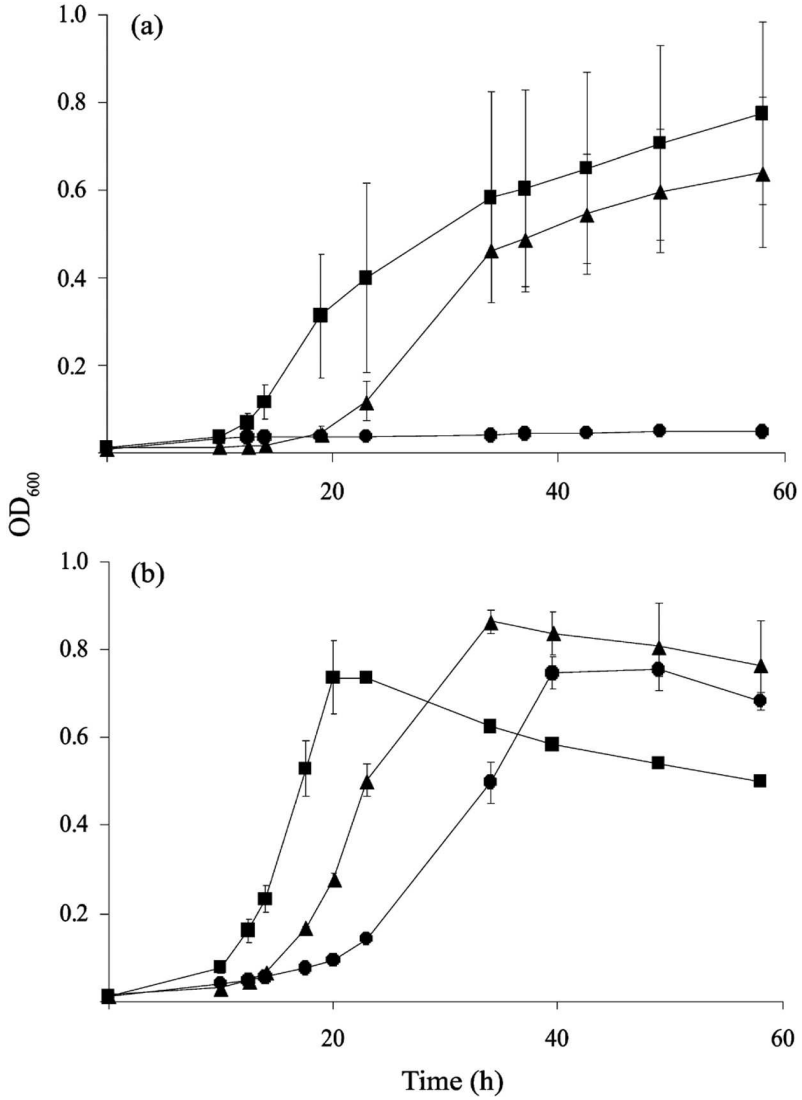

Figure 2.2. Growth of three naphthalene degrading bacteria on mineral salts media with naphthalene crystals (a) or pyruvate (b). Unlike *P. putida* NCIB 9816-4 (■) and *Ralstonia* sp. strain U2 (▲), which grew equally well on pyruvate and naphthalene, strain CJ2 (●) grew only in MSB with pyruvate but not in MSB saturated with naphthalene. The experimental values represent the mean and standard deviation of triplicate experiments.

different masses of naphthalene. This procedure has been shown to buffer the aqueous naphthalene concentration at levels proportional to the added mass (Morasch et al. 2001). Once an equilibrium was established between XAD7 bound naphthalene and aqueous naphthalene, strain CJ2 was inoculated (initial cell density=$1.56x10^6$ CFUs ml^{-1}) into media with initial aqueous concentrations of naphthalene of approximately 23, 40, 55, 78, or 100 μM, as determined by HPLC analysis of aqueous naphthalene in sterile media. Growth was strongly inhibited when the initial naphthalene concentration in the media was higher than 78 μM. However, strain CJ2 grew well when the initial naphthalene concentration of the media was at or below 55 μM (Figure 2.3). This indicates that growth inhibition by naphthalene is concentration dependent, with optimum growth occurring at ~40 μM and inhibitory effects manifest above ~78 μM.

2.4.6 Direct inhibition by naphthalene

The hypotheses for explaining the inhibitory effect of naphthalene on strain CJ2 are: (i) naphthalene itself could be directly inhibitory or toxic when present at high concentrations; (ii) the metabolism of naphthalene could lead to the accumulation of toxic or inhibitory metabolites when a high concentration of naphthalene is available to the cells; or (iii) both naphthalene and its metabolites play a role in growth inhibition.

To determine if naphthalene is directly toxic to strain CJ2, we measured the growth of CJN110, a NagR1 regulatory mutant of CJ2 that is unable to grow on naphthalene (Jeon et al., 2006), in MSB amended with 6 mM glucose in the presence of naphthalene at concentrations that were inhibitory or non-inhibitory to the wild type strain. Partially inhibited growth occurred on glucose in the presence of 23 μM

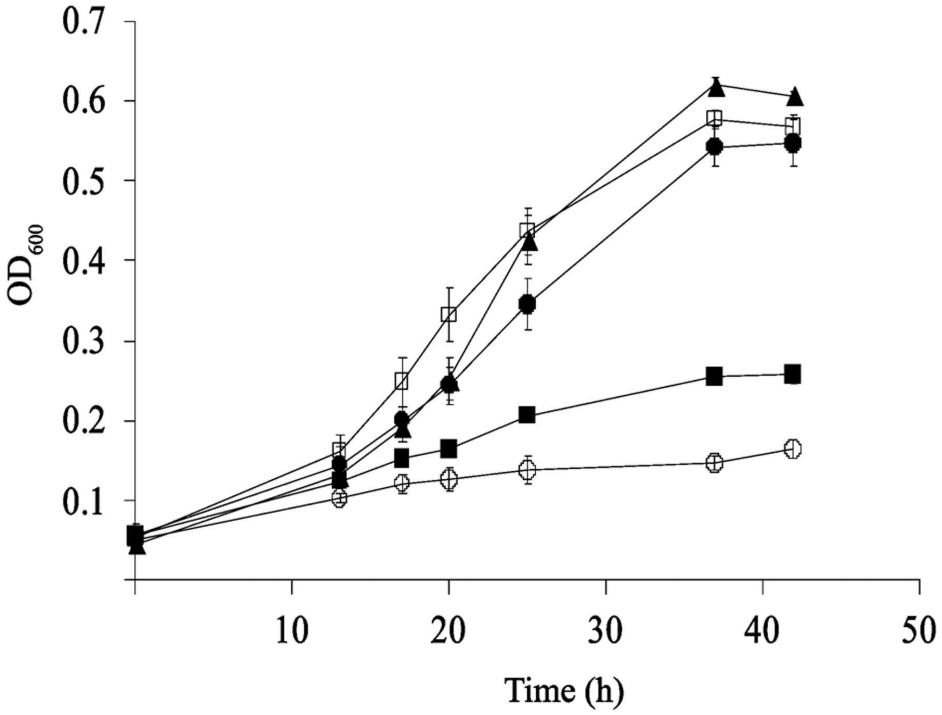

Figure 2.3. Growth of strain CJ2 in MSB media with initial aqueous naphthalene concentrations (□, 23 mM; ▲, 40 mM; ●, 55 mM; ■, 78 mM; ○, 100 mM naphthalene) buffered by XAD-7 resin. Growth was inhibited at concentrations of 78 μM and higher. The experimental values represent the mean and standard deviation of triplicate experiments.

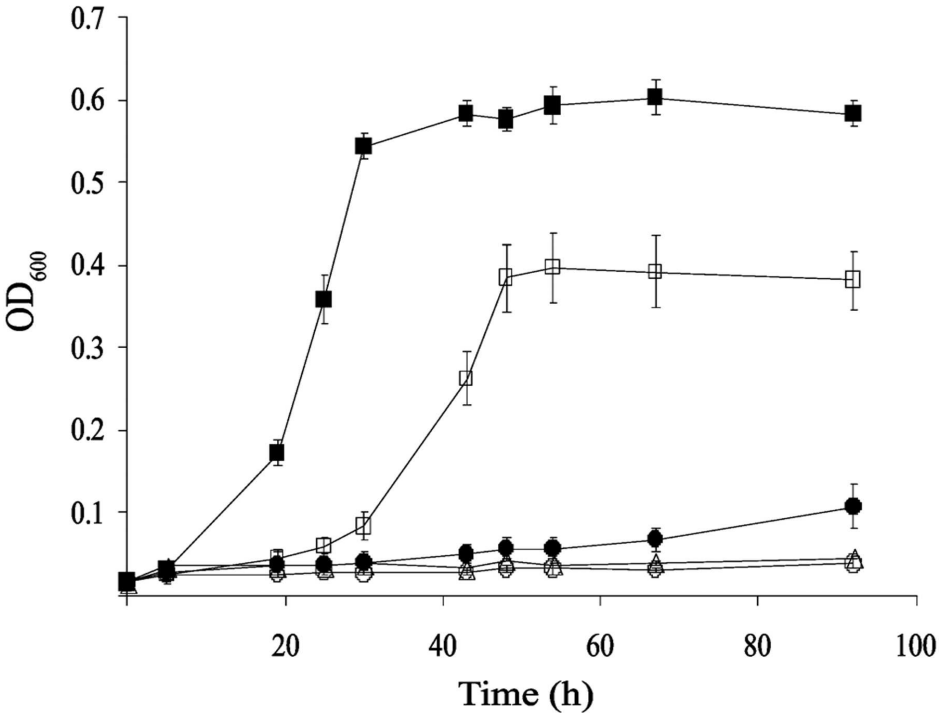

Figure 2.4. Growth of a regulatory mutant of strain CJ2 (strain CJN110, NagR-) in glucose with or without naphthalene. The experimental values represent the mean and standard deviation of triplicate experiments. (■, glucose, no naphthalene; □, glucose + 23 mM naphthalene; ●, glucose + 40 mM naphthalene; ○, glucose + 55 mM naphthalene; Δ, 23 mM naphthalene, no glucose.)

naphthalene. However, at all other naphthalene concentrations growth on glucose was severely inhibited (Figure 2.4). Because strain CJN110 is unable to metabolize naphthalene, inhibition of growth was not due to the production of potentially toxic naphthalene metabolites. Therefore, naphthalene has a direct inhibitory or toxic effect on strain CJN110 derived from strain CJ2.

2.4.7 Evidence for the production of toxic metabolites

In order to explore the relationship between naphthalene concentration and growth inhibition, cell viability and naphthalene concentration were monitored over the course of a growth experiment. Strain CJ2 was inoculated into tubes containing MSB with 6 mM glucose or 0.1 g of XAD7 and initial aqueous concentrations of 31, 47, and 86 μM, respectively.

Growth occurred as expected in the cultures containing 6 or 10 mg naphthalene (Figure 2.5a), with both culture conditions reaching an OD_{600} near 0.68 and cultures containing 10 mg growing slightly slower than those containing 6 mg. However, in tubes containing 12 mg of naphthalene, growth was severely inhibited and did not exceed an OD_{600} of 0.13. The aqueous naphthalene concentration dropped below 10 μM in cultures with 6 mg (Figure 2.5b), suggesting strain CJ2 metabolized naphthalene faster than it was diffusing from the XAD7 resin. In cultures containing 10 or 12 mg there was an initial increase in the aqueous naphthalene concentration, indicating a new equilibrium was established upon the addition of cells. The subsequent decrease in naphthalene concentration shows that even the inhibited cultures were metabolizing naphthalene.

Though growth was inhibited in cultures containing 12 mg naphthalene, viable cells were detected until 34 hours (Figure 2.5c). However, after 34 hours no viable cells were detected, and the loss of viability corresponded with the appearance of the

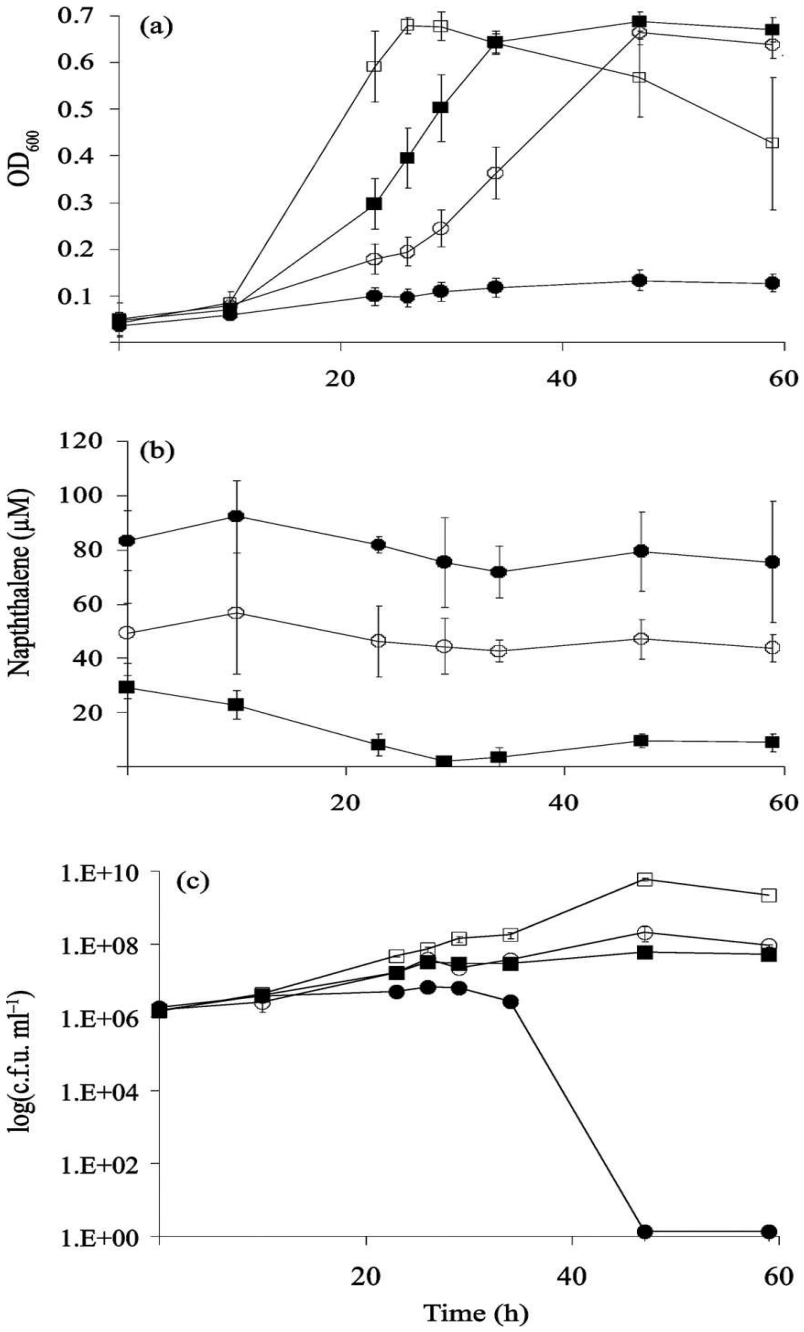

Figure 2.5. The relationship between cell growth, aqueous naphthalene concentration, and cell viability. Strain CJ2 was inoculated into MSB with glucose (□) or 0.1 g XAD7 and 6 (■), 10 (○), or 12 (●) mg naphthalene. Optical density (a), aqueous naphthalene concentration (b), and viable cells (c) were monitored. Inoculum density was held constant at 9.8×10^6 CFUs.

light orange color in the media, which appeared between 34 and 47 hours. These results suggest that not only does naphthalene have an inhibitory effect, but also naphthalene metabolism by inhibited cells results in the accumulation of a naphthalene metabolite that is toxic to the cells. It should be noted, that even though there was no visible color accumulation prior to 34 hours it is possible that a low level of the toxic metabolite had accumulated and was responsible for growth inhibition.

2.4.8 Analysis of toxic accumulated metabolites

Previous reports have suggested that the accumulation of an orange metabolite in naphthalene metabolizing cultures results from the abiotic oxidative transformation of 1,2-dihydroxynaphthalene to 1,2-naphthoquinone (Auger et al., 1995; Davies and Evans, 1964; Murphy and Stone, 1955). Spectrophotometric scans (240 to 400 nm) of 1,2-naphthoquinone standards and colored media from naphthalene-inhibited cultures of strain CJ2 suggested that 1,2-naphthoquinone was present at concentrations between 50 and 100 μM (data not shown). Therefore, we used HPLC to compare 1,2-naphthoquinone standards (dissolved in MSB) with media from strain CJ2 cultures that were either successfully grown on naphthalene or cultures that were inhibited by naphthalene and had accumulated orange-colored metabolites.

Analysis of 1,2-naphthoquinone dissolved in MSB revealed that it too was unstable in aqueous media . When 50 μM 1,2-naphthoquinone was analyzed by HPLC shortly after dissolution in MSB, there was one major peak with a retention time of 20 minutes (peak II in Figure 2.6a). A probable oxidation product with a retention time of 24 minutes (peak III in Figure 2.6a) also appeared. However, after 50 μM 1,2-naphthoquinone was incubated for 48 hours in sterile MSB peak II was no longer detected, while new peaks (I and IV) with retention times of 15 and 26 min (respectively) were abiotically produced (Figure 2.6b). Analysis of the colored medium from a naphthalene-inhibited culture detected three peaks: one peak (II)

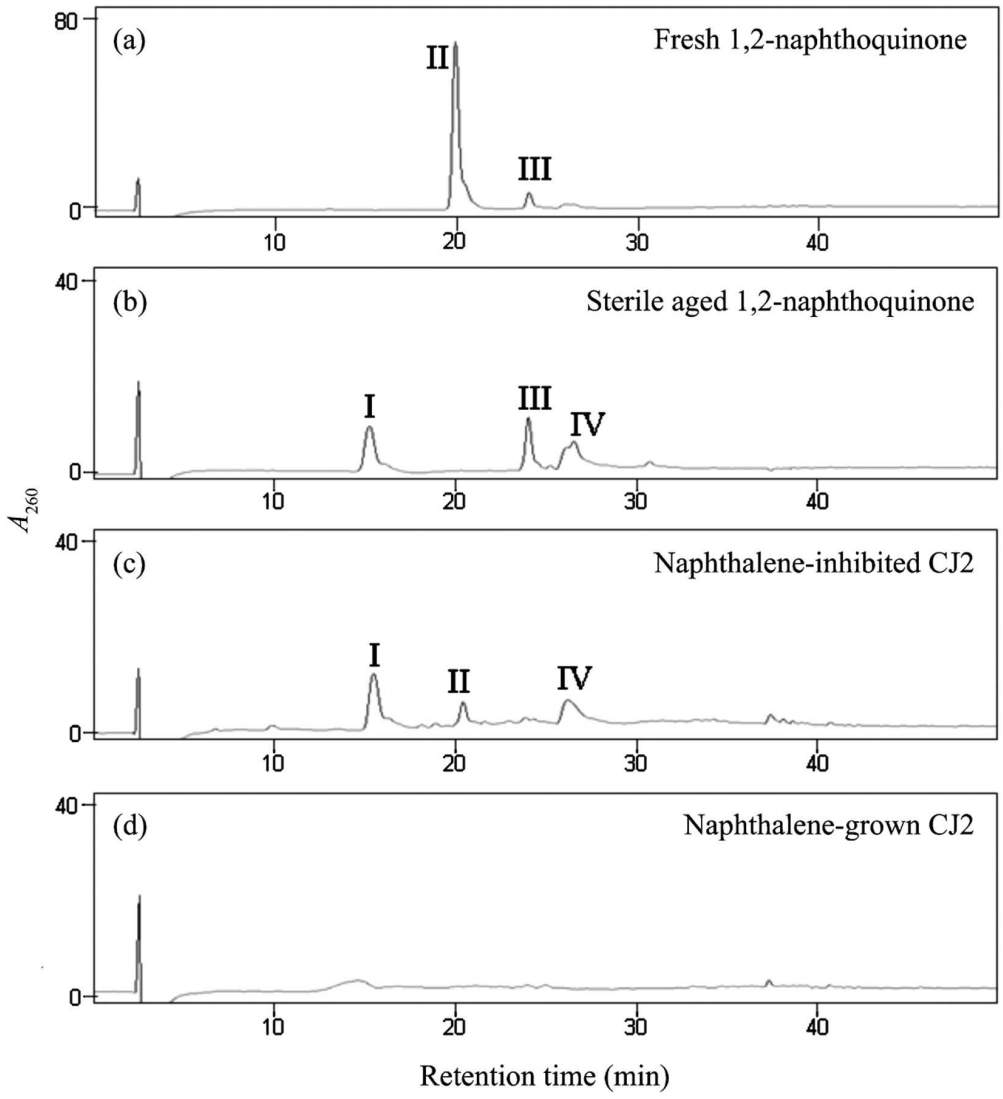

Figure 2.6. Analysis of naphthalene metabolites by HPLC. Chromatograms of 50 μM 1,2-naphthoquinone freshly dissolved in MSB media (a), 50 μM 1,2-naphthoquinone aged in sterile MSB media for 48 hours (b), culture medium from naphthalene-inhibited strain CJ2 (c), and culture medium from naphthalene-grown strain CJ2 (d). Note that the vertical scale in panel A is twice that of the other panels.

corresponds with the primary peak of freshly dissolved 1,2-naphthoquinone, while the other two peaks, I and IV, correspond with daughter products of aged 1,2-naphthoquinone (Figure 2.6c). No peaks of putative inhibitory metabolites were present in the uncolored medium from cultures of CJ2 that successfully grew on naphthalene (Figure 2.6d). Chemical instability, ineffective derivatization procedures, and lack of authentic standards prevented GC/MS identification of the putative toxic compounds eluting as peaks I and IV in the inhibited culture of strain CJ2 (Figure 2.6c). Support for 1,2-naphthoquinone's (peak II) contribution to toxicity was obtained in assays showing that growth of strain CJ2 was completely inhibited in MSB-glucose medium when 1,2-naphthoquinone was ~50 µM (data not shown).

2.5 Discussion

The isolation of strain CJ2 has provided a unique opportunity to investigate the genetics and physiology of a bacterium that is linked to the in situ biodegradation of naphthalene in contaminated sediment. Sequencing of the naphthalene catabolic genes revealed a novel arrangement of structural and regulatory genes in strain CJ2 (Jeon et al., 2006). In this study, we gained insight into the physiology of naphthalene metabolism in strain CJ2 by comparing it to two archetypal naphthalene degrading bacteria. Our data from respirometry, metabolite detection by GC/MS, and enzyme assays showed that strain CJ2 metabolizes naphthalene via the gentisate pathway. Growth assays revealed that strain CJ2 cannot grow on naphthalene at concentrations above 78 µM, and that metabolic imbalances may lead to inhibition and toxicity.

Bacteria that metabolize aromatic hydrocarbons face the challenge of acquiring carbon and energy from compounds that are potentially toxic (Ramos et al., 2002; Sikkema et al., 1995). The inability of potential biodegrading populations to tolerate aromatic hydrocarbon toxicity may contribute to the persistence of pollutants in the

environment. The mechanisms of toxicity are generally believed to be disruption of biological membranes (Sikkema et al., 1995) and the production of toxic metabolites (e.g., Park et al., 2004). The lipophilic character of aromatic hydrocarbons can alter membrane fluidity, permeablize the membrane, and cause swelling of the lipid bilayer. Alteration of membrane structure can disrupt energy transduction and the activity of membrane associated proteins (Sikkema et al., 1995). Additionally, metabolites of aromatic compounds, such as catechols and quinones, can be more toxic than the parent compound due to an increase in solubility, production of reactive oxygen species, or adduct formation with DNA and proteins (Penning et al., 1999; Schweigert et al., 2001).

In the present investigation we have shown that *Polaromonas naphthalenivorans* CJ2 is susceptible to both (i) direct naphthalene inhibition and (ii) formation of toxic intermediate metabolites. Naphthalene inhibited the growth of strain CJ2 at concentrations 55 μM (Figure 2.4), which is well below naphthalene's aqueous saturation point (230 μM). Naphthalene has been reported to be toxic to the archetypal naphthalene degraders, *P. putida* G7 and *P. putida* NCIB 9816-4, but only under nitrogen- or oxygen-limiting conditions (Ahn et al., 1998) or during incubation in soil amended with a high concentration (0.2% w/v) of naphthalene crystals (Park et al., 2004), respectively. We found that inhibition of strain CJ2 by naphthalene was independent of metabolism, and, based on the study of Sikkema et al. (1994), we speculate that the mechanisms of direct inhibition are likely to be related to impaired membrane function.

In addition to growth inhibition, naphthalene metabolism by strain CJ2 at inhibitory concentrations resulted in the accumulation of toxic oxidation products derived from 1,2-naphthoquinone, which resulted in a complete loss of viability (Figure 2.6c). Davies and Evans (1964) showed that a 25 μM solution of 1,2-

dihydroxynaphthalene is converted by nonenzymatic oxidation to 1,2-naphthoquinone at a rate of approximately 20% per minute at pH 6.5. 1,2-Naphthoquinone has been reported to accumulate and inhibit both growth and naphthalene metabolism when ferrous and magnesium salts are omitted from growth media (Murphy and Stone, 1955) or when naphthalene bioavailability is increased by surfactant addition (Auger et al., 1995). Our analysis by HPLC suggests that 1,2-naphthoquinone (presumably produced abiotically from 1,2-dihydroxynaphthalene) and two abiotic transformation products of 1,2-naphthoquinone accumulate when strain CJ2 is exposed to inhibitory concentrations of naphthalene.

Strain CJ2 was shown to metabolize naphthalene in situ by stable isotope probing, which suggests that strain CJ2 is an active member of the naphthalene-degrading population in the sediment (Jeon et al., 2003). Strain CJ2 has evolved, apparently successfully, to occupy a niche as naphthalene degrader even though naphthalene has a strong inhibitory effect and subsaturation levels of naphthalene can result in toxic metabolite accumulation. It is possible that strain CJ2 never experienced selective pressure to develop greater tolerance to naphthalene because adsorption to soil and metabolism of naphthalene by other bacteria kept naphthalene concentrations well below inhibitory levels. If this is the case, strain CJ2 may not have evolved adaptation mechanisms frequently associated with tolerance to aromatic compounds such as *cis*-to-*trans* isomerization of unsaturated fatty acids and efflux pumps (Ramos et al., 2002). Furthermore, the accumulation of 1,2-naphthoquinone-related oxidation products might be due to unrealistic naphthalene concentrations imposed in laboratory incubations combined with the slow growth of strain CJ2. An enzyme in the naphthalene catabolic pathway may have a low specific activity that is only problematic when the concentration of naphthalene exceeds a threshold. Another possibility is that, if strain CJ2 is adapted to low naphthalene bioavailability in soil,

the bacterium has evolved to accumulate as much naphthalene as possible, whether through active uptake or through modifications of the cell membrane and envelope. Thus, when presented with naphthalene at the concentrations used in this study, strain CJ2 accumulated naphthalene to inhibitory and toxic quantities.

This study also showed that strain CJ2 metabolizes naphthalene via gentisate using the *nag*-type pathway found in *Ralstonia* sp. strain U2. Metabolism of aromatics via gentisate has been studied less extensively than metabolism via catechol, and it is not clear whether one pathway has an advantage over the other. A study investigating bacteria that metabolize 3-chlorobenzoate suggested that microorganisms using the gentisate pathway have lower maximum specific growth rates and lower apparent half-saturation constants for oxygen and 3-chlorobenzoate; thus, they may be well adapted to substrate- and/or oxygen-limited conditions (Krooneman et al., 2000). If these same characteristics are applicable to strain CJ2, they could help explain why strain CJ2 was successful in naphthalene-contaminated sediments despite being sensitive to inhibitory effects of naphthalene.

3. FIELD-BASED STABLE ISOTOPE PROBING REVEALS THE IDENTITIES OF BENZOIC ACID-METABOLIZING MICROORGANISMS AND THEIR IN SITU GROWTH IN AGRICULTURAL SOIL.

3.1 Abstract

We used a combination of Stable Isotope Probing (SIP), GC/MS-based respiration, isolation/cultivation, and quantitative PCR procedures to discover the identity and in situ growth of soil microorganisms that metabolize benzoic acid. We added [^{13}C] or [^{12}C]benzoic acid (100 µg) once, four times, or five times at 2-day intervals to agricultural field plots. After monitoring $^{13}CO_2$ evolution from the benzoic acid-dosed soil, field soils were harvested and used for nucleic acid extraction and for cultivation of benzoate-degrading bacteria. Exposure of soil to benzoate increased the number of culturable benzoate degraders compared to unamended soil, and exposure to benzoate shifted the dominant culturable benzoate degraders from *Pseudomonas* species to *Burkholderia* species. Isopycnic separation of heavy [^{13}C]DNA from the unlabeled fraction allowed T-RFLP analyses to confirm that distinct 16S rRNA genes were localized in the heavy fraction. Phylogenetic analysis of sequenced 16S rRNA genes revealed a predominance (15 of 58 clones) of *Burkholderia* species in the heavy fraction. Isolate *Burkholderia sp*. strain EBA09 shared 99.5% 16S rRNA sequence similarity with a group of clones representing the dominant RFLP pattern, and the T-RFLP fragment for strain EBA09 and a clone from that cluster matched the fragment enriched in the [^{13}C]DNA fraction. Growth of the population represented by EBA09 during the field-dosing experiment was demonstrated using MPN-PCR and primers targeting EBA09 and closely related *Burkholderia hospita* species. Thus, the target population identified by SIP not only actively metabolized benzoic acid, but reproduced in the field upon the addition of the substrate.

3.2 Introduction

Soil environments are commonly carbon limited (Alden et al., 2001), and carbon input through decomposition, industrial spills, or other disturbance can lead to an increase in microbial activity (Nyman, 1999). In order to understand population dynamics of bacteria in soils, it is necessary to understand which organisms respond to increases in carbon availability and how the population changes. Investigations using stable isotope probing (SIP) are particularly suited to identifying bacteria that metabolize a specific carbon compound, because cellular biomarkers used to identify organisms become ^{13}C-labeled when organisms metabolize and incorporate ^{13}C from the labeled substrate (Boschker et al., 1998; Buckley et al., 2006; Leigh et al., 2007; Madsen, 2006; Manefield et al., 2002; Neufeld et al., 2007; Radajewski et al., 2000). The growth of bacteria identified by DNA-SIP can be inferred, because, at minimum, two generations are required for DNA to be fully labeled with ^{13}C due to semi-conservative DNA replication. Researchers can use phylogenetic analysis of labeled sequences, along with chemical knowledge of both the labeled compound and the experimental environment, to gain further insight into the physiology of the metabolically active population. Furthermore, the successful isolation of a strain representative of an active population identified by SIP allows for more detailed genetic and physiological investigation (Jeon et al., 2003; Jeon et al., 2006; Kasai et al., 2006; Liou et al., 2008; Pumphrey and Madsen, 2007).

Benzoic acid is a naturally occurring aromatic acid that enters soil environments through plant decomposition and root exudates. Soil with growing or decomposing quackgrass contained approximately 30 or 80 nmol benzoic acid g^{-1} dry soil, respectively (Baziramakenga et al., 1995). Although a diverse number of bacteria are known to metabolize benzoic acid (Biodegradative Strain Database,

http://bsd.cme.msu.edu/jsp/InfoController.jsp?object=Chemical&id=C_benzo8), to our knowledge there are no in situ studies identifying populations that metabolize benzoic acid in soil. Aerobic metabolism of benzoic acid occurs through either dihydroxylation of benzoate by benzoate 1,2-dioxygenase (BenABC) with subsequent ortho cleavage of catechol by catechol 1,2-dioxygenase (Harwood and Parales, 1996) or through conversion to benzoyl-CoA with subsequent ring cleavage (Gescher et al., 2002). Benzoic acid is also a common intermediate metabolite in metabolic pathways for aromatic pollutants such as benzonitrile, biphenyl, and toluene. The extensively studied biphenyl degrader, *Burkholderia xenovorans* LB400, encodes both the catechol *ortho* cleavage pathway as well as the benzoyl-coenzyme A pathway (Denef et al., 2006). In *B. xenovorans* LB400, the benzoate dioxygenase pathway converted benzoate more rapidly than metabolism via coenzyme A activation and resulted in faster growth (Denef et al., 2006).

In this study, we investigated the dynamics of a benzoic acid metabolizing population in an agricultural field during multiple amendments of benzoic acid. To discover the identity of microorganisms that metabolize benzoic acid and measure their in situ growth in soil we employed a combination of SIP, GC/MS-based respiration, isolation/cultivation. Furthermore, to confirm the growth of the active population identified by SIP, we used MPN-PCR to quantify the population in situ.

3.3 Materials and Methods

3.3.1 Bacterial strains

Burkholderia xenovorans LB400 was originally isolated from a site contaminated with polychlorinated biphenyls (Bedard et al., 1986), and was a gift from G. Zylstra, Rutgers University. Additional strains, isolated during this study, were used to verify the specificity of PCR primers used to detect *Burkholderia* strain

EBA09 included *Burkholderia* spp. EBA01, EBA02, EBA03, EBA04, EBA05, EBA07, EBA11, EBA14, EBA15, and EBA16, *Pseudomonas* sp. EBA13, *Arthrobacter* sp. EBA06, *and Cupriavidus* sp. EBA17.

3.3.2 Soil field treatments for respiration, stable isotope probing, cultivation, and population monitoring

The application of SIP in the field is based on methods developed by Padmanaban et al. (2003) and DeRito et al. (2005). A small field plot (~ 1 m^2) of Collamer silt loam at the Cornell University Agricultural Experiment Station, Ithaca, NY was leveled and cleared of vegetation several days prior to the experiment. A grid of dosing points (on 15-cm centers marked by screw-cap canning jar bands) was laid out to accommodate all treatments in triplicate. For the SIP experiment, soil in the field was dosed four times with 100 μg of benzoic acid in 50 μl H_2O every 48 hours and a fifth time 24 hours after the fourth dose. Three treatments varied in the amount of [^{13}C]benzoic acid added to the soil. For the first treatment, soils received five doses of [^{12}C]benzoic acid, the second treatment received four doses of [^{12}C]benzoic acid with a final dose of [^{13}C]benzoic acid, and the third treatment received five doses of [^{13}C]benzoic acid. Immediately following the final dose, septum-covered chambers were placed over the treated soils to allow headspace analysis. In parallel with the respiration/SIP procedures, additional soil-plot treatments were dosed with unlabeled benzoic acid or left unamended. These soils were used in experiments utilizing cultivation and MPN-PCR techniques. A table was placed over the plot (0.8 m high) to protect the experiment from rain and direct exposure to sunlight.

3.3.3 GC/MS analysis of CO_2

Analysis of CO_2 respired from soil was conducted as previously described (DeRito et al., 2005). A Hewlett-Packard HP5890 gas chromatograph (Wilmington, DE) equipped with an HP5971A mass-selective detector was used for the respiration analyses. With high-purity helium as the carrier gas, a Hewlett-Packard Pora Plot Q column (25 m by 0.32 mm, 10 um film thickness) was used to separate carbon dioxide from other gaseous components. The detector was operated at an electron energy of 70 eV and a detector voltage of 2,000 V. The ion source pressure was maintained at 1×10^{-5} torr. A splitless injection was used, and the GC oven was isothermal at 60°C. CO_2 eluted at 1.18 min. Single-ion monitoring allowed simultaneous quantification of both $^{12}CO_2$ (m/z = 44) and $^{13}CO_2$ (m/z = 45). The concentration of $^{13}CO_2$ was quantified using calibration curves prepared using external standards (Scott Specialty Gases, Plumsteadville, PA). The net $^{13}CO_2$ produced from metabolism of the [^{13}C]benzoic acid was calculated by subtracting background $^{13}CO_2$ produced by the native microbial community from soil organic matter. Background $^{13}CO_2$ was inferred from direct measurement of $^{12}CO_2$ adjusted to the known fixed ratio of ^{12}C to ^{13}C in naturally occurring carbon (1.11%). This ratio was confirmed analytically. Net $^{13}CO_2$ values from replicate chambers were averaged at each time point.

3.3.4 DNA extraction

DNA was extracted from soil according to the method of Griffiths et al. (2000). Extractions were performed by combining 0.5 g (wet weight) of soil with 0.5 ml of hexadecyltrimethylammonium bromide (CTAB) extraction buffer and 0.5 ml of phenol-chloroform-isoamyl alcohol (25:24:1, pH=8.0) in Lysing Matrix E tubes (MO BIO Laboratories, Carlsbad, CA). CTAB extraction buffer is prepared by mixing equal volumes of 10% (wt/vol) CTAB in 0.7 M NaCl with 240 mM potassium

phosphate buffer, pH 8.0. Samples were homogenized with a bead-beater (BioSpec Products, Bartlesville, OK) for 30 s, and the aqueous phase was separated by centrifugation (16,000 *g*) for 5 min at 4°C. The aqueous phase was moved to a 1.5 ml tube and phenol was removed by mixing an equal volume of chloroform-isoamyl alcohol (24:1) followed by centrifugation (16,000 *g*) for 5 min at 4°C. DNA was precipitated from the aqueous layer with 2 volumes of 30% (wt/vol) polyethylene glycol 6000 for 2 hours at room temperature. The precipitated DNA was pelleted by centrifugation (16,000 g), washed with ice cold 70% ethanol, and air dried prior to resuspension in TE (pH=8.0).

3.3.5 Isopycnic centrifugation and gradient fractionation

Density gradient ultracentrifugation and subsequent fractionation were performed according to the method of Lueders et al. (2004). 100 ng of extracted DNA were added to a CsCl solution in TE buffer (pH=8.0) to a final volume of 5.5 ml and an average density of 1.729 g ml^{-1}. The ultracentrifugation tubes were sealed and centrifuged at 146000 g_{av} and 20°C for at least 60 hours. The centrifuged gradients were fractionated from bottom to top into ~300 µl fractions by displacing the gradient with sterile water from the top of the tube with a HPLC pump. The density of each fraction was determined by measuring the refractive index of a subsample using an AR200 digital refractometer (Leica Microsystems). DNA was precipitated from the CsCl fractions with polyethylene glycol as above, and precipitated DNA was washed with 70% ethanol and suspended in 35 µl TE. Primarily two fractions (1.70-1.71 and 1.747 g ml^{-1}) were analyzed.

3.3.6 T-RFLP

T-RFLP protocols and analyses of the fragments were performed as described by Cadillo-Quiroz et al. (2006). FAM-labeled amplicons were generated from community DNA from 1 µl of selected gradient fractions using the FAM-27f (5'-AGAGTTTGATCCTGGCTCAG), which was fluorescently labeled on the 5' end with Carboxifluorescein, and 1492r (5'-TACGGYTACCTTGTTACGACTT) primers (Integrated DNA Technologies, USA). The labeled 16S rRNA genes were generetated using Thermo-Start® PCR Master Mix (ABgene, United Kingdom), with 0.5 µM of each primer and 1.5 mM $MgCl_2$. The following PCR conditions were used: 94°C for 15 min; 34 cycles consisting of 94°C for 30s, 55°C for 1 min, 72°C for 1 min; followed by 72°C for 5 min. Amplicons were purified (Qiagen PCR Purification kit), and 100 ng of pooled, triplicate PCR reactions were digested with 5 units of *MspI* (New England Biolabs, USA) for 3 h at 37°C. Purified digested products were concentrated in a vacuum centrifuge, and then resuspended with a mix of Hi Di-Formamide (Applied Biosystems, USA) and Gene Scan 500-Liz marker (12 µl ml−1; Applied Biosystems, USA). Fragments were resolved with an Applied BioSystems 3730xl DNA Analyser (Bio Resources Center, Cornell University). Terminal restriction fragment length and peak height were determined using Peak Scanner™ (Applied Biosystems).

3.3.7 PCR cloning, restriction digestion, and sequencing

PCR amplification of 16S rRNA genes from gradient fractions using universal eubacterial primers 27f and 1492r was performed as described previously (Bakermans et al., 2002; DeRito et al., 2005). The product was ligated into the vector pCR2.1 (TA cloning; Invitrogen) by following the manufacturer's recommended protocol. Following transformation of plasmids into host cells and blue/white screening,

colonies with inserts were verified by PCR with vector-specific primers (5'-GTAACGGCCGCCAGTGTGCT and 5'-CAGTGTGATGGATATCTGCA) that flanked the cloning region. Amplicons were digested with *Hae*III and *Hha*I, and RFLP patterns were analyzed on 3% MetaPhore agarose gels (BioWhittaker; Molecular Applications, Rockland, Maine) with a 100-bp ladder (Promega) as a marker. Clones that were selected for sequencing were grown overnight in 5 ml of Luria-Bertani broth with kanamycin (50 μg/ml), pelleted, and plasmids were purified (QiaPrep spin miniprep kit; QIAGEN, Santa Clarita, Calif.).

Sequencing (Cornell University DNA Sequencing Facility) was conducted with four primers: M13 forward (5'-TGTAAAACGACGGCCAGT-3'), M13 reverse (5'-AACAGCTATGACCATG-3'), 531 reverse (5'-TACCGCGGCTGCTGGCAC-3'), and 533 forward (5'-GTGCCAGCMGCCGCGG-3'). Raw sequence data were assembled into full-length sequences using the program SEQMAN II (DNASTAR, Inc.). After assembly, the consensus sequence was verified manually by referring to the corresponding ABI chromatograms of the sequencing reactions, and Bellerophon (Huber et al., 2004) was used to check for chimeras. Phylogenetic relationships were discerned by the neighbor-joining method using the computational tools of Lasergene (DNASTAR, Madison, WI) and ClustalX (Thompson et al., 1997).

3.3.8 Isolation of benzoate-metabolizing bacteria

Benzoate metabolizing bacteria were isolated from soils that were left unamended or treated with benzoic acid as in the field experiment. For both treatments, 1 g soil was serially diluted in phosphate-buffered solution, spread plated onto MSB agar plates (Stanier et al., 1966) with 0.01% (0.7 mM) sodium benzoate in duplicate, and incubated at room temperature. For each treatment, 30 individual colonies from the two highest dilutions were randomly selected and checked for purity

by streaking on R2A agar plates. Confirmed pure cultures were grown again on MSB agar with 0.01% benzoate, and isolates that maintained the benzoate-metabolizing phenotype were stored at -80°C for later characterization of the cultures. Eleven genetically distinct isolates were distinguished by 16S rRNA gene fingerprinting as described above.

3.3.9 Amplification of the benzoate 1,2-dioxygenase large subunit gene in isolated bacteria

A 540-bp fragment of the benzoate 1,2-dioxygenase alpha subunit gene was amplified from selected isolates using primers BAf1 (5'-GCRCARGAYAGCCAGATTCCC) and BAr2 (5'-GGTGGCMGCYTAGTTCCAGTG), which were designed from the homologous regions of *benA* of *Acinetobacter baylyi* ADP1 and *xylX* of *Pseudomonas putida* TOL plasmid pWW0 (Francisco et al., 2001; Harayama et al., 1991; Neidle et al., 1991). The *benA* fragment was amplified with the following program: 95°C for 15 min with 5 initial cycles of 94°C for 30 sec, 60°C for 30 sec (-1° per cycle), and 70°C for 45 sec, followed by 35 cycles of 95°C for 30 sec, 54° for 45 sec, 70°C for 45 sec, and a 1 min extension at 68°C. The resulting amplicons were sequenced directly using the PCR primers.

3.3.10 MPN-PCR

Quantification of bacteria identified by SIP by MPN-PCR was performed as previously described (Fredslund et al., 2001). In parallel with the field SIP experiment, three sets of triplicate soils were dosed with 100 µg benzoic acid in 50 µl water every 48 hours. Triplicate (0.5 g) soil samples were collected and stored at -80°C at times 0 (untreated), 48 (1 dose), 144 (3 doses), and 192 hours (5 doses). DNA

was extracted as described above from each soil sample, and the primer Burkhospita1F (5'-AAAGGCCTCGCGCTCAAG) was designed using the 16S rRNA gene sequence from isolate EBA09 and cloned 16S rRNA sequences D603, D617, and D638 (generated in this study) using Primrose software (Ashelford et al., 2002). A 180 bp amplicon was generated when Burkhospita1F was used in combination with the universal eubacterial primer 342r (5'-CTGCTGCSYCCCGTAG). Tenfold dilution series of the extracted DNA were made and 1 µl was used as template in a 20 µl PCR with the following program: 15 min at 95°C; 32 cycles of 30 sec at 95°C, 30 sec at 60°C, 45 sec at 70°C; 4 min at 70°C; and final hold at 4°C. The second highest dilution to produce the target 180-bp amplicon was used as a starting point for triplicate 3-fold dilution series. The freeware MPN calculator (VB6 version; Michael Curiale [http://www.i2workout.com/mcuriale/mpn/index.html]) was used to calculate the MPN abundance of populations related to strain EBA09 in soil samples dosed with benzoate.

3.3.11 Nucleotide sequence accession numbers

The nucleotide sequence data reported here have been submitted to GenBank under accession no. EU677388 to EU677420.

3.4 Results

3.4.1 Benzoic acid metabolism at a field site

In order to investigate the dynamics of the benzoic acid-metabolizing community in the field agricultural study site, we carried out a dosing regime based on that established by DeRito et al. (2005). For the first treatment, soils received five doses of [^{12}C]benzoic acid, the second treatment received four doses of [^{12}C]benzoic acid with a final dose of [^{13}C]benzoic acid, and the third treatment received five doses

of [^{13}C]benzoic acid. Monitoring of benzoic acid metabolism in the field was determined by GC/MS analysis of $^{13}CO_2$ respired from the soil after the final dose (Figure 3.1). In soils exposed to [^{13}C]benzoic acid, a net increase in respired $^{13}CO_2$ above background levels was observed, whereas no increase was seen in soils receiving [^{12}C]benzoic acid. The $^{13}CO_2$ respired from soils receiving a single dose of [^{13}C]benzoic acid amounted to 17% of the labeled carbon added to the soil. Respired $^{13}CO_2$ was nearly identical between soils that received 5 doses of ^{13}[C]benzoic acid and soils that received 4 doses of ^{12}[C]benzoic acid with a final dose of ^{13}[C]benzoic acid. This suggested two things: (i) that benzoic acid was metabolized quickly-- little or no residual ^{13}[C]benzoic acid remained in soils receiving prior doses: and (ii) the ^{13}C-labeled biomass (produced via assimilation of early doses of ^{13}[C]benzoic acid) was relatively stable and not subject to further metabolism during the experiment.

3.4.2 Community profiles of density-resolved DNA

Triplicate soil samples from each of the three field treatment were collected and pooled. DNA was extracted, and the [^{13}C]DNA was separated from [^{12}C]DNA by isopycnic centrifugation. We used T-RFLP to compare community profiles from heavy (1.747 g ml^{-1}) and light (1.70-1.71 g ml^{-1}) fractions taken from the CsCl gradient of each field treatment (Figure 3.2). Figures 3.2A and 3.2B show results of our positive- and negative-control treatments, respectively, that received unlabeled benzoate. As expected, the light fraction (Figure 3.2A) featured a complex T-RFLP pattern typical of heterogenous populations in a soil community and the heavy fraction (Figure 3.2B) that was virtually free of signals (except for a spurious peak at 491 bp that was also present in our reagent blank). All other T-RFLP patterns should be interpreted relative to Figure 3.2B and according to contrasts between heavy and light fractions in a given treatment.

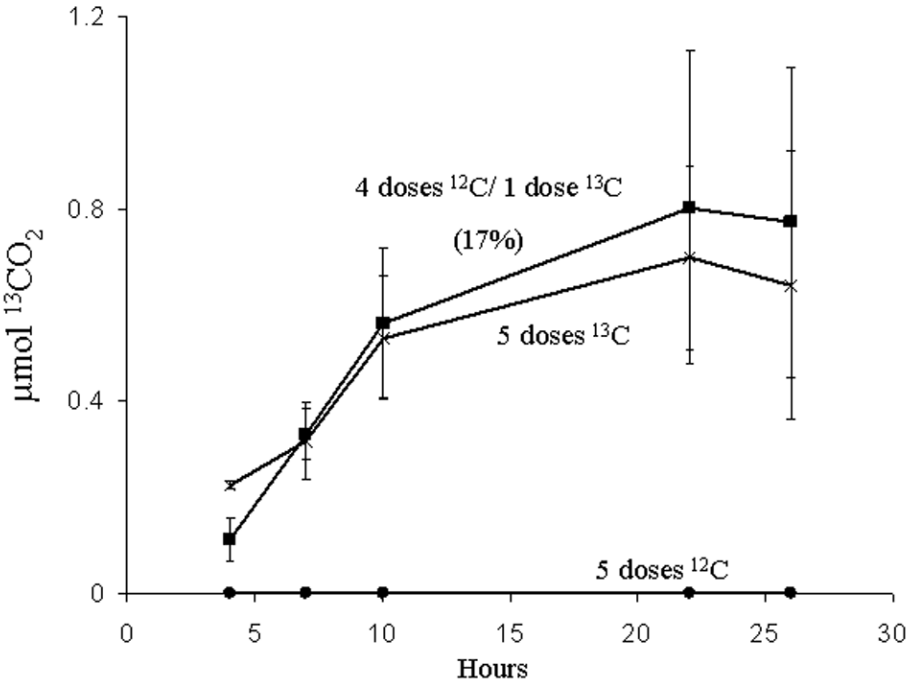

Figure 3.1. Confirmation of [^{13}C]benzoic acid metabolism measured as net $^{13}CO_2$ respiration from the agricultural field study site. $^{13}CO_2$ was produced from soils receiving 5 doses of 100 µg [^{12}C]benzoic acid (●), 4 doses of 100 µg [^{12}C]benzoic acid and a final 100 µg dose of [^{13}C]benzoic acid (■), or 5 doses of 100 µg [^{13}C]benzoic acid (×). The percentage in parentheses shows the proportion of the total added [^{13}C]carbon recovered as $^{13}CO_2$ from the treatment receiving a single dose of [^{13}C]benzoic acid. Experimental values represent the mean and standard deviation of triplicate samples.

For the three treatments, the distribution of T-RFLP signals within a gradient was consistent with type of benzoic acid label (^{13}C or ^{12}C) the treatment received. In contrast to the treatment receiving only [^{12}C]benzoic acid (discussed above), T-RFLP signals in the DNA from soil receiving 5 doses of [^{13}C]benzoic acid were enhanced in the heavy fraction (Figure 3.2F) compared to the light fraction of the gradient (Figure 3.2E). The peak corresponding to a fragment length of 139 bp, in particular, showed enrichment as the density of the gradient increased (Figure 3.2F). This suggested that the population represented by the 139 bp fragment was metabolizing the benzoic acid and fully incorporated the ^{13}C-label into its biomass. Three peaks, corresponding to fragment sizes of 128, 139, and 149 bp were shared by all treatments, which suggests that one or all of the organisms represented by these fragments were members of the benzoic acid metabolizing community.

3.4.3 Identifying active benzoic acid metabolizing bacteria

We pursued two methods to investigate the identities of active benzoic acid-metabolizing bacteria: cultivation and cloning plus sequencing 16S rRNA genes. Prior to cultivating benzoic acid metabolizing isolates, soil was either dosed with benzoic acid as in the SIP experiment or left unamended. Plate counts showed that culturable benzoic acid-metabolizing isolates from the unamended soil were present at $3.9x10^5$ CFU g^{-1} soil, while successive benzoate additions increased the number of benzoic acid degraders nearly 10-fold to $3.3x10^6$ CFU g^{-1} soil. Comparison of RFLP patterns generated from 16S rRNA gene amplicons digested with *Hae*III and *Hha*I and subsequent 16S rRNA gene sequencing revealed that 16 of 24 selected isolates from the highest dilutions of the unamended soil were *Pseudomonas* species. However, when the soil was exposed to benzoic acid, 14 of 17 isolates from the highest dilutions were *Burkholderia* species.

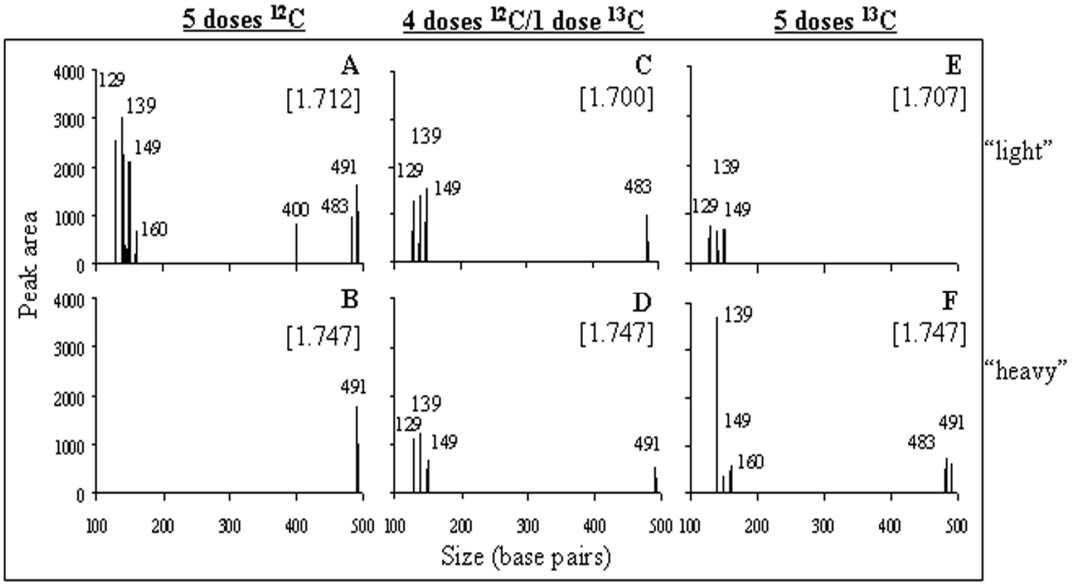

Figure 3.2 Microbial community composition represented by T-RFLP profiles from three fractions collected from CsCl gradients containing DNA extracted from soils receiving (A) 5 doses of 100 µg [^{12}C]benzoic acid, (C) 4 doses of 100 µg [^{12}C]benzoic acid and a final 100 µg dose of [^{13}C]benzoic acid, or (E) 5 doses of 100 µg [^{13}C]benzoic acid. The buoyant density (g ml^{-1}) of the fractions are shown in brackets.

In addition to the above culture-based investigation, a 16S rRNA gene clone library was prepared from the heavy (1.747 g ml^{-1}) fraction (Figure 3.2F) of the treatment that received 5 doses of [^{13}C]benzoic acid. Fifty eight clones were screened by comparing RFLP patterns following double digestion with HhaI and HaeIII. There were 25 unique RFLP patterns, and 22 clones representing 12 unique RFLP patterns were sequenced. No chimeras were detected with Bellerophon. BLAST analysis of cloned sequences revealed clones representing the predominant RFLP pattern (15 of 58 clones) were *Burkholderia* species.

A phylogenetic tree was generated using complete 16S rRNA gene sequences from 11 isolates cultured from soil amended with benzoic acid and 19 cloned 16S rRNA sequences (Figure 3.3). One group of isolated *Burkholderia* strains, EBA05, EBA07, EBA09, and EBA11, clustered near *Burkholderia hospita* and *Burkholderia* sp. TH2. The latter is known to metabolize benzoate and chlorobenzoates (Suzuki et al., 2001). Remarkably, this group of isolates clustered together with three clones representing the dominant RFLP pattern from the [^{13}C]DNA fraction, suggesting we had successfully isolated representatives of the benzoic acid metabolizing population that was active in the field. Isolate EBA09 was found to have 99.5% sequence similarity with this group of clones. Furthermore, the T-RFLP pattern for isolate EBA09 and clones from that cluster revealed a 139 bp fragment (data not shown), which matches the fragment enriched in the [^{13}C]DNA fraction from the field (Figure 3.2).

3.4.4 Phylogenetic analysis of benzoate 1,2-dioxygenase genes

A 540-bp fragment of the gene encoding the benzoate 1,2-dioxygenase alpha subunit was amplified from isolates EBA05, EBA07, and EBA09. The amplified

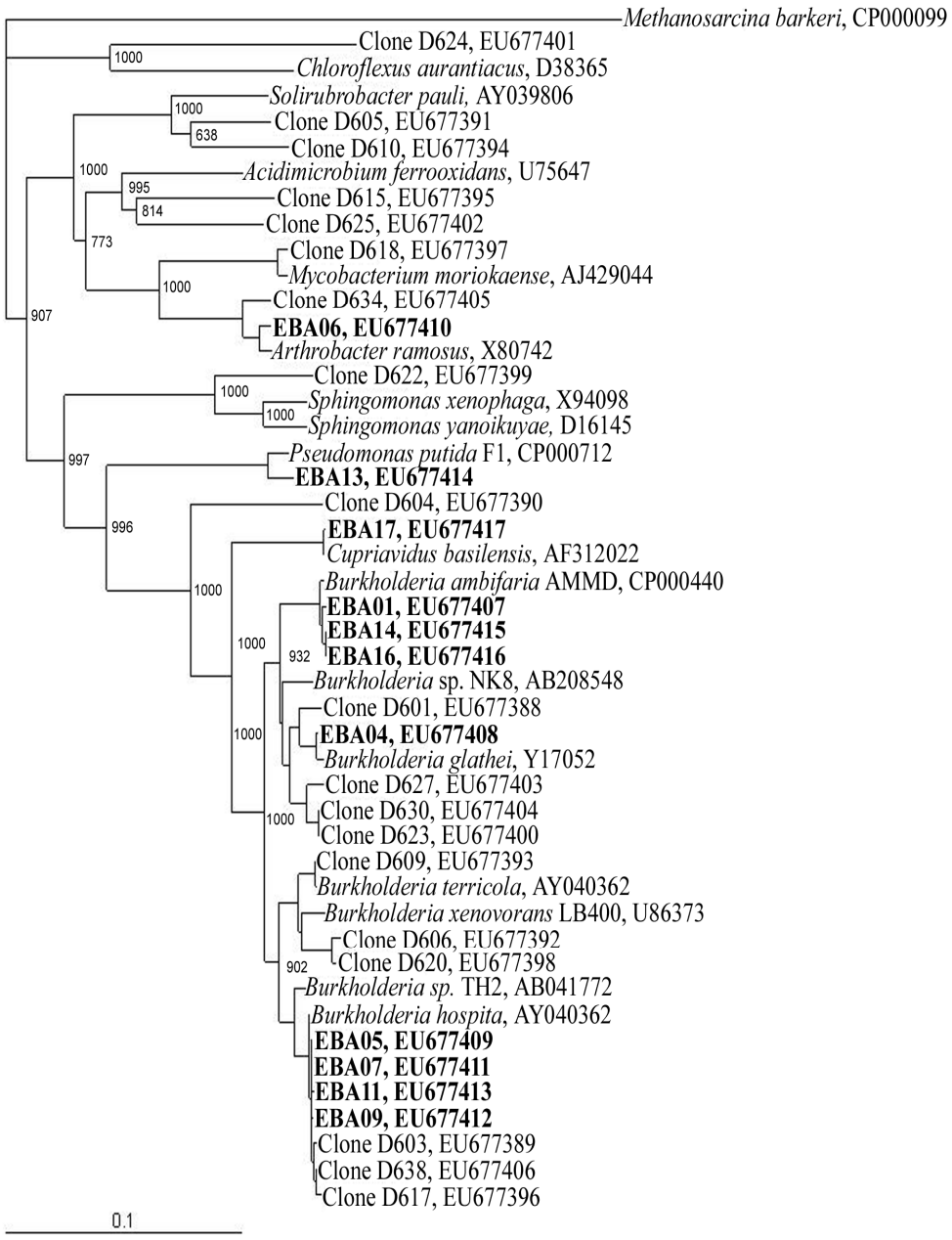

Figure 3.3. Phylogenetic analysis of 11 benzoate metabolizing isolates and 19 cloned 16S rRNA genes (~1400 bp) derived from ^{13}C-labeled DNA from soils receiving 5 doses of [^{13}C]benzoic acid. Isolates are in bold, clones are in plain text, and 17 reference strains are in italics. Accession numbers for reference sequences are given.

benA fragments were sequenced and subjected to phylogenetic analysis along with other benzoate 1,2-dioxygenase, toluate 1,2-dioxygenase, and chlorobenzoate dioxygenase genes (Figure 3.4). The resulting phylogenetic tree shows the *benA* genes from the isolates are closely related to the nonfunctional *benA* in *Burkholderia* sp. TH2 (Suzuki et al., 2002), as well chlorobenzoate dioxygenase genes from *Burkholderia* sp. NK8 (Francisco et al., 2001), *Burkholderia* sp. TH2, and *Burkholderia cepacia* 2CBS (Haak et al., 1995), which are able to metabolize chlorinated benzoates.

3.4.5 Growth of the Burkholderia populations in the field during the benzoate-dosing regime

To demonstrate growth of the population represented by EBA09 upon addition of benzoic acid in the field, we performed MPN-PCR on archived DNA extracts using a primer targeting the 16S gene of EBA09 and closely related *Burkholderia hospita* species (Figure 3.5). Specificity of the primer was tested by performing PCR on unrelated *Burkholderia* species as well as all of the isolates from the benzoic acid amended soil, which included *Burkholderia, Pseudomonas, Arthrobacter, and Cupriavidus* species. We only obtained the expected 180 bp amplicon from isolates EBA05, EBA07, and EBA09, which share at least 99.4% sequence similarity. The DNA used in the MPN-PCR assay was extracted from three sets of triplicate soils that were dosed with 100 μg benzoic acid in 50 μl water every 48 hours and triplicate soils that were unamended. The soils treatments for the MPN-PCR assay occurred simultaneously with the field SIP experiment, so the field conditions for each were identical. At time 0, the target population was present at slightly under 100,000 copies per gram of soil, with little change after 48 hours. However, after 144 hours, the population underwent approximately two doublings, as the target population had

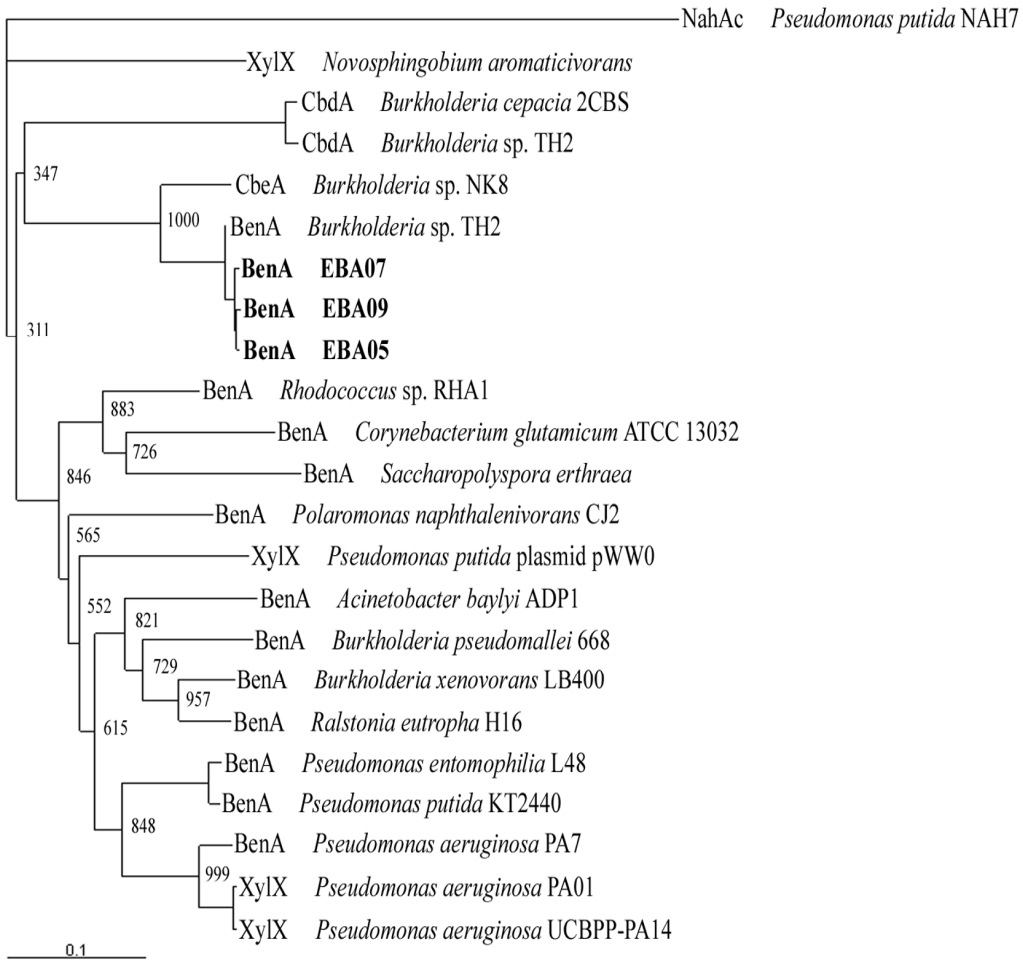

Figure 3.4. Phylogenetic analysis inferred from the alignment of 175 amino acid positions predicted from *benA* sequences amplified from isolates (EBA05, EBA07, and EBA09; accession numbers EU677418, EU677419, and EU677420, respectively; in bold) as well as 19 reference sequences for benzoate 1,2-dioxygenase (benA), toluate 1,2-dioxygenase (xylX), and chlorobenzoate dioxygenase (cbdA and cbeA) sequences from GenBank. The naphthalene dioxygenase, *nahAc*, from *Pseudomonas putida* G7 is the outgroup.

increased to 4.5-4.8x10^5 copies per gram of soil. Clearly, the target population identified by stable isotope probing not only actively metabolized benzoic acid, but also reproduced in the field after the addition of the substrate.

3.5 Discussion

In this study, we found that successive addition of benzoic acid to a field soil resulted in the growth of *Burkholderia* species that were also identified as the primary degraders of benzoic acid in situ by SIP. Although identifying an organism by DNA-SIP implies growth, MPN-PCR quantification of the population identified in our SIP experiment confirmed the population underwent approximately two doublings. Furthermore, enumeration of culturable benzoic acid degraders suggested *Pseudomonas* species were initially the more abundant benzoic acid degraders, but the addition of benzoic acid to the soil caused a shift in the community yielding greater numbers of *Burkholderia* species. According to the rRNA operon copy number database (Klappenbach et al., 2001; http://ribosome.mmg.msu.edu/rrndb/index.php), species from the genus *Burkholderia* have an average of 4.94 16S rRNA gene copies. Assuming the EBA09 population detected in the MPN-PCR assay has 5 16S rRNA gene copies per cell, the population increased from about 2×10^4 cells per gram of soil to just over 9×10^4 cells per gram of soil during the experiment. Following the final dose of benzoic acid, the number of culturable benzoate degrading *Burkholderia* were approximately 35 to 40 times higher than those detected by MPN-PCR, which used a primer designed to detect only populations closely related to *Burkholderia* sp. EBA09. This discrepancy between the final number of culturable *Burkholderia* species and the EBA09 population measured by MPN-PCR is likely due to the specificity of the PCR primers used in the MPN-PCR assay, and the likelihood that the EBA09 population is a subset of the total benzoic acid-metabolizing community. Despite this difference, a

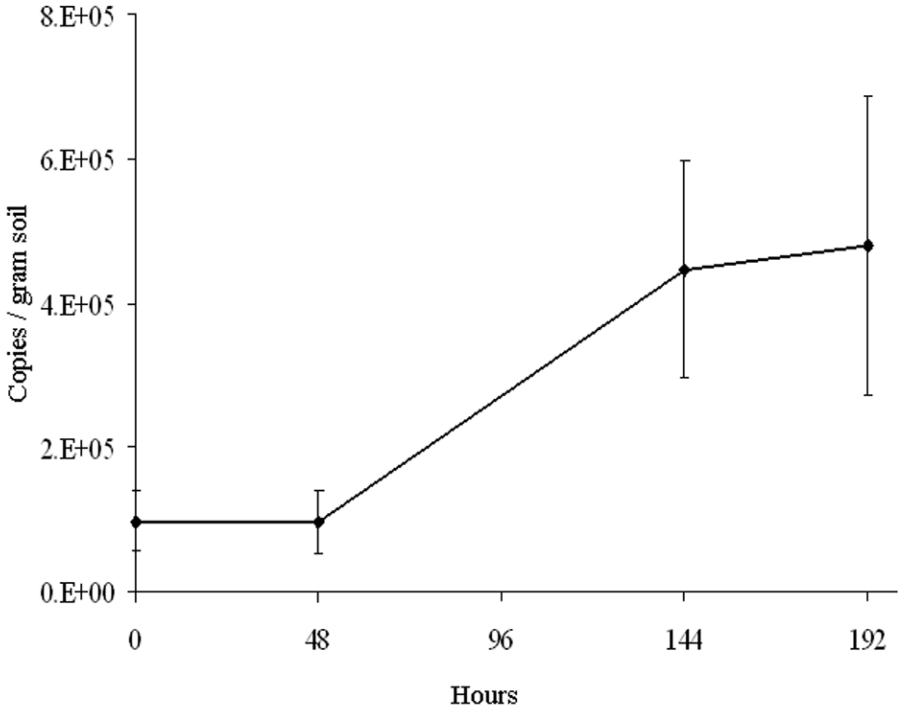

Figure 3.5. Quantification of EBA09-like population in the field by MPN-PCR during growth on benzoic acid. Experimental values represent the average copy number of the target 16S rRNA gene from triplicate soil samples. Error bars represent the standard deviation.

measured increase in *Burkholderia* species after the addition of benzoic acid is consistent between culture and non-culture-based methods.

The population numbers obtained by MPN-PCR indicated a slowdown in growth between 144 and 196 hours (Figure 3.5), which could indicate that nutrients other than carbon were becoming scarce and limiting the growth of the EBA09-related population. If this were the case, it could have implications for microbial communities in soils receiving repeated carbon inputs. The high rRNA gene copy number found in many *Burkholderia* species is associated with bacteria that employ a copiotrophic ecological strategy (Klappenbach et al., 2000). Copiotrophic populations are expected to respond quickly to the added carbon and exhaust other nutrients (e.g., N and P), which may subsequently limit their activity. This could explain why there was not greater enrichment of the 139 bp fragment in the heavy DNA fraction from the sample that received only 1 dose of [^{13}C]benzoic acid after 4 doses of [^{12}C]benzoic acid (Figure 3.2). By the time the ^{13}C-labeled substrate was added, nutrients other than carbon may have been limiting, causing the *Burkholderia* sp. EBA09 population to grow at a slower rate. If the experiment had been extended another 48-96 hours, it is possible that oligotrophic populations, which tend to have higher affinities for nutrients, might have replaced the *Burkholderia* population as the active benzoic acid-degraders within the community.

In order for bacteria to take advantage of an introduced carbon source, they must have a combination of genes and physiology that enable them to compete for and utilize a substrate. Species within the genus *Burkholderia* are widespread in soil environments, ecologically versatile, and capable of metabolizing aromatic compounds (Coenye and Vandamme, 2003; O'Sullivan and Mahenthiralingam, 2005). Other studies have suggested *Burkholderia* species are the primary degraders of aromatic compounds in soil environments. For example, in soils amended with 2- and

3-chlorobenzoate, *Burkholderia* species were the dominant indigenous culturable degraders of the added compounds (Gentry et al., 2001; Gentry et al., 2004). Another study using SIP found *Burkholderia* species to be the primary degraders of polychlorinated biphenyls (Tillman et al., 2005). The ecological versatility of *Burkholderia* is attributed to their multireplicon genomes, which can be larger than 9 Mb (Chain et al., 2006). Such large genomes allow metabolic versatility, and the presence of mobile genetic elements can promote genomic plasticity and general adaptability (Lessie et al., 1996). The isolation of *Burkholderia* sp. EBA09 will allow subsequent experimentation to examine the genetic and physiological characteristics that enabled ecological success of the bacterium upon the introduction of benzoic acid in the field.

4. DYNAMIC SECONDARY ION MASS SPECTROMETRY (SIMS) IMAGING OF MICROBIAL POPULATIONS UTILIZING ^{13}C-LABELED SUBSTRATES IN PURE CULTURE AND IN SOIL.

4.1 Abstract

We demonstrate that dynamic secondary ion mass spectrometry (SIMS)-based ion microscopy can provide a means of measuring ^{13}C assimilation into individual bacterial cells grown on ^{13}C-labeled organic compounds in the laboratory and in field soil. We grew pure cultures of *Pseudomonas putida* NCIB 9816-4 in minimal media with known mixtures of ^{12}C- and ^{13}C-glucose and analyzed individual cells via SIMS imaging. Individual cells yielded signals of masses 12, 13, 24, 25, 26, and 27 as negative secondary ions indicating the presence of $^{12}C^-$, $^{13}C^-$, $^{24}(^{12}C_2)^-$, $^{25}(^{12}C^{13}C)^-$, $^{26}(^{12}C^{14}N)^-$, and $^{27}(^{13}C^{14}N)^-$ ions, respectively. We verified that ratios of signals taken from the same cells only changed modestly during a ~4.5-min period of sputtering with primary scanning by the erosive O_2^+ beam of the dynamic SIMS instrument. There was a clear relationship between mass 27 and 26 signals in *Psuedomonas putida* cells grown in media containing varying proportions of ^{12}C- to ^{13}C-glucose: a standard curve was generated to predict ^{13}C-enrichment in unknown samples. We then used two strains of *Pseudomonas putida* able to grow on either all or only a part of a mixture of ^{13}C-labeled and unlabeled carbon sources to verify that differential ^{13}C signals measured by SIMS were due to ^{13}C assimilation into cell biomass. Finally, we made three key observations after applying SIMS ion microscopy to soil samples from a field experiment receiving ^{12}C- or ^{13}C-phenol: (i) cells enriched in ^{13}C were heterogeneously distributed among soil populations; (ii) ^{13}C-labeled cells were detected in soil that was dosed a single time with ^{13}C-phenol; and (iii) in soil that received 12 doses of ^{13}C-phenol, 27% of the cells in the total community were more

than 90% ^{13}C-labeled.

4.2 Introduction

Linking the identity of active microorganisms with their function *in situ* is a central challenge in environmental microbiology (Madsen, 2005). Techniques such as stable isotope probing (SIP), which combine molecular identification methods with isotopic tracers (Boschker et al., 1998; Buckley et al., 2006; Leigh et al. 2007; Lu and Conrad, 2005; Madsen, 2005, 2006; Manefield et al., 2002; Neufeld et al., 2007; Radajewski et al., 2000; Whiteley et al. 2007), are proving to be effective and insightful means for identifying metabolically active microorganisms (Jeon et al., 2003; Kasai et al., 2006; Liou et al. 2008; Pumphrey and Madsen, 2008). The growing application of such techniques in microbial ecology has increased interest in developing microscopic techniques that both confirm the role of microorganisms that are identified through SIP and measure the amount of isotopic label individual cells have incorporated the into their biomass.

When suitable probes are available, fluorescent in situ hybridization (FISH) is an effective means of microscopic identification of microorganisms (Wagner et al., 2003), and can be combined with techniques using radioactive and stable isotopes to identify metabolically active microorganisms. The localization of radioactive isotopes can be determined through microautoradiography, and when used in combination with FISH, can provide insight into the structure and function of microbial communities (Lee et al., 1999; Ouverney and Fuhrman 1999). For the localization and measurement of stable isotopes, Raman microspectroscopy (Huang et al., 2004; Huang et al., 2007) and secondary ion mass spectrometry (SIMS) are potentially powerful methods that have been successfully combined with FISH.

SIMS is a technique that can characterize the isotopic composition of a sample by first bombarding the sample surface with a primary ion beam, and then separating and measuring the resulting secondary ions by mass spectrometry (Chandra, 2005; Chandra and Morrison, 2000). To date researchers have applied various SIMS techniques to pure cultures and environmental samples to measure ^{13}C, ^{15}N, as well as inorganic isotopes in bacteria. Early pioneering studies applying SIMS to microbial systems used a SIMS ion microprobe in combination with fluorescent in-situ hybridization (FISH) to show that methane-consuming *Archaea* in anoxic marine sediments were naturally ^{13}C-depleted (Orphan et al., 2001; Orphan et al., 2002). A SIMS ion microprobe was also used in combination with autoradiography and FISH to show CH_4 and CO_2 consumption by methanotrophic microbial mats (Treude et al., 2007). Time of flight SIMS (TOF-SIMS) has been used to measure inorganic carbon and nitrogen assimilation in individual bacterial cells and fungal hyphae (Cliff et al., 2002), and to distinguish *Bacillus subtilis* spores grown on different media based elemental signatures (Cliff et al., 2005). Lechene et al. (2006) demonstrated the use of nanometer-scale SIMS (NanoSIMS) to show ^{15}N fixation by *Teredinibacter turnerae* and not *Enterococcus faecalis* in pure culture, and NanoSIMS was able to distinguish ^{15}N-enriched *Pseudomonas fluorescens* that were added to a soil matrix (Herrmann et al., 2007). Application of NanoSIMS to a biofilm dominated by sulfate-reducing bacteria showed the aggregation of extracellular proteins and biogenic zinc sulfide crystals (Moreau et al., 2007). The use of an oligonucleotide probe labeled with iodized cytidine was combined with NanoSIMS to visualize both *Escherichia coli* grown on different amounts of ^{13}C and ^{15}N, and an archaeal population from a municipal solid waste bioreactor growing on ^{13}C-methanol (Li et al., 2008).

SIMS technology has tremendous potential to aid investigations examining the role of bacteria in the biodegradation of organic pollutants. DeRito et al. (2005) used

dynamic SIMS ion microscopy to provide qualitative evidence that a soil community exposed to ^{13}C-phenol was enriched in ^{13}C relative to a population that received an equal amount of ^{12}C-phenol. However, in this study the increased ^{13}C signal detected by SIMS was qualitative, and the amount of ^{13}C incorporated into the bacterial biomass was unclear. A related ratio imaging approach applied to dynamic SIMS ion microscopy clearly distinguished ^{13}C-labeled from unlabeled cells in soil samples (Chandra et al., 2008). In the present investigation, we show that it is possible to use dynamic SIMS ion microscopy to measure the degree of isotopic enrichment in single cells from pure cultures grown on mixtures of ^{12}C- and ^{13}C-labeled organic substrates. In addition, using pure-culture experiments to generate a dose-response curve, we estimated the degree of ^{13}C-labeling in bacterial cells from a soil community that received ^{13}C-phenol in a series of field soil experiments.

4.3 Methods

4.3.1 Bacterial strains and growth conditions

Standards of ^{13}C-labeled bacteria grown in known ratios of ^{13}C- and ^{12}C-glucose were prepared by growing the naphthalene-degrading bacterium *Pseudomonas putida* NCIB 9816-4 (Serdar and Gibson 1989) overnight in mineral salts broth (MSB) (Stanier et al., 1966) amended with 1 g$\cdot$ L^{-1} total glucose while varying the proportion of ^{13}C in the pool (Sigma ^{13}C-glucose; 99 % purity). Initial proportions of the ^{13}C label varied from 1% (natural abundance) to 25, 50, 75, or 99% ^{13}C-glucose. To show that metabolism of ^{13}C-glucose caused proportionate labeling of cells, *P. putida* NCIB 9816-4 and *P. putida* NCIB 9816-4.C (Stuart-Keil et al., 1998), a strain cured of the plasmid encoding naphthalene-catabolic genes, were grown in 6 ml MSB amended with 0.1% ^{13}C-glucose (6mg) and 10 mg ^{12}C-naphthalene (unlabeled) crystals in tubes sealed with a Teflon®-lined septa. Bacterial growth and metabolism of the substrates

were monitored by optical density and headspace analysis of respired CO_2 by GC/MS, respectively. Pure culture samples were fixed for SIMS microscopy by adding 100 µl of bacterial culture to 300 µl of 4% formaldehyde.

4.3.2 GC/MS analysis of CO_2

Procedures used were those of DeRito et al. (2005). A Hewlett-Packard HP5890 gas chromatograph (Wilmington, DE) equipped with an HP5971A mass-selective detector was used for CO_2 analyses. With high-purity helium as the carrier gas, a Hewlett-Packard Pora Plot Q column (25 m by 0.32 mm, 10 µm film thickness) was used to separate CO_2 from other gaseous components. The detector was operated at an electron energy of 70 eV and a detector voltage of 2,000 V. The ion source pressure was maintained at 1×10^{-5} torr. A splitless injection was used, and the GC oven was isothermal at 60°C. Single-ion monitoring allowed simultaneous quantification of both $^{12}CO_2$ (m/z = 44) and $^{13}CO_2$ (m/z = 45). The concentration of CO_2 was quantified using calibration curves prepared using external standards (Scott Specialty Gases, Plumsteadville, PA).

4.3.3 Soil field treatments

Soil samples produced in experiments by DeRito et al. (2005) were analyzed in this study. Briefly, a soil plot (Collamer silt loam) at the Cornell University Agricultural Experiment Station, Ithaca, NY was level and free of vegetation. A table was placed over the plot (0.8 m high) to protect the experiment from rain and direct exposure to sunlight. Three soil treatments received 12 daily doses of phenol, with each 20 µl dose containing 200 µg of phenol. The first treatment received only ^{12}C-phenol and the second treatment received only ^{13}C-phenol. The third treatment received 11 daily doses of ^{12}C-phenol and a single dose of 13C-phenol on the twelfth

day. A fourth treatment was not dosed with phenol for the first 11 days, but received a single dose of ^{13}C-phenol on the twelfth day. Twenty-four hours following the final dose, one-tenth of a gram of surface soil was aseptically collected from the field treatments, fixed in 4% formaldehyde (1 ml), and stored in screw-cap glass vials.

4.3.4 SIMS imaging

Procedures used were those of Chandra et al. (2008). A small drop (~2 μl) from the formaldehyde-fixed samples was smeared on the polished surface of sterile silicon wafer pieces (Silicon Quest International, Santa Clara, CA, about 1 cm^2 surface area). The samples were air dried and heat-fixed to the silicon substrate by passing rapidly (~2 sec) over a flame prior to SIMS analysis. A CAMECA IMS-3f SIMS ion microscope was used in the study. A 5.5 keV mass filtered primary ion beam of O_2^+ (about 100-200 nA beam current with a spot size of 60 μm) was raster scanned over a 250 μm^2 or 500 μm^2 region, depending on the need of a particular analysis, for imaging studies. A 60 μm contrast aperture and 150 μm transfer optics were employed in the imaging mode for the detection of negative secondary ion signals. SIMS images of masses 12, 13, 24, 25, 26, and 27, primarily representing contributions from $^{12}C^-$, $^{13}C^-$, $^{24}(^{12}C_2)^-$, $^{25}(^{13}C^{12}C)^-$, $^{26}(^{12}C^{14}N)^-$, and $^{27}(^{13}C^{14}N)^-$, respectively, were recorded for designated times on the Photometrics CCD camera capable of 14 bits per pixel image digitization. It should be noted that under these instrumental conditions of mass resolution of the ion microscope imaging mode, mass interfering species like $^{13}(^{12}CH)^-$, $^{26}(^{13}C_2)^-$, $^{25}(^{12}C_2H)^-$, $^{27}(^{13}C_2H)^-$, and $^{27}(^{13}C^{14}N)^-$ cannot be separated from the species of interest like $^{25}(^{12}C^{13}C)^-$, $^{26}(^{12}C^{14}N)^-$, and $^{27}(^{13}C^{14}N)^-$. However, the enhancement of signals reflected in ion microscopy images of masses 13, 25 and 27 from ^{13}C-labeled phenol treated cells compared to controls does provide meaningful imaging of ^{13}C incorporation in individual bacterial cells.

4.3.5 Image analysis

Computer image processing was performed with DIP Station (Haydon Image Processing Group). To measure the mean signal intensities for corresponding masses (i.e. 27 and 26), the images of corresponding masses from the same field of view were overlayed and registered. A region of interest (ROI) was drawn within an individual bacteria cell on one image, copied onto the same cell in the corresponding image, and the mean pixel intensities for the corresponding ROIs between the two images were measured. The relationship between masses 27 and 26 was calculated as percent mass 27 of the combined mass 26 and mass 27 signals using the following equation:

$$\%\ \text{mass } 27 = \left[\frac{\text{mass } 27}{(\text{mass } 26 + \text{mass } 27)} \right] \times 100$$

Ratio imaging provided a direct comparison of the enhancement of ^{13}C signals in individual bacterial cells due to the treatment with ^{13}C-labeled phenol in direct comparison to the unlabeled phenol treatment. For ratio imaging, the corresponding SIMS bacterial images were calibrated to a single contrast scale; then the ^{13}C signal was divided by the ^{12}C signal using the NIH's ImageJ software. The result is an image in which the value of each pixel is the ratio of one mass image to the other. A color gradient map was then applied to each ratio image in Adobe Photoshop, where 2:1=cyan, 1:1=magenta, and 0=yellow. This color scale allows clear distinction between the highest ratios (cyan, where $^{27}(^{13}C^{14}N)^-$ is greater than $^{26}(^{12}C^{14}N)^-$), the 1:1 ratios (magenta), and the fractional ratios (yellow, where 13C isotopes are scarce or not present). The resulting image distinguishes which bacteria are assimilating the ^{13}C-labeled compound and which are not. Overlay images were created using Metamorph® software.

4.3.6 Automated image processing

Analysis of secondary ion signal intensities of SIMS images was performed with Metamorph Software (Molecular Devices). A 1:1 correspondence was established between the DIP Station and Metamorph analyses of the pure culture standard images by first generating a mass 27 and mass 26 composite image for each field of view analyzed using ImageJ (NIH). ROIs were determined by generating a segmented image with minimum and maximum region widths and heights of 2 and 10 pixels respectively at specific graylevels above a background intensity specific to each composite image. ROIs identified in composite images were transferred to corresponding mass 27 and mass 26 images to quantify average ROI pixel intensities. Field soil SIMS images and images from the pure culture experiments involving *P. putida* NCIB 9816-4 (wild-type) *P. putida* NCIB 9816-4.C (cured of pDTG1) were analyzed in the same manner as the automated analysis of the pure culture ^{13}C-glucose standards.

4.4 Results

4.4.1 Effect of continuous ion beam sputtering on the constancy of isotope ratios

Our standard SIMS protocol for analyzing microbiological samples began with ~1 min of primary O_2^+ beam exposure used for fine focusing and signal stabilization. Then, images of masses 12, 13, 24, 25, 26 and 27 as negative secondary ions from each field of view revealed the presence of $^{12}C^-$, $^{13}C^-$, $^{24}(^{12}C_2)^-$, $^{25}(^{13}C^{12}C)^-$, $^{26}(^{12}C^{14}N)^-$, and $^{27}(^{13}C^{14}N)^-$ in individual bacterial cells. The surface sputtering mechanism utilized by dynamic SIMS is a destructive process and masses are imaged one at a time; therefore, it is essential to know that mass signals and calculated isotopic ratios from microbiological samples are consistent throughout the time images are recorded.

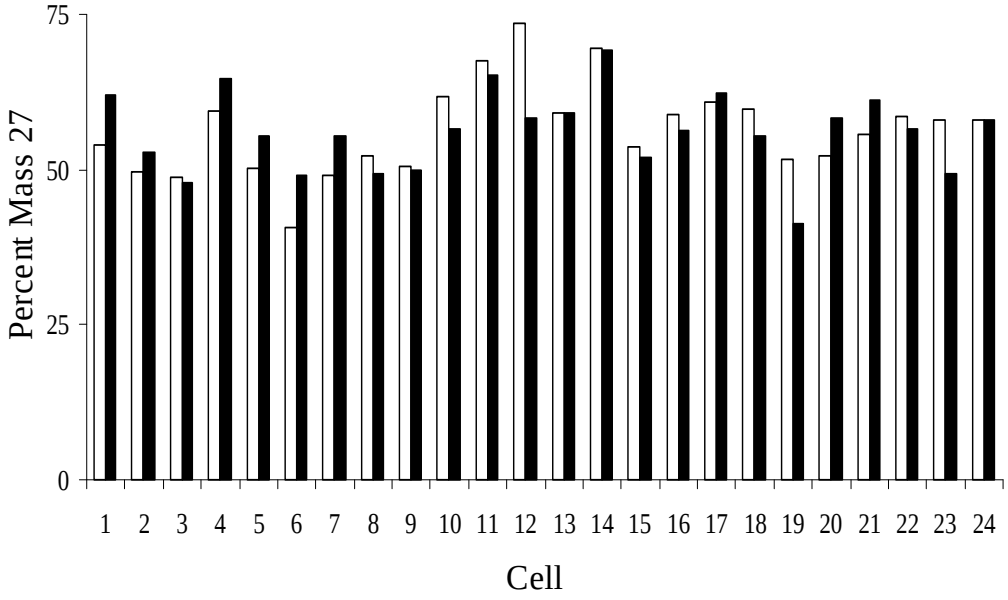

Figure 4.1. A comparison of the change in mass 27 and mass 26 signal intensities detected by SIMS in *P. putida* NCIB 9816-4 cells grown on ^{13}C-glucose after exposure to the O_2^+ beam for 4.5 min. The percent mass 27 for each cell was calculated from signal intensities from an initial measurement of mass 27 and 26 ions (white bars) and signal intensities from a subsequent measurement after 4.5 minutes of exposure to the O_2^+ beam (black bars). Image analysis was performed using DIP station software.

The percent mass 27 relative to mass 26 before and after the 4.5 minute beam exposure was calculated and used to compare the change in signals from *Pseudomonas putida* NCIB 9816-4 cells grown on 99% ^{13}C-glucose (Figure 4.1). The vertical axis in Figure 4.1 did not reach 100% because several ions besides $^{26}(^{12}C^{14}N)^-$ contribute to the mass 26 signal (see below). Among the 24 cells randomly examined the average change in the percent mass 27 was 0.3% ± 5.8%, with only two cells showing a change of more than 10%. This shows that the destructive dynamic SIMS sampling process under our experimental conditions caused minimal change in signal ratios over the time typically needed to record images; thus, dynamic SIMS ion microscopy can provide reliable data for determining isotope ratios in bacterial samples.

4.4.2 Measurement of ^{13}C incorporation by pure cultures

To determine whether dynamic SIMS ion microscopy could distinguish between cells that are unlabeled, partially labeled, or fully labeled with ^{13}C, we grew pure cultures of *Pseudomonas putida* NCIB 9816-4 in minimal media with known mixtures of ^{12}C- and ^{13}C-glucose. Masses 12, 13, 24, 25, 26, and 27 were measured via SIMS imaging, and the average signal intensity for individual cells was measured both by hand drawing regions of interest (ROIs) within cells using DIP station and by using Metamorph® to automatically select ROIs by intensity (Figure 4.2). Data generated from images of mass 27 and 26 are shown because these two masses provide optimal resolution among the available secondary ions. The other secondary ions produced similar data to mass 27 and mass 26 for pure cultures, but have been found to be less effective for soil samples (DeRito et al., 2005; Chandra et al., 2008). Plotting the intensity of ^{13}C containing masses against the intensity of ^{12}C containing masses for individual cells revealed increases in slope that corresponded with an

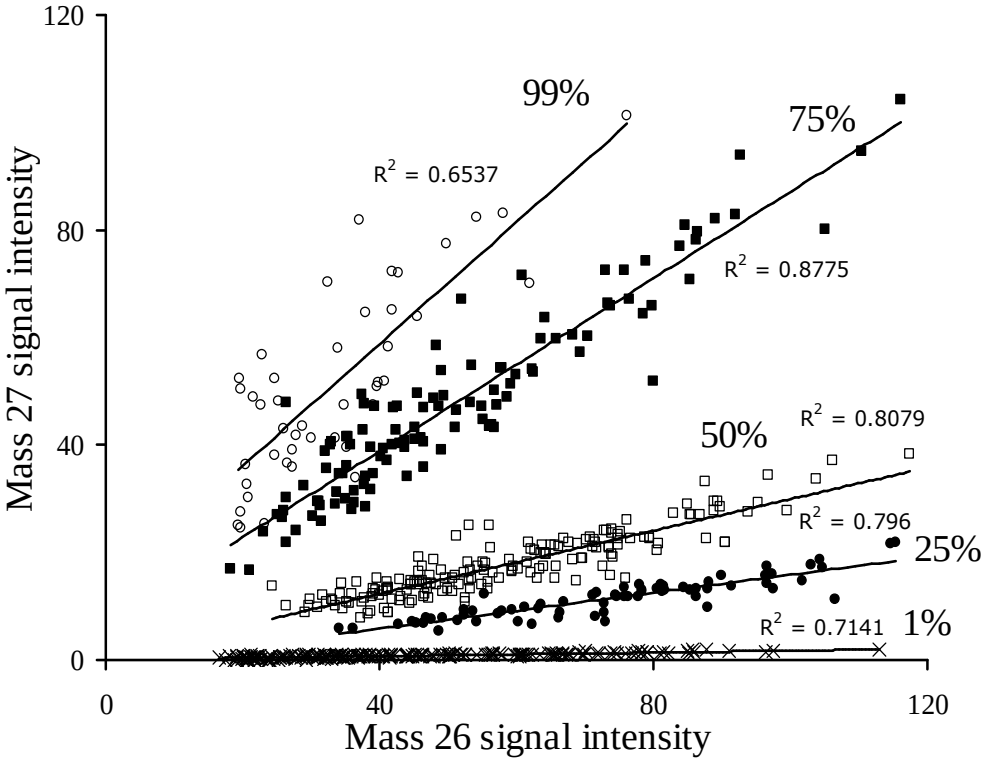

Figure 4.2. A scatter plot showing the relationship between mass 27 and mass 26 signal intensities from individual cells of *P. putida* NCIB 9816-4 grown on 1 g· L^{-1} total glucose while varying the proportion of ^{13}C label from 99 to 75, 50, 25, or 1%. Each data point represents an individual bacterial cell whose mass 27 and mass 26 signals were determined using SIMS. Up to 200 determinations were completed for each growth condition. Images were recorded by dynamic SIMS ion microscopy and signal intensities were measured with Metamorph® software.

increase in ^{13}C-glucose in the growth medium (Figure 4.2). Plotting signal intensities from individual cells also showed that though signal intensity can vary greatly between cells with similar ^{13}C-enrichment, the ratios between signal intensities (i.e. mass 27 to mass 26) are consistent.

Standard curves were generated by plotting the average percent mass 27 values calculated from the mass 27 and 26 signals from individual cells, which were grown on various proportions of ^{13}C-glucose. For each growth condition, 60 individual bacteria cells were measured manually and up to 200 individual bacteria cells were measured using a procedure with Metamorph® software to automatically select ROIs by intensity and size. Cultures were grown on glucose whose ^{13}C proportions varied from 1%, 25%, 50%, 75%, or 99% ^{13}C-glucose. Both manually measured images and the automated procedure using Metamorph® software produced equivalent standard curves (Figure 4.3). The percent mass 27 values shows that as ^{13}C increases in cellular biomass, the $(^{13}C_2)^-$ secondary ion makes a greater contribution to the mass 26 signal than the $(^{12}C^{14}N)^-$ secondary ion. Despite the influence of interfering masses, there is a positive correlation between mass 27 and 26 signals recorded by dynamic SIMS ion microscopy and the ratio of ^{13}C- to ^{12}C-glucose in the growth media (Figure 4.3). This relationship can be used to quantitatively estimate ^{13}C enrichment in samples with unknown carbon isotope ratios.

In order to demonstrate that an enriched signal measured by SIMS was due to metabolism and incorporation of the ^{13}C, we conducted experiments with wild-type *P. putida* NCIB 9816-4 and *P. putida* NCIB 9816-4.C, which was cured of pDTG1, the plasmid encoding naphthalene-catabolic genes. Both the wild-type and cured strain were grown in minimal media containing a mixture of ^{13}C-glucose and unlabeled (^{12}C) naphthalene crystals and we monitored growth (OD), respiration, and mass 27/mass 26 ratios in individual cells using SIMS (Figure 4.4). As expected, the highest OD

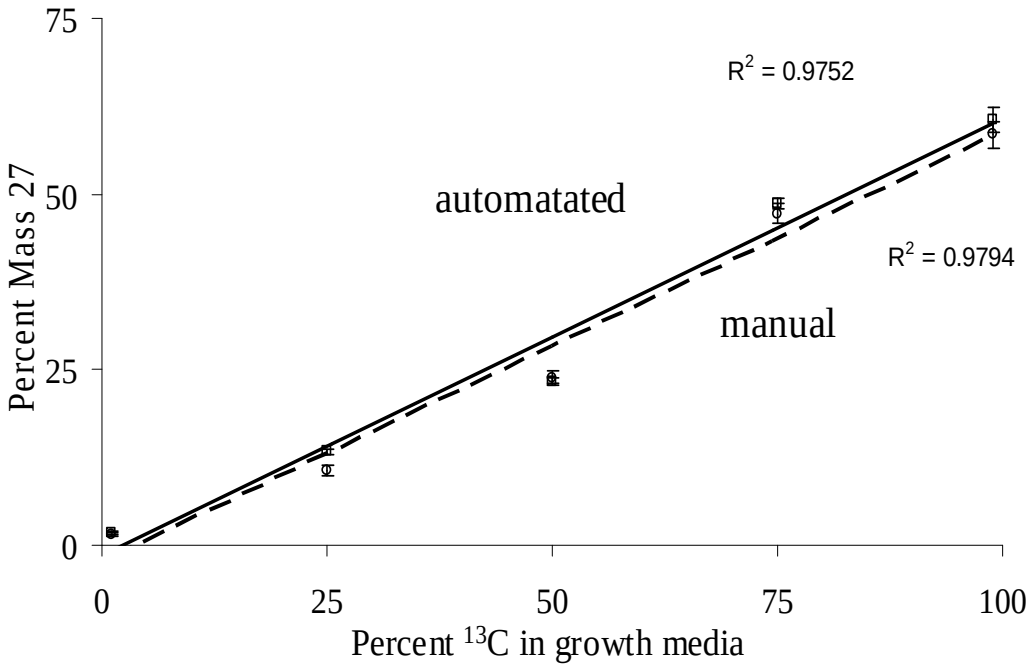

Figure 4.3. Standard curves generated from pure cultures of *P. putida* NCIB 9816-4 grown on 0.1% glucose composed of 99, 75, 50, 25, or 1% ^{13}C-glucose. Plotted points represent the mean percent mass 27 values calculated from the mass 27 and mass 26 signal intensities from individual cells that were measured by automated selection with Metamorph® software (×, solid trendline) or manually with DIP station software (+, dashed trendline). Error bars represent the 95% confidence interval for the mean of each sample. A total of 60 determinations for each growth condition were completed manually, and up to 200 were completed automatically.

reading (Figure 4.4A) was achieved by the wild-type strain, able to utilize both glucose and naphthalene. The cured strain reached only moderate density (Figure 4.4A), confirming it was growing on glucose, not naphthalene. The wild-type strain released high amounts of both labeled and unlabeled CO_2 (from glucose and naphthalene, respectively; Figure 4.4 B), while the cured strain only respired $^{13}CO_2$, indicating the cured strain only metabolized the ^{13}C-glucose. As expected from the above trends in growth and respiration, the ratios of masses 27/26 in individual cells showed that the wild-type strain exhibited a low proportion of mass 27 in its biomass because its cell carbon was derived from both labeled and unlabeled substrates (Figure 4.4C). In contrast, cured cells were fully labeled with ^{13}C (Figure 4.4C), which indicates the naphthalene was not incorporated into the cellular biomass and had little to no influence on the SIMS signal. Using the standard curve generated from pure culture standards (Figure 4.3), the percent mass 27 values in the wild-type cells suggested mixed isotopic compositions that ranged between 30-70% ^{13}C for individual cells, confirming the wild-type strain metabolized and incorporated both the ^{13}C-glucose and ^{12}C-naphthalene.

4.4.3 Measurement of ^{13}C incorporation by phenol-degraders in soil

Confident in our methods to measure carbon isotope composition in bacteria, we applied SIMS ion microscopy to soil communities that were exposed to ^{12}C- or ^{13}C-phenol in the field. We plotted the mass 27 and mass 26 signal intensities from soil treatments that received twelve 20-µl doses (200 µg phenol per dose) of either ^{13}C- or unlabeled phenol (Figure 4.5). The pattern of labeling clearly shows that many cells in the soil receiving ^{13}C-phenol were enriched in ^{13}C compared to cells from soil receiving only ^{12}C-phenol. The mass 27 and 26 signal intensities from the ^{12}C-phenol

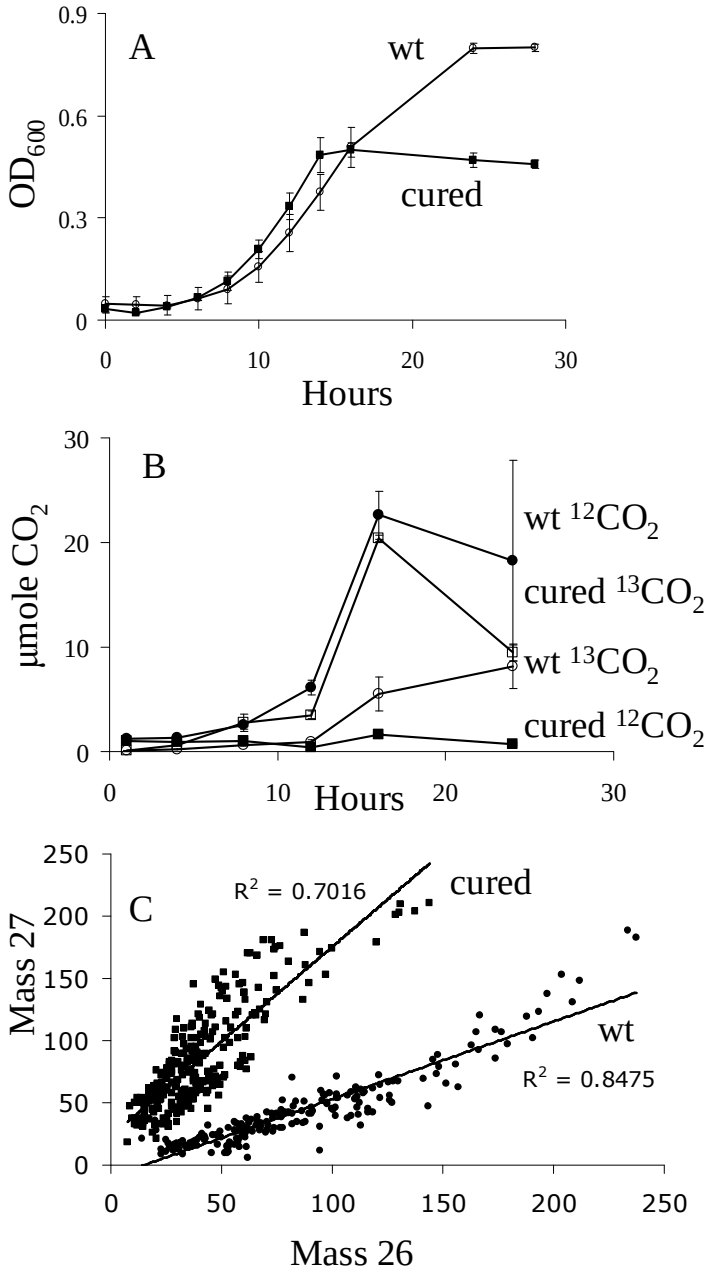

Figure 4.4. The metabolism of naphthalene or glucose by *P. putida* NCIB 9816-4 and *P. putida* NCIB 9816-4.C is shown by (a) growth in MSB amended with unlabeled naphthalene crystals and 0.1% ^{13}C-glucose, (b) production of $^{13}CO_2$ and $^{12}CO_2$ respired during growth on the substrates shown in (a), and (c) mass 27 and 26 signal intensities for individual wild-type (wt) or cured *P. putida* NCIB 9816-4 cells after growth on the media in (a). Signal intensities were measured with Metamorph® software.

treatment were consistent with intensities shown in Figures 4.2 and 4.3. The mass 27 and 26 signal intensities from the ^{13}C-phenol treatment indicated a much more diverse distribution in terms of ^{13}C content: data in Figure 4.5 clearly show cells containing a low (natural abundance) of ^{13}C, as well as cells exhibiting a high degree of ^{13}C enrichment. Overlay images created by combining mass 27 images (green) and mass 26 images (red) confirmed that the soil microbial community exposed to ^{13}C-phenol contained heterogeneous populations, with many cells showing no incorporation of the ^{13}C-label and others showing a range of ^{13}C incorporation (Figure 4.6A). It is not possible to distinguish metabolically inactive cells from those that grew on phenol in the ^{12}C-phenol treatment (Figure 4.6B). Images created by overlaying the intensity of mass 27 onto mass 26 for individual cells, provided a means of direct, semi-quantitative assessment of ^{13}C incorporation (Figure 4.6C). High mass 27 signals in cells (blue in Figure 4.6C) clearly metabolized ^{13}C-phenol; while cells showing low (natural abundance) mass 27 signals in cells (yellow in Figure 4.6C) did not. An image of a comparable soil sample stained with DAPI (Figure 4.6D) is provided for comparison with the SIMS images. The absence of any ^{13}C signal in many cells in these images (Figure 4.6) reinforce the information from Figure 4.4 that signal intensity is a result of ^{13}C assimilation, not caused by physical association between the cell and an added labeled chemical.

To estimate percent ^{13}C-enrichment in individual cells from the soil community dosed with either labeled or unlabeled phenol, the percent mass 27 was calculated for each ROI measured using Metamorph®, and percent ^{13}C-enrichment was estimated using the standard curve generated from pure cultures (Figure 4.3). Cells from the 4 field-dosing treatments were grouped according to percent ^{13}C-enrichment by 10% intervals to show the distribution of ^{13}C in the populations that

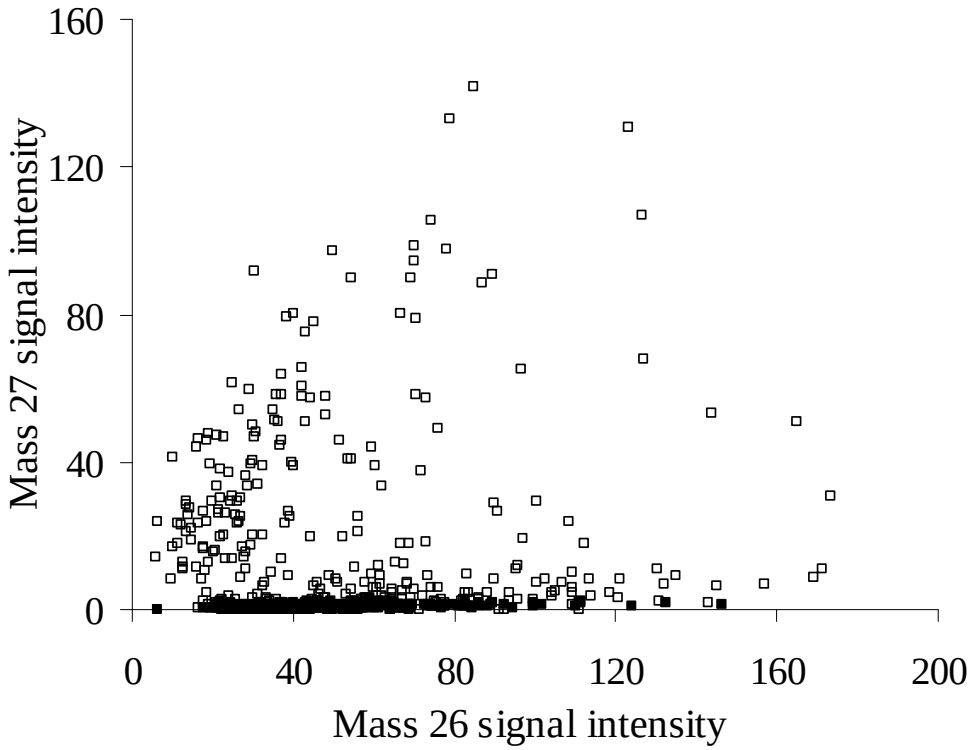

Figure 4.5. A scatter plot showing the relationship between mass 27 and mass 26 signal intensities of bacterial cells detected by SIMS in soils exposed to 12 doses of ^{13}C-phenol (□) or ^{12}C-phenol (■). The signal intensities of 481 regions of interest (ROIs) from images of soil receiving ^{12}C-phenol and 327 ROIs from images of soil receiving ^{13}C-phenol were measured with Metamorph® software.

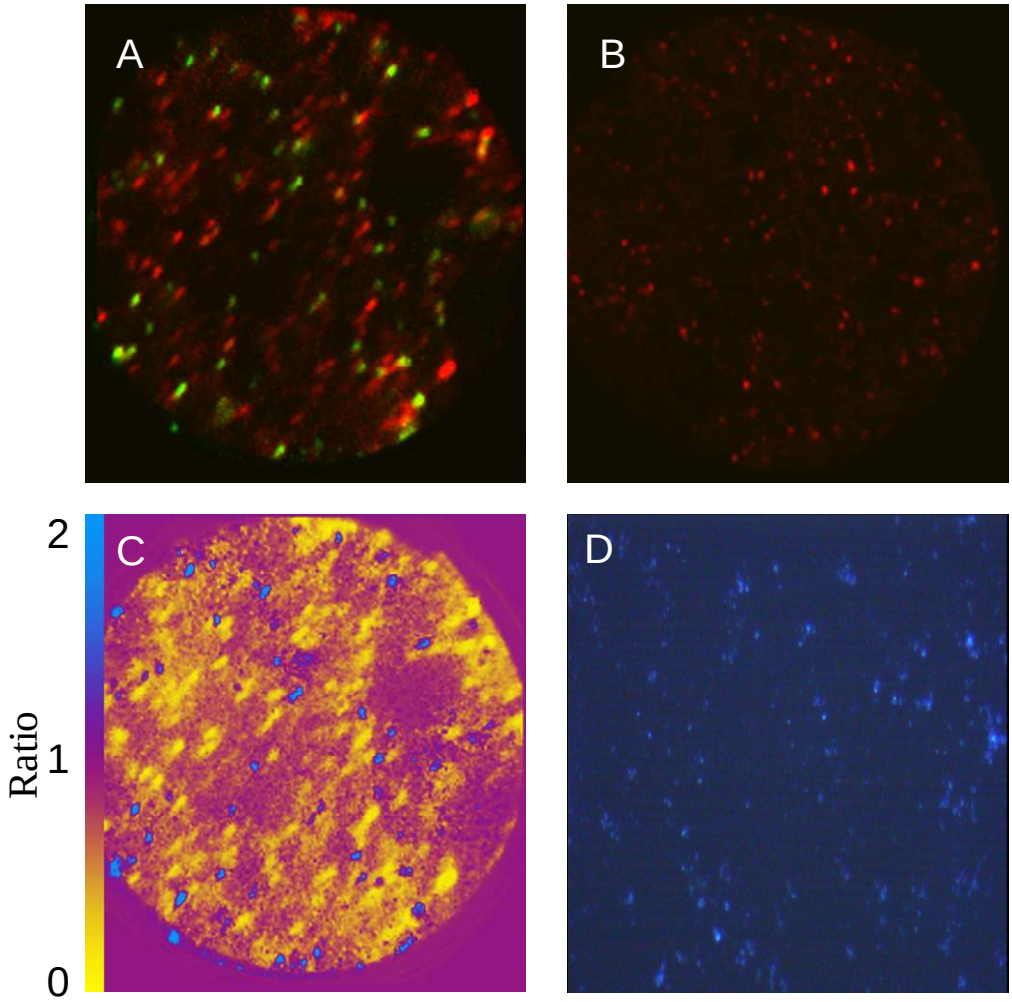

Figure 4.6. A comparison of mass 27 and mass 26 SIMS images. Mass 27 (green) to mass 26 (red) overlay of field samples dosed with (A) ^{13}C-phenol or (B) ^{12}C-phenol. (C) A mass 27 to mass 26 ratio image of the same ^{13}C-phenol exposed soil. (D) DAPI image, 40x magnification, of comparable soil sample not exposed to the O_2^+ beam.

received ^{12}C- or ^{13}C-phenol (Figure 4.7). For the control treatment of soil dosed 12 times with ^{12}C-phenol, 98% (473 of 481) of the cells were found to have less than 10% ^{13}C in their biomass. The distribution of ^{13}C in cells from soil dosed 12 times with ^{13}C-phenol differed markedly from the control treatment: only 30% (99 of 327) of the cells from soil dosed with ^{13}C-phenol were found to be less than 10% ^{13}C-labeled; while 27% of the cells were more than 90% ^{13}C-labeled, suggesting many cells were metabolizing the ^{13}C-phenol exclusively. The remainder of signals from cells in the multiple ^{13}C-phenol treatment were of intermediate intensity (from 20% to 80 % enrichment), which was likely due to a combination of mixotrophy, carbon cross-feeding, and possible heterogeneous distribution of ^{13}C-phenol in the soil matrix.

Cells enriched with ^{13}C above background levels were also detected in the two soil treatments that received a single dose of ^{13}C-phenol. From the soil community that only received a single dose of ^{13}C-phenol (no unlabled substrate), 61% (704 of 1150) were less than 10% labeled, while 33% contained between 10 and 20% ^{13}C-label, 4% of the cells contained between 20 and 30% label, and a small number of cells contained between 30 and 60% ^{13}C-label (Figure 4.7). Like the treatment with no prior exposure, the soil community exposed to unlabeled phenol (11 prior doses), 60% (147 of 242) of the community was less than 10% labeled; however, 14% of the population was labeled with 20-30% ^{13}C, and 7% of the cells contained between 30% and 40% ^{13}C-label. No detected cells in either treatment that received a single dose of ^{13}C-phenol were greater than 70% ^{13}C-labeled, though the possibility of >90% labeling of rare cells cannot be dismissed. Although multiple doses of ^{13}C-phenol were necessary for detection the of fully labeled cells, dynamic SIMS ion microscopy was sensitive enough to distinguish between ^{13}C-labeled cells and unlabeled cells in soil after exposure to a single dose of 200 µg ^{13}C-phenol for 24 hours. These cells are

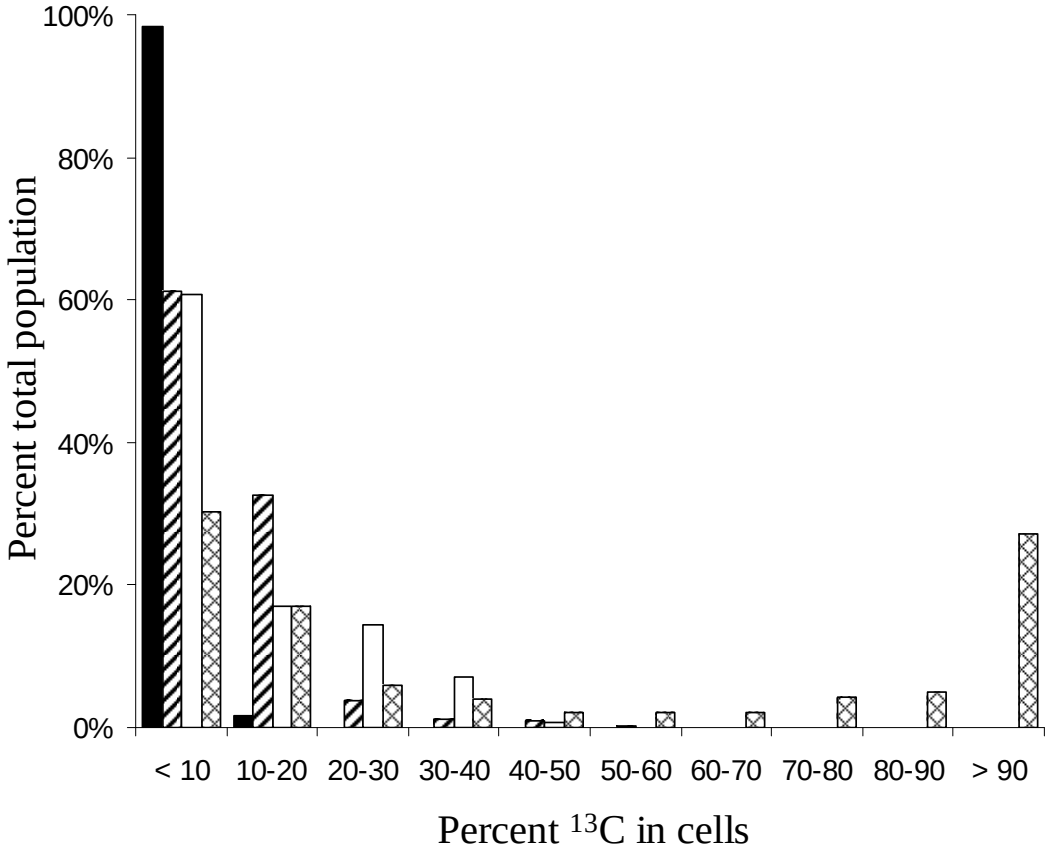

Figure 4.7. A bar graph comparing the distribution of ^{13}C signal intensity in individual bacterial cells responding to four types of phenol treatments in a field-soil experiment. The four treatments were: (i) the soil was soil dosed 12 times with ^{12}C-phenol (black bars, 481 ROIs measured) over a period of 12 days; (ii) no phenol was added for the first 11 days, only a single dose of ^{13}C-phenol was added prior to sampling at the end of day 12 (diagonal lines, 1150 ROIs measured); (iii) during the same 12-day period, the soil was soil dosed 11 times with ^{12}C-phenol with a final dose of ^{13}C-phenol (white bars, 242 ROIs measured); and (iv) soil was dosed 12 times with ^{13}C-phenol (cross hatching, 327 ROIs measured). For each treatment, the percent ^{13}C-enrichment of individual cells was estimated using the standard curve (Figure 4.3) generated from pure cultures of *P. putida* NCIB 9816-4 grown on known amounts of ^{13}C-glucose. Cells were categorized by 10% intervals. Ratios were calculated from signal intensities measured with Metamorph® software.

likely to be the primary phenol degraders; not cells labeled through carbon cross-feeding.

4.5 Discussion

In this study, we demonstrate the use of dynamic SIMS ion microscopy to measure ^{13}C-incorporation into individual bacteria grown in two settings: laboratory media and field soil. It was first necessary to show that although the primary ion beam used in SIMS erodes the sample surface, we could obtain reliable and consistent images of bacteria (Figure 4.1). Overall, we found that signal change during SIMS analysis processing was minimal over exposure times typically needed to collect images. However, occasionally signals from a small number of cells would disappear or appear during image acquisition, presumably due to changes to the sample surface caused by the primary ion beam and exposure of new cells hidden beneath the sampling plane. To increase the likelihood of reliable signals it is advisable to optimize and limit exposure times, sequentially record images of corresponding ions (i.e. mass 26 then mass 27), and collect data from a large sample size.

For dynamic SIMS ion microscopy assays to allow inferences about metabolic function, it was necessary to link substrate assimilation to ^{13}C signal detection. For this purpose, we chose two strains of *Pseudomonas putida*, one with and one without a naphthalene catabolic plasmid. Absence of the plasmid prevented cells from incorporating carbon from naphthalene when cells were exposed to a mixture of ^{13}C-glucose and unlabeled naphthalene. The data (Figure 4.4) clearly showed that ^{13}C signal intensity (measured by SIMS) was proportionate to the degree of ^{13}C-substrate respiration and growth. It was possible to measure ^{13}C incorporation in bacteria by imaging masses 12, 13, 24, 25, 26, and 27 representing contributions from $^{12}(^{12}C^-)$, $^{13}(^{13}C^-)$, $^{24}(^{12}C_2)^-$, $^{25}(^{13}C^{12}C)^-$, $^{26}(^{12}C^{14}N)^-$, and $^{27}(^{13}C^{14}N)^-$ secondary ions, respectively

(Figures 4.2 and 4.3). Unlike NanoSIMS and TOF-SIMS techniques, dynamic SIMS ion microscopy does not provide the ion resolution needed to distinguish the ion species of interest from potentially interfering species of the same mass. However, using pure cultures grown on known amounts of ^{13}C, we were able to show that the relationship between mass 26 and mass 27 signal intensities strongly correlated with ^{13}C-enrichment in cells (Figures 4.2 and 4.4).

When we measured the distribution of ^{13}C in a soil microbial community that had respired ^{13}C-phenol in situ, dynamic SIMS ion microscopy allowed us to quantify ^{13}C incorporated into individual cells (Figures 4.5 and 4.7). Using the calibration and image-processing procedures developed here and applied to our prior field soil experiments (DeRito et al., 2005), we found that when soil was dosed 12 times with ^{13}C-phenol, 27% of the soil microbial populations assimilated at least 90% of their cell carbon from the added ^{13}C phenol. The majority of cells however, were partially ^{13}C-labeled. Because the phenol was applied to soil, it is likely that the availability of phenol was not even and that gradients were present. Thus, some cells may have metabolized phenol exclusively, but did not acquire enough phenol to become fully labeled. It is also likely that mixotrophs in the population were metabolizing ^{13}C-phenol as well as other non-labeled substrates. Carbon cross-feeding may also lead to partial ^{13}C-labeling as bacteria metabolize by-products and other cellular components from the primary phenol degraders. We note that a substantial portion of the soil community treated with ^{13}C-phenol never delivered a ^{13}C-signal above background (approximately 60% from soil treated with one dose of ^{13}C-phenol and 30% from soil treated with 12 doses ^{13}C-phenol). These are likely dormant cells or ones that utilize substrates other that phenol, or simply ones whose growth rate on phenol is relatively slow. Understanding the physiology and ecological role of soil populations found to be inactive by SIMS microscopy is a major research frontier.

In order for dynamic SIMS ion microscopy to be maximally insightful as a tool in microbial ecology, researchers should be able to use SIMS in combination with techniques that identify individually labeled cells that are isotopically enriched. We are exploring feasibility of using oligonucleotide probes in combination with dynamic SIMS ion microscopy. Additionally, different methods of sample preparation are being explored, such as cryogenic sample preparation, which may help improve image quality and quantitative analysis.

REFERENCES

Adamczyk, J., Hesselsoe, M., Iverson, N., Horn, M., Lehner, A., Nielsen, P.H., Schloter, M., Roslev, P., and Wagner, M. (2003) The isotope array, a new tool that employs substrate-mediated labeling of rRNA for determination of microbial community structure and function. *Appl Environ Microbiol* **69**: 6875-6889.

Ahn, I.S., Ghiorse, W.C., Lion, L.W., and Shuler, M.L. (1998) Growth kinetics of *Pseudomonas putida* G7 on naphthalene and occurrence of naphthalene toxicity during nutrient deprivation. *Biotechnol Bioeng* **59:** 587-594.

Alden, L., Demoling, F., and Bååth, E. (2001) Rapid method of determining factors limiting growth in soil. *Appl Environ Microbiol* **67:** 1830-1838.

Allen, C.C.R., Boyd, D.R., Larkin, M.J., Reid, K.A., Sharma, N.D., and Wilson K. (1997) Metabolism of naphthalene, 1-naphthol, indene, and indole by *Rhodococcus* sp. strain NCIMB12038. *Appl Environ Microbiol* **63**: 151-155.

Amann, R.I, Ludwig, W., and Schleifer, K.-H. (1995) Phylogenetic identification and in situ detection of individual microbial cells without cultivation. *Microbiol Rev* **59**: 143-169.

Ashelford, K.E., Weightman, A.J., and Fry, J.C. (2002) PRIMROSE: a computer program for generating and estimating the phylogenetic range of 16S rRNA oligonucleotide probes and primers in conjunction with the RDP-II database. *Nucleic Acids Res* **30:** 3481–3489.

Auger, R.L., Jacobson, A.M., and Domach, M.M. (1995) Effect of nonionic surfactant addition on bacterial metabolism of naphthalene: Assessment of toxicity and overflow metabolism potential. *J Hazard Mater* **43:** 263-272.

Bakermans, C., and Madsen, E.L. (2002) Diversity of 16S rDNA and naphthalene dioxygenase genes from coal-tar-waste-contaminated aquifer waters. *Microb Ecol* **44**: 95–106.

Baziramakenga, R., Simard, R.R., and Leroux, G.D. (1995) Determination of organic acids in soil extracts by ion chromatography. *Soil Biol Biochem* **27:** 349-356.

Bedard, D.L., Unterman, R., Bopp, L.H., Brennan, M.J., Haberl, M.L., and Johnson, C. (1986) Rapid assay for screening and characterizing microorganisms for the ability to degrade polychlorinated biphenyls. *Appl Environ Microbiol* **51**: 761-768.

Behrens, S., Lösekann, T., Pett-Ridge, J., Weber, P.K., Ng, W.O., Stevenson, B.S., Hutcheon, I.D., Relman, D.A., Spormann, A.M. (2008) Linking microbial phylogeny to metabolic activity at the single-cell level by using enhanced element labeling-catalyzed reporter deposition fluorescence in situ hybridization (EL-FISH) and NanoSIMS. *Appl Environ Microbiol* **74**: 3143-3150.

Borodina, E., Cox, M.J., McDonald, I.R., and Murrell, J.C. (2005) Use of DNA-stable isotope probing and functional gene probes to investigate the diversity of methyl chloride-utilizing bacteria in soil. *Environ Microbiol* **7**: 1318-1328.

Boschker, H.T.S., Nold, S.C., Wellsbury, P.,Bos, D., de Graaf, W., Pel, R., Parkes, R.J., and Cappenburg, T.E. (1998) Direct linking of microbial populations to specific biogeochemical processes by ^{13}C-labelling of biomarkers. *Nature* **392:** 801-804.

Buckley, D.H., Huangyutitham, V., Hsu, S.-F., and Nelson, T.A. (2007a) Stable isotope probing achieved by disentangling the effects of genome G+C content and isotope enrichment on DNA density. *Appl Environ Microbiol* **73**: 3189-3295.

Buckley, D.H., Huangyutitham, V., Hsu, S.F., Nelson, T.A. (2007b) Stable isotope probing with $^{15}N_2$ reveals novel noncultivated diazotrophs in soil. *Appl Environ Microbiol* **73**: 3196-3204.

Bull, I.D., Parekh, N.R., Hall, G.H., Ineson, P., and Evershed, R.P. (2000) Detection and classification of atmospheric methane oxidizing bacteria in soil. *Nature* **405**: 175-178.

Butler, J.L., Williams, M.A., Bottomley, P.J., and Myrold, D.D. (2003) Microbial community dynamics associated with rhizosphere carbon flow. *Appl Environ Microbiol* **69**: 6793-6800.

Cadillo-Quiroz H., Bräuer, S., Yashiro, E., Sun, C., Yavitt, J., and Zinder, S. (2006) Vertical profiles of methanogenesis and methanogens in two contrasting acidic peatlands in central New York State, USA. *Environ Microbiol* **8**: 1428-40.

Castaing, R. and Slodzian, G. (1962) Microanalyse par e´mission ionique secondaire. *J Microsc* **1**: 395–410.

Cébron, A., Bodrossy, L., Stralis-Pavese, N., Singer, A.C., Thompson, I.P., Prosser, J.I., and Murrell, J.C. (2007a) Nutrient amendments in soil DNA stable isotope probing experiments reduce the observed methanotroph diversity. *Appl Environ Microbiol* **73**: 798-807.

Cébron, A., Bodrossy, L., Chen, Y., Singer, A.C., Thompson, I.P., Prosser, J.I., and Murrell, J.C. (2007b) Identity of active methanotrophs in landfill cover soil as revealed by DNA-stable isotope probing. *FEMS Microbiol Ecol*. **62**: 12-23.

Cerdan, P., Wasserfallen, A., Rekik, M., Timmis, K.N. and Harayama, S. (1994) Substrate specificity of catechol 2,3-dioxygenase encoded by TOL plasmid pWWO of *Pseudomonas putida* and its relationship to cell growth. *J Bacteriol* **176:** 6074-6081.

Chain P.S., Denef, V.J., Konstantinidis, K.T., Vergez, L.M., Agulló, L., Reyes, V.L., Hauser, L., Córdova, M., Gómez, L., González, M., Land, M., Lao, V., Larimer, F., LiPuma, J.J., Mahenthiralingam, E., Malfatti, S.A., Marx, C.J., Parnell, J.J., Ramette, A., Richardson, P., Seeger, M., Smith, D., Spilker, T., Sul, W.J., Tsoi, T.V., Ulrich, L.E., Zhulin, I.B., and Tiedje, J.M. (2006) *Burkholderia xenovorans* LB400 harbors a multi-replicon, 9.73-Mbp genome shaped for versatility. *Proc Natl Acad Sci USA* **103:** 15280-15287.

Chandra, S. (2005) Quantitative imaging of subcellular calcium stores in mammalian LLC-PK_1 epithelial cells undergoing mitosis by SIMS ion microscopy. *Eur Cell Biol* **84**: 783-797.

Chandra, S., Pumphrey, G., Abraham, J.M., and Madsen, E.L. (2008) Dynamic SIMS ion microscopy imaging of individual bacterial cells for studies of isotopically labeled molecules. *Appl Surf Sci* (In press).

Chandra, S., Smith, D.R., and Morrison, G.H. (2000) Subcellular imaging by dynamic SIMS ion microscopy. *Anal Chem* **72**: 104A-114A.

Cliff, J.B., Gaspar, D.J., Bottomley, P.J., and Myrold, D.D. (2002) Exploration of inorganic C and N assimilation by soil microbes with time-of-flight secondary ion mass spectrometry. *Appl Environ Microbiol* **68**: 4067-4073.

Cliff, J.B., Jarman, K.H., Valentine, N.B., Golledge, S.L., Gaspar, D.J., Wunschel, D.S., and Wahl, K.L. (2005) Differentiation of spores of *Bacillus subtilis* grown in different media by elemental characterization using time-of-flight secondary ion mass spectrometry. *Appl Environ Microbiol* **71**: 6524-6530.

Coenye, T. and Vandamme, P. (2003) Diversity and significance of *Burkholderia* species occupying diverse ecological niches. *Environ Microbiol* **5:** 719-729.

Crawford, R.L., Hutton, S.W. and Chapman, P.J. (1975) Purification and properties of gentisate 1,2-dioxygenase from *Moraxella osloensis*. *J Bacteriol* **121:** 794-799.

Crossman, Z.M., Abraham, F., and Evershed, R.P. (2004) Stable isotope pulse-chasing and compound specific stable carbon isotope analysis of phospholipid fatty acids to assess methane oxidizing bacterial populations in landfill cover soils. *Environ Sci Technol* **38**: 1359-1367.

Davies, J.I. and Evans, W.C. (1964) Oxidative metabolism of naphthalene by soil pseudomonads. The ring-fission mechanism. *Biochem J* **91:** 251-261.

Denef, V.J., Klappenbach, J.A., Patrauchan, M.A., Florizone, C., Rodrigues, J.L.M., Tsoi, T.V., Verstraete, W., Eltis, L.D., and Tiedje, J.M. (2006) Genetic and genomic insights into the role of benzoate-catabolic pathway redundancy in *Burkholderia xenovorans* LB400. *Appl Environ Microbiol* **72:** 585-595.

Dennis, J.J. and Zylstra, G.J. (2004) Complete sequence and genetic organization of pDTG1, the 83-kilobase naphthalene degradation plasmid from *Pseudomonas putida* NCIB 9816-4. *J Mol Biol* **341:** 753-768.

DeRito, C.M., Pumphrey, G.M., and Madsen, E.L. (2005) Use of field-based stable isotope probing to identify adapted populations and track carbon flow through a phenol-degrading soil microbial community. *Appl Environ Microbiol* **78:** 58-65.

Dorn, E. and Knackmuss, H.-J. (1978) Chemical structure and biodegradability of halogenated aromatic compounds. *Biochem J* **174:** 85-94.

Dumont, M.G. and Murrell, J.C. (2005) Stable isotope probing – linking microbial identity to function. *Nat Rev Microbiol* **3:** 499-504.

Dumont, M.G., Radajewski, S.M., Miguez, C.B., McDonald, I.R., and Murrell, J.C. (2006) Identification of a complete methane monooxygenase operon from soil by combining stable isotope probing and metagenomic analysis. *Environ Microbiol* **8**: 1240-1250.

Francisco, P. B., Ogawa, N., Suzuki, K., and Miyashita, K. (2001) The chlorobenzoate dioxygenase genes of *Burkholderia* sp. NK8 involved in the catabolism of chlorobenzoates. *Microbiol* **147**:121-133.

Fredslund, L., Flemming, E., Jacobsen, C.S., and Johnsen, K. (2001) Development and application of a most-probable-number-PCR assay to quantify flagellate populations in soil samples. *Appl Environ Microbiol* **67:** 1613-1618.

Fuenmayor, S.L., Wild, M., Boyes, A.L. and Williams, P.A. (1998) A gene cluster encoding steps in conversion of naphthalene to gentisate in *Pseudomonas* sp. Strain U2. *J Bacteriol* **180:** 2522-2530.

Gallagher, E., McGuinness, L., Phelps, C., Young, L.Y., and Kerkhof, L.J. (2005) ^{13}C-carrier DNA shortens the incubation time needed to detect benzoate-utilizing denitrifying bacteria by stable-isotope probing. *Appl Environ Microbiol* **71**: 5192-5196.

Gentry, T.J., Newby, D.T., Josephson, K.L., and Pepper, I.L. (2001) Soil microbial population dynamics following bioaugmentation with a 3-chlorobenzoate-degrading bacterial culture. *Biodegrad* **349:** 349-357.

Gentry, T.J., Wang, G., Rensing, C., and Pepper, I.L. (2004) Chlorobenzoate-degrading bacteria in similar pristine soils exhibit different community structures and population dynamics in response to anthropogenic 2-, 3-, and 4-chlorobenzoate levels. *Microb Ecol* **48:** 90-102.

Gescher, J., Zaar, A., Mohamed, M., Schägger, H., and Fuchs, G. (2002) Genes coding for a new pathway of aerobic benzoate metabolism in *Azoarcus evansii*. *J Bacteriol* **184:** 6301-6315.

Ginige, M.P., Hugenholtz, P., Daims, H., Wagner, M., Keller, J., and Blackall, L.L. (2004) Use of stable-isotope probing, full-cycle rRNA analysis, and fluorescence in situ hybridization-microautoradiography to study a methanol-fed denitrifying microbial community. *Appl Environ Microbiol* **70**: 588-596.

Ginige, M.P., Keller, J., and Blackall, L.L. (2005) Investigation of an acetate-fed denitrifying microbial community by stable isotope probing, full-cycle rRNA analysis, and fluorescent in situ hybridization-microautoradiography. *Appl Environ Microbiol* **71**: 8683-8691.

Griffiths R.I., Whiteley, A.S., O'Donnell, A.G., and Bailey, M.J. (2000) Rapid method for coextraction of DNA and RNA from natural environments for analysis of ribosomal DNA- and rRNA-based microbial community composition. *Appl Environ Microbiol* **66:** 5488-5491.

Griffiths, R.I., Manefield, M., Ostle, N., McNamara, N., O'Donnell, A.G., Bailey, M.J., and Whiteley, A.S. (2004) $^{13}CO_2$ pulse labelling of plants in tandem with stable isotope probing: methodological considerations for examining microbial function in the rhizosphere. *J Microbiol Methods* **58**: 119-129.

Guerquin-Kern, J.-L., Wu, T.-D., Quintana, C., and Croisy, A. (2005) Progress in analytical imaging of the cell by dynamic secondary ion mass spectrometry (SIMS microscopy). *Biochim Biophys Acta* **1724:** 228-238.

Haak, B., Fetzner, S., and Lingens, F. (1995) Cloning, nucleotide sequence, and expression of the plasmid-encoded genes for the two-component 2-

halobenzoate1,2-dioxygenase from *Pseudomonas cepacia* 2CBS. *J Bacteriol* **177**: 667-675.

Habe, H. and Omori, T. (2003) Genetics of polycyclic aromatic hydrocarbon metabolism in diverse aerobic bacteria. *Biosci Biotechnol Biochem* **67**: 225-243.

Haichar, F.Z., Achouak, W., Christen, R., Heulin, T., Marol, C., Marais, M.F., Mougel, C., Ranjard, L., Balesdent, J., and Berge, O. (2007) Identification of cellulolytic bacteria in soil by stable isotope probing. *Environ Microbiol* **9**: 625-634.

Hamberger, A., Horn, M.A., Dumont, M.G., Murrell, J.C., and Drake, H.L. (2008) Anaerobic consumers of monosaccharides in a moderately acidic fen. *Appl Environ Microbiol* **74**: 3112-3120.

Handelsman, J. (2004) Metagenomics: application of genomics to uncultured microorganisms. *Microbiol Mol Bio Rev* **68**: 669-685.

Hanson, J.R., Macalady, J.L., Harris, D., and Scow, K.M. (1999) Linking toluene degradation with specific microbial populations in soil. *Appl Environ Microbiol* **65**: 5403-5408.

Harayama S., Rekik, M., Bairoch, A., Neidle, E.L., and Ornston, L.N. (1991) Potential DNA slippage structures acquired during evolutionary divergence of *Acinetobacter calcoaceticus* chromosomal benABC and *Pseudomonas putida* TOL pWW0 plasmid xylXYZ, genes encoding benzoate dioxygenases. *J Bacteriol* **173**: 7540-7548.

Harwood, C.S. and Parales, R.E. (1996) The β-ketoadipate pathway and the biology of self-identity**.** *Annu Rev Microbiol* **50**: 553-590.

Hatamoto, M., Imachi, H., Ohashi, A., and Harada, H. (2007) Identification and cultivation of anaerobic, syntrophic long-chain fatty acid-degrading microbes from mesophilic and thermophilic methanogenic sludges. *Appl Environ Microbiol* **73**: 1332-1340.

Herrmann A.M., Clode, P.L., Fletcher, I.R., Nunan, N., Stockdale, E.A., O'Donnell, A.G., and Murphy, D.V. (2007) A novel method for the study of the biophysical interface in soils using nano-scale secondary ion mass spectrometry. *Rapid Commun Mass Spectrom* **21:** 29-34.

Héry, M., Singer, A.C., Kumaresan, D., Bodrossy, L., Stralis-Pavese, N., Prosser, J.I., Thompson, I.P., and Murrell, J.C. (2008) Effect of earthworms on the community structure of active methanotrophic bacteria in a landfill cover soil. *ISME J* **2**: 92-104.

Hori, T., Noll, M., Igarashi, Y., Friedrich, M.W., and Conrad, R. (2007) Identification of acetate-assimilating microorganisms under methanogenic conditions in anoxic rice field soil by comparative stable isotope probing of RNA. *Appl Environ Microbiol* **73**: 101-109.

Huang, W.E., Griffiths, R.I., Thompson, I.P., Bailey, M.J., and Whiteley, A.S. (2004) Raman microscopic analysis of single microbial cells. *Anal Chem* **76**: 4452-4458.

Huang, W.E., Stoecker, K., Griffiths, R., Newbold, L., Daims, H., Whiteley, A.S., and Wagner, M. (2007) Raman-FISH: combining stable-isotope Raman spectroscopy and fluorescence in situ hybridization for the single cell analysis of identity and function. *Environ Microbiol* **8**: 1878-1889.

Huber T., Faulkner, G., and Hugenholtz, P. (2004) Bellerophon: a program to detect chimeric sequences in multiple sequence alignments. *Bioinformatics* **20**:2317-2319.

Hugenholtz, P. (2002) Exploring prokaryotic diversity in the genomic era. *Genome Biol* **3**: reviews0003.1-0003.8.

Hutchens, E., Radajewski, S., Dumont, M.G., McDonald, I.R., and Murrell, J.C. (2004) Analysis of methanotrophic bacteria in Movile Cave by stable isotope probing. *Environ Microbiol* **6**: 111-120.

Jeon, C.O., Park, W., Padmanabhan, P., DeRito, C., Snape, J.R. and Madsen, E.L. (2003) Discovery of a bacterium, with distinctive dioxygenase, that is responsible for in situ biodegradation in contaminated sediment. *Proc Natl Acad Sci USA* **100:** 13591-13596.

Jeon, C.O., Park, M., Ro, H.S., Park, W. and Madsen, E.L. (2006) The naphthalene catabolic (*nag*) genes of *Polaromonas naphthalenivorans* CJ2: evolutionary implications for two gene clusters and novel regulatory control. *Appl Environ Microbiol* **72:** 1086-1095.

Kasai, Y., Takahata, Y., Manefield, M., and Watanabe, K. (2006) RNA-based stable isotope probing and isolation of anaerobic benzene-degrading bacteria from gasoline-contaminated groundwater. *Appl Environ Microbiol* **72**: 3586-3592.

Kittelmann, S. and Friedrich, M.W. (2008a) Identification of novel perchloroethene-respiring microorganisms in anoxic river sediment by RNA-based stable isotope probing. *Environ Microbiol* **10**: 31-46.

Kittelmann, S. and Friedrich, M.W. (2008b) Novel uncultured Chloroflexi dechlorinate perchloroethene to trans-dichloroethene in tidal flat sediments. *Environ Microbiol* **10**: 1557-70.

Klappenbach, J.A., Dunbar, J.M., and Schmidt, T.M. (2000) rRNA Operon copy number reflects ecological strategies of bacteria. *Appl Environ Microbiol* **66**:1328-1333.

Klappenbach, J.A., Saxman, P.R., Cole, J.R., and Schmidt, T.M. (2001) rrnDB: The ribosomal RNA operon copy number database. Nucleic Acids Res. **29**: 181-4.

Krooneman J., Sliekers, A.O., Pedro Gomes, T.M., Forney, L.J. and Gottshal, J.C. (2000) Characterization of 3-chlorobenzoate degrading aerobic bacteria isolated under various environmental conditions. *FEMS Microbiol Ecol* **32:** 53-59.

Kulakov, L.A, Chen, S., Allen, C.R., and Larkin, M.J. (2005) Web-type evolution of *Rhodococcus* gene clusters associated with utilization of naphthalene. *Appl Environ Microbiol* **71**: 1754-1764.

Kulakova, A.N., Reid, K.A., Larkin, M.J., Allen, C.R., and Kulakov, L.A. (1996) Isolation of *Rhodococcus rhodocrous* NCIMB13064 derivatives with new biodegradative abilities. *FEMS Microbiol Lett* **145**: 227-231.

Kunapuli, U., Lueders, T., and Meckenstock, R.U. (2007) The use of stable isotope probing to identify key iron-reducing microorganisms involved in anaerobic benzene degradation. *ISME J* **1**: 643-653.

Laurie, A.D. and Lloyd-Jones, G. (1999a) The *phn* genes of *Burkholderia* sp. strain RP007 constitute a divergent gene cluster for polycyclic aromatic hydrocarbon catabolism. *J Bacteriol* **181**: 531-540.

Laurie, A.D. and Lloyd-Jones, G. (1999b) Conserved and hybrid meta-cleavage operons from PAH-degrading *Burkholderia* RP007. *Biochem Biophys Res Commun* **262**: 308-314.

Lear, G., Song, B., Gault, A.G., Polya, D.A., and Lloyd, J.R. (2007) Molecular analysis of arsenate-reducing bacteria within Cambodian sediments following amendment with acetate. *Appl Environ Microbiol* **73**: 1041-1048.

Lechene, C., Hillion, F., McMahon, G., Benson, D., Kleinfield, A.M., Kampf, J.P., Distel, D., Luyten, Y., Bonventre, J., Hentschel, D., Park, K.M., Ito, S., Schwartz, M., Benichou, G., and Slodzian, G. (2006) High-resolution quantitative imaging of mammalian and bacterial cells using stable isotope mass spectrometry. *J Biol* **5:** 20-49.

Lee, H.J., Villaume , J., Cullen, D.C., Kim, B.C. and Gu, M.B. (2003) Monitoring and classification of PAH toxicity using an immobilized bioluminescent bacteria. *Biosens Bioelectron* **18:** 571-577.

Lee, N., Nielsen, P.H., Andreasen, K.H., Juretschko, S.J., Nielsen, L., Schleifer, K.-H., and Wagner, M. (1999) Combination of fluorescent in situ hybridization and microautoradiography—a new tool for structure-function analyses in microbial ecology. *Appl Environ Microbiol* **65**: 1289-1297.

Leigh, M.B., Pellizari, V., Uhlík, O., Sutka, R., Rodrigues, J., Ostrom, N.E., Zhou, J., and Tiedje, J.M. (2007) Biphenyl-utilizing bacteria and their functional genes in a pine root zone contaminated with polychlorinated biphenyls (PCBs). *ISME Journal* **1**: 134-148.

Lessie T. G., Hendrickson, W., Manning, B.D., and Devereux, R. (1996) Genomic complexity and plasticity of *Burkholderia cepacia*. *FEMS Microbiol Lett* **144:** 117-128.

Li, T, Wu, T.D., Mazéas, L., Toffin, L., Guerquin-Kern, J.L., Leblon, G., and Bouchez, T. (2008) Simultaneous analysis of microbial identity and function using NanoSIMS. *Environ Microbiol* **10**: 580-588.

Lin, J.L., Radajewski, S., Eshinimaev, B.T., Trotsenko, Y.A., McDonald, I.R., and Murrell, J.C. (2004) Molecular diversity of methanotrophs in Transbaikal soda lake sediments and identification of potentially active populations by stable isotope probing. *Environ Microbiol* **6**: 1049-1060.

Liou, J. S-C., DeRito, C.M. and Madsen, E.L. (2008) Field-based and laboratory stable isotope probing surveys of the identities of both aerobic and anaerobic benzene-metabolizing microorganisms in freshwater sediment. *Environ Microbiol* (IN PRESS)

Lu, Y. and Conrad, R. (2005) In situ stable isotope probing of methanogenic archaea in the rice rhizosphere. *Science* **309**: 1088-1090.

Lu, Y., Lueders, T., Friedrich, M.W., and Conrad, R. (2005) Detecting active methanogenic populations on rice roots using stable isotope probing. *Environ Microbiol* **7**: 326-336.

Lu, Y., Rosencrantz, D., Liesack, W., and Conrad, R. (2006) Structure and activity of bacterial community inhabiting rice roots and the rhizosphere. *Environ Microbiol* **8**: 1351-1360.

Lu, Y., Abraham, W.R., and Conrad, R. (2007) Spatial variation of active microbiota in the rice rhizosphere revealed by in situ stable isotope probing of phospholipid fatty acids. *Environ Microbiol* **9**: 474-481.

Lueders, T., Manefield, M., and Friedrich, M.W. (2004a) Enhanced sensitivity of DNA-and rRNA-based stable isotope probing by fractionation and quantitative analysis of isopycnic centrifugation gradients. *Environ Microbiol* **61**: 73–78.

Lueders, T., Wagner, B., Claus, P., and Friedrich, M.W. (2004b) Stable isotope probing of rRNA and DNA reveals a dynamic methylotroph community and trophic interactions with fungi and protozoa in oxic rice field soil. *Environ Microbiol* **6**: 60-72.

Lueders, T., Pommerenke, B., and Friedrich, M.W. (2004c) Stable-isotope probing of microorganisms thriving at thermodynamic limits: syntrophic propionate oxidation in flooded soil. *Appl Environ Microbiol* **70**: 5778-5786.

Madsen, E. L. (2005) Identifying microorganisms responsible for ecologically significant biogeochemical processes. *Nature Reviews Microbiol* **3**: 439-446.

Madsen, E.L. (2006) The use of stable isotope probing techniques in bioreactor and field studies on bioremediation. *Curr Opin Biotechnol* **17**: 92-97.

Mahmood, S., Paton, G.I., and Prosser, J.I. (2005) Cultivation-independent in situ molecular analysis of bacteria involved in degradation of pentachlorophenol in soil. *Environ Microbiol* **7**: 1349-1360.

Manefield, M., Whitely, A.S., Griffiths, R.I., and Bailey, M.J. (2002) RNA stable isotope probing, a novel means of linking community function to phylogeny. *Appl Environ Microbiol* **68**: 5367-5373.

Manefield, M., Griffiths, R., McNamara, N.P., Sleep, D., Ostle, N., and Whiteley, A. (2007) Insights into the fate of a ^{13}C labelled phenol pulse for stable isotope probing (SIP) experiments. *J Microbiol Methods* **69**: 340-344.

Maron, P.-A., Ranjard, L., Mougel, C., and Lemanceau, P. (2007) Metaproteomics: A new approach for studying functional microbial ecology. *Microb Ecol* **53**: 486-493.

Mauclaire, L., Pelz, O., Thullner, M., Abraham, W.-R., and Zeyer, J. (2003) Assimilation of toluene along a bacteria-protist food chain determined by ^{13}C-enrichment of biomarker fatty acids. *J Microbiol Methods* **55**: 635-649.

Maxfield, P.J., Hornibrook, E.R., and Evershed, R.P. (2006) Estimating high-affinity methanotrophic bacterial biomass, growth, and turnover in soil by phospholipid fatty acid ^{13}C labeling. *Appl Environ Microbiol* **72**: 3901-3907.

Maxfield, P.J., Hornibrook, E.R., and Evershed, R.P. (2008) Acute impact of agriculture on high-affinity methanotrophic bacterial populations. *Environ Microbiol* **10**: 1917-1924.

Mohanty, S.R., Bodelier, P.L., Floris, V., and Conrad, R. (2006) Differential effects of nitrogenous fertilizers on methane-consuming microbes in rice field and forest soils. *Appl Environ Microbiol* **72**: 1346-1354.

Morasch B., Annweiler, E., Warthmann, R.J. and Meckenstock, R.U. (2001) The use of a solid adsorber resin for enrichment of bacteria with toxic substrates and to identify metabolites: degradation of naphthalene, O-, and m-xylene by sulfate-reducing bacteria. *J Microbiol Methods* **44:** 183-191.

Moreau, J. W., Weber, P.K., Martin, M.C., Gilbert, B., Hutcheon, D.I., Banfield, J.F. (2007) Extracellular proteins limit the dispersal of biogenic nanoparticles. *Science* **316**: 1600-1603.

Morris, S.A., Radajewski, S., Willison, T.W., and Murrell, J.C. (2002) Identification of the functionally active methanotroph population in a peat soil microcosm by stable-isotope probing. *Appl Environ Microbiol* **68**: 1446-1453.

Murase, J. and Frenzel, P. (2007) A methane-driven microbial food web in a wetland rice soil. *Environ Microbiol* **9**: 3025-3034.

Murphy, J.F. and Stone, R.W. (1955) The bacterial dissimilation of naphthalene. *Can J Microbiol* **1:** 579-588.

Neidle, E.L., Hartnett, C., Ornston, L.N., Bairoch, A., Rekik, M., and Harayama, S. (1991) Nucleotide sequences of the *Acinetobacter calcoaceticus* benABC genes for benzoate 1,2-dioxygenase reveal evolutionary relationships among multicomponent oxygenases. *J Bacteriol* **173**: 5385-5395.

Nercessian, O., Noyes, E., Kalyuzhnaya, M.G., Lidstrom, M.E., and Chistoserdova, L. (2005) Bacterial populations active in metabolism of C1 compounds in the sediment of Lake Washington, a freshwater lake. *Appl Environ Microbiol* **71**: 6885-6899.

Neufeld, J.D., Vohra, J., Dumont, M.G., Lueders, T., Manefield, M., Friedrich, M.W., and Murrell, J.C. (2007a) DNA stable-isotope probing. *Nature Protocols* **2**: 860-866.

Neufeld, J.D., Schäfer, H., Cox, M.J., Boden, R., McDonald, I.R., and Murrell, J.C. (2007b) Stable-isotope probing implicates *Methylophaga* spp. and novel Gammaproteobacteria in marine methanol and methylamine metabolism. *ISME J* **1**: 480-491.

Neufeld, J.D., Wagner, M., and Murrell, J.C. (2007c) Who eats what, where, and when? Isotope labeling experiments are coming of age. *ISME J* **1**: 103-110.

Neufeld, J.D., Chen, Y., Dumont, M.G., and Murrell, J.C. (2008) Marine methylotrophs revealed by stable-isotope probing, multiple displacement amplification and metagenomics. *Environ Microbiol* **10**: 1526-1535.

Noll, M., Frenzel, P., and Conrad, R. (2008) Selective stimulation of type I methanotrophs in a rice paddy soil by urea fertilization revealed by RNA-based stable isotope probing. *FEMS Microbiol Ecol*. **65**: 125-132.

O'Sullivan, L. A. and Mahenthiralingam, E. (2005) Biotechnology potential within the genus *Burkholderia*. *Lett Appl Microbiol* **41:** 8-11.

Orphan, V.J., House, C.H., Hinrichs, K.U., McKeegan, K.D., and DeLong, E.F. (2001) Methane-consuming archaea revealed by directly coupled isotopic and phylogenetic analysis. *Science*. **293**: 484-487.

Orphan, V.J., House, C.H., Hinrichs, K.U., McKeegan, K.D., and DeLong, E.F. (2002) Multiple archaeal groups mediate methane oxidation in anoxic cold seep sediments. *Proc Natl Acad Sci U S A* **99**: 7663-7668.

Osaka, T., Yoshie, S., Tsuneda, S., Hirata, A., Iwami, N., and Inamori, Y. (2006) Identification of acetate- or methanol-assimilating bacteria under nitrate-reducing conditions by stable-isotope probing. *Microb Ecol* **52**: 253-266.

Osaka, T., Ebie, Y., Tsuneda, S., and Inamori, Y. (2008) Identification of the bacterial community involved in methane-dependent denitrification in activated sludge using DNA stable-isotope probing. *FEMS Microbiol Ecol* **64**: 494-506.

Ouverney, C.C. and Fuhrman, J.A. (1999) Combined microautoradiography–16s rRNA probe technique for determination of radioisotope uptake by specific microbial cell types in situ. *Appl Environ Microbiol* **65**: 1746-1752.

Pacholski, M.L. and Winograd, N. (1999) Imaging with mass spectrometry. *Chem Rev* **99**: 2977– 3005.

Padmanabhan, P., Padmanabhan, S., DeRito, C., Gray, A., Gannon, D., Snape, J.R., Tsai, C.S., Park, W., Jeon, C., and Madsen, E.L. (2003) Respiration of

^{13}C-labeled substrates added to soil in the field and subsequent 16S rRNA gene analysis of ^{13}C-labeled soil DNA. *Appl Environ Microbiol* **69**: 1614–1622.

Parales, R.E. (2003) The role of active-site residues in naphthalene dioxygenase. *J Ind Microbiol Biotechnol* **30**: 271-278.

Park, W., Jeon, C.O., Cadillo, H., DeRito, C. and Madsen, E.L. (2004) Survival of naphthalene-degrading *Pseudomonas putida* NCIB 9816-4 in naphthalene-amended soils: toxicity of naphthalene and its metabolites. *Appl Microbiol Biotechnol* **64:** 429-435.

Pelz, O., Chatzinotas, A., Andersen, N., Bernasconi, S.M., Hesse, C., Abraham, W.-R., and Zeyer, J. (2001) Use of isotopic and molecular techniques to link toluene degradation in denitrifying aquifer microcosms to specific microbial populations. *Arch Microbiol* **175**: 270-281.

Penning, T.M., Burczynski, M.E., Hung, C.F., McCoull, K.D., Palackal, N.T. and Tsuruda, L.S. (1999) Dihydrodiol dehydrogenases and polycyclic aromatic hydrocarbon activation: generation of reactive and redox active o-quinones. *Chem Res Toxicol* **12:** 1-18.

Pernthaler, A., Pernthaler, J., and Amann, R. (2002) Fluorescence in situ hybridization and catalyzed reporter deposition for the identification of marine bacteria. *Appl Environ Microbiol* **68:** 3094–3101.

Peteranderl R. and Lechene, C. (2004) Measure of carbon and nitrogen stable isotope ratios in cultured cells. *J Am Soc Mass Spectrom* **15**: 478-485.

Peters, C.A., Knightes, C.D. and Brown, D.G. (1999) Long-term composition dynamics of PAH-containing NAPLs and implications for risk assessment. *Environ Sci Technol* **33**: 4499-4507.

Pombo, S.A., Pelz, O., Schroth, M.H., and Zeyer, J. (2002) Field-scale ^{13}C-labeling of phospholipid fatty acids (PLFA) and dissolved inorganic cabon: tracing acetate assimilation and mineralisation in a petroleum hydrocarbon-contaminated aquifer. FEMS Microbiol Ecol **41**: 259-267.

Pombo, S.A., Kleikemper, J., Schroth, M.H., and Zeyer, J. (2005) Field-scale isotopic labelling of phospholipid fatty acids from acetate degrading sulfate-reducing bacteria. FEMS Microbiol Ecol **51**: 197-201.

Popa, R., Weber, P.K., Pett-Ridge, J., Finzi, J.A., Fallon, S.J., Hutcheon, I.D., Nealson, K.H., and Capone, D.G. (2007) Carbon and nitrogen fixation and metabolite exchange in and between individual cells of *Anabaena oscillarioides*. *ISME J* **1:** 354–360.

Pumphrey, G.M. and Madsen, E.L. (2007) Naphthalene metabolism and growth inhibition by naphthalene in *Polaromonas naphthalenivorans* strain CJ2. *Microbiol* **153:** 3730-3738.

Pumphrey, G.M. and Madsen, E.L. (2008) Field-based stable isotope probing reveals the identities of benzoic acid-metabolizing microorganisms and their in situ growth in agricultural soil. **74**: 4111-4118.

Qiu, Q., Noll, M., Abraham, W.R., Lu, Y., and Conrad, R. (2008) Applying stable isotope probing of phospholipid fatty acids and rRNA in a Chinese rice field to study activity and composition of the methanotrophic bacterial communities in situ. *ISME J* **2**: 602-614.

Radajewski, S., Ineson, P., Parekh, N.H., and Murrell, J.C. (2000) Stable-isotope probing as a tool in microbial ecology. *Nature* **403**: 646-649.

Ramos, J.L., Duque, E., Gallegos, M.T., Godoy, P., Ramos-Gonzalez, M.I., Rojas, A., Teran, W. and Segura, A. (2002) Mechanisms of solvent tolerance in gram-negative bacteria. *Annu Rev Microbiol* **56:** 743-768.

Rangel-Castro, J.I., Killham, K., Ostle, N., Nicol, G.W., Anderson, I.C., Scrimgeour, C.M., Ineson, P., Meharg, A., and Prosser, J.I. (2005) Stable isotope probing analysis of the influence of liming on root exudate utilization by soil microorganisms. *Environ Microbiol* **7**: 828-838.

Serdar, C.M. and Gibson D.T. (1989) Isolation and characterization of altered plasmids in mutant strains of *Pseudomonas putida* NCIB 9816. *Biochem Biophys Res Commun* **164**: 764-771.

Samanta, S.K., Singh, O.V. and Jain, R.K. (2002) Polycyclic aromatic hydrocarbons: environmental pollution and bioremediation. *Trends Biotechnol* **20:** 243-248.

Schwarz, J.I., Lueders, T., Eckert, W., and Conrad, R. (2007) Identification of acetate-utilizing Bacteria and Archaea in methanogenic profundal sediments of Lake Kinneret (Israel) by stable isotope probing of rRNA. *Environ Microbiol* **9**: 223-37.

Schweigert, N., Zehnder, A.J. and Eggen, R.I. (2001) Chemical properties of catechols and their molecular modes of toxic action in cells, from microorganisms to mammals. *Environ Microbiol* **3:** 81-91.

Shrestha, M., Abraham, W.R., Shrestha, P.M., Noll, M., and Conrad, R. (2008) Activity and composition of methanotrophic bacterial communities in planted rice

soil studied by flux measurements, analyses of pmoA gene and stable isotope probing of phospholipid fatty acids. *Environ Microbiol* **10**: 400-412.

Sikkema, J., de Bont, J.A. and Poolman, B. (1994) Interactions of cyclic hydrocarbons with biological membranes. *J Biol Chem* **269:** 8022-8028.

Sikkema, J., de Bont, J.A. and Poolman, B. (1995) Mechanisms of membrane toxicity of hydrocarbons. *Microbiol Rev* **59:** 201-222.

Singleton, D.R., Powell, S.N., Sangaiah, R., Gold, A., Ball, L.M., and Aitken, M.D. (2005) Stable-isotope probing of bacteria capable of degrading salicylate, naphthalene, or phenanthrene in a bioreactor treating contaminated soil. *Appl Environ Microbiol* **71**: 1202-1209.

Singleton, D.R., Sangaiah, R., Gold, A., Ball, L.M., and Aitken, M.D. (2006) Identification and quantification of uncultivated Proteobacteria associated with pyrene degradation in a bioreactor treating PAH-contaminated soil. *Environ Microbiol* **8**: 1736-1745.

Singleton, D.R., Hunt, M., Powell, S.N., Frontera-Suau, R., and Aitken, M.D. (2007) Stable-isotope probing with multiple growth substrates to determine substrate specificity of uncultivated bacteria. *J Microbiol Methods* **69**: 180-187.

Singh, B.K. and Tate, K. (2007) Biochemical and molecular characterization of methanotrophs in soil from a pristine New Zealand beech forest. *FEMS Microbiol Lett* **275**: 89-97.

Singh, B.K., Tate, K.R., Kolipaka, G., Hedley, C.B., Macdonald, C.A., Millard, P., and Murrell, J.C. (2007) Effect of afforestation and reforestation of pastures on the activity and population dynamics of methanotrophic bacteria. *Appl Environ Microbiol* **73**: 5153-5161.

Sota, M., Yano, H., Ono, A., Miyazaki, R., Ishii, H., Genka, H., Top, E.M. and Tsuda, M. (2006) Genomic and functional analysis of the IncP-9 naphthalene-catabolic plasmid NAH7 and its transposon Tn4655 suggests catabolic gene spread by a tyrosine recombinase. *J Bacteriol* **188:** 4057-4067.

Stanier, R.Y., Palleroni, N.J. and Doudoroff, M. (1966) The aerobic pseudomonads: a taxonomic study. *J Gen Microbiol* **43:** 159–271.

Stuart-Keil, K.G., Hohnstock, A.M., Drees, K.P., Herrick, J.B., and Madsen, E.L. (1998) Plasmids responsible for horizontal transfer of naphthalene catabolism genes between bacteria at a coal tar-contaminated site are homologous to pDTG1 from *Pseudomonas putida* NCIB 9816-4. *Appl Environ Microbiol* **64**: 3633-3640.

Suzuki, K., Ogawa, N., and Miyashita, K. (2001) Expression of 2-halobenzoate dioxygenase genes (cbdSABC) involved in the degradation of benzoate and 2-halobenzoate in *Burkholderia* sp. TH2. *Gene* **262**: 137-145.

Suzuki, K., Ichimura, A., Ogawa, N., Hasebe, A., and Miyashita, K. (2002) Differential expression of two catechol 1,2-dioxygenases in *Burkholderia* sp. Strain TH2. *J Bacteriol* **184**: 5714-5722.

Thompson, J.D., Gibson, T.J., Plewniak, F., Jeanmougin, F., and Higgins, D.G. (1997) The ClustalX windows interface: flexible strategies for multiple sequence alignment aided by quality analysis tools. *Nucleic Acids Res* **24**: 4876-4882.

Tillman, S., Strömpl, C., Timmis, K.N., and Abraham, W.-R. (2005) Stable isotope probing reveals the dominant role of *Burkholderia* species in aerobic degradation of PCBs. *FEMS Microbiol Ecol* **52:** 207-217.

Treonis, A.M., Ostle, N.J., Stott, A.W., Primrose, R., Grayston, S.J., Ineson, P. (2004) Identification of groups of metabolically-active rhizosphere microorganisms by stable isotope probing of PLFAs. *Soil Biol Biochem* **36**: 533-537.

Treude, T., Orphan, V., Knittel, K., Gieseke, A., House, C.H., and Boetius, A. (2007) Consumption of methane and CO_2 by methanotrophic microbial mats from gas seeps of the anoxic Black Sea. *Appl Environ Microbiol* **73**: 2271-2283.

von Wintzingerode, F., Göbel, U.B., and Stackebrandt, E. (1997) Determination of microbial diversity in environmental samples: pitfalls of PCR-based rRNA analysis. *FEMS Microbiol Rev* **21**: 213-229.

Wagner, M., Horn, M., and Daims, H. (2003) Fluorescence in situ hybridization for the identification and characterisation of prokaryotes. *Curr Opin Microbiol* **6**: 302-309.

Webster, G., Watt, L.C., Rinna, J., Fry, J.C., Evershed, R.P., Parkes, R.J., and Weightman, A.J. (2006) A comparison of stable-isotope probing of DNA and phospholipid fatty acids to study prokaryotic functional diversity in sulfate-reducing marine sediment enrichment slurries. *Environ Microbiol* **8**: 1575-89.

Whiteley, A.S., Thomson, B., Lueders, T., and Manefield, M. (2007) RNA stable isotope probing. *Nature Protocols* **2**: 838-844.

Xu, Y., Yan, D.Z. and Zhou, N.Y. (2006) Heterologous expression and localization of gentisate transporter Ncg12922 from *Corynebacterium glutacmicum* ATCC 13032. *Biochem Biophys Res Commun* **346**: 555-561.

Xue, W. and Warshawsky, D. (2005) Metabolic activation of polycyclic and heterocyclic aromatic hydrocarbons and DNA damage: A review. *Toxicol Appl Pharmacol* **206:** 73-93.

Yen, K.M. and Gunsalus, I.C. (1982) Plasmid gene organization: Naphthalene/salicylate oxidation. *Proc Natl Acad Sci USA* **79:** 874-878.

Yen, K.M and Serdar, C.M. (1988) Genetics of naphthalene catabolism in pseudomonads. *Crit Rev Microbiol* **15:** 247-268.

Zhou, N.Y., Al-Dulayymi, J., Baird, M.S. and Williams, P.A. (2002) Salicylate 5-hydroxylase from *Ralstonia* sp. strain U2: a monooxygenase with close relationships to and shared electron transport proteins with naphthalene dioxygenase. *J Bacteriol* **184:** 1547-1555.